

**Investigating novel drug targets and the  
biosynthetic pathways of lipids in  
mycobacteria**

By

**AMRITA KAUR RANA**

A thesis submitted to The University of Birmingham  
for the Degree of Doctor of Philosophy

School of Chemistry  
College of Engineering and Physical Sciences  
The University of Birmingham

September 2013

UNIVERSITY OF  
BIRMINGHAM

**University of Birmingham Research Archive**

**E-theses repository**

This unpublished thesis/dissertation is copyright of the author and/or third parties. The intellectual property rights of the author or third parties in respect of this work are as defined by The Copyright Designs and Patents Act 1988 or as modified by any successor legislation.

Any use made of information contained in this thesis/dissertation must be in accordance with that legislation and must be properly acknowledged. Further distribution or reproduction in any format is prohibited without the permission of the copyright holder.

## ABSTRACT

The spread of the tuberculosis (TB) has been further accelerated by the emergence of multi- and extensively-drug resistant *Mycobacterium tuberculosis* strains, thereby further increasing the need to characterise novel drug targets and develop anti-TB agents. The cell wall of *M. tuberculosis* plays a key role in survival of the pathogen in the host cell, making it an attractive drug target. The findings in this thesis present three different studies that contribute to the discovery of novel drug targets. Using a whole-cell screening approach and the generation of spontaneous drug-resistant mutants in *M. smegmatis*, a surrogate model of *M. tuberculosis*, we identified a new inhibitor which targets glycerol metabolism. The two remaining studies involved studying the biosynthetic pathways of critical cell-wall components. In this first study, Conditional expression specialised transduction essentiality test was used to confirm the essentiality of MSMEG3859 in *M. smegmatis*, an enzyme which generates mannose donors that are utilised in the biosynthesis of higher order Phosphatidyl-*myo*-inositol mannosides, Lipomannan (LM) and Lipoarabinomannan (LAM), important immunomodulators in mycobacteria. Furthermore, a deletion mutant of Protein kinase H (PknH) in *M. tuberculosis* was used to demonstrate its importance in the production of LM/LAM and Phthiocerol dimycoserates, a glycolipid that is also involved in TB pathogenesis. Thus, both Ppm1 and PknH can potentially be used as future therapeutic targets against *M. tuberculosis*.

## **DECLARATION**

The work presented in this thesis was carried out in the School of Biosciences at the University of Birmingham, U.K., B15 2TT during the period September 2009 to September 2013. The work in this thesis is original except where acknowledged by references.

No portion of the work is being, or has been submitted for a degree, diploma or any other qualification at any other University.

## ACKNOWLEDGMENTS

I would like to take this opportunity to thank all the people who have made this incredible four year experience and ultimately this thesis possible. First and foremost, I would like to express my sincere gratitude and appreciation to my supervisor, Professor Gurdyal S. Besra, for granting me the opportunity to study in his lab. I still remember me asking him if he was sure when he offered me this opportunity. I think one of the biggest obstacles that I have had to overcome in this PhD is my lack of confidence in my capabilities, but I'm thankful to the many people that have helped me to believe in myself. I would like to thank Dr Liam R. Cox for all his valuable help and advice throughout this PhD and always pointing me in the right direction.

Very special thanks to Kiran who provided valuable guidance during my first few months of my PhD. Further thanks to Dr Apoorva Bhatt for always readily offering his technical expertise at every point of this PhD, helping me write my first paper and giving innumerable suggestions whenever things didn't go to plan. I would also like to thank Albel, Luke and Sid for all their help and useful tips in some of the experiments done in this thesis. I would like to thank Dr. Anaximandro Gómez-Velasco and Prof. Yossef Av-Gay from the University of British Columbia for performing some of the experiments that appears in Chapter 4 including radiolabelling, mass spectrometry (lipidomics) and immunostaining.

I would also like to thank Mimi and Usha for all their valuable help and advice whenever I needed it throughout my PhD. My special thanks to everyone in the Besra lab who has contributed in making these four years very memorable. Special mention to Monika, Shipra,

Veemal and Natacha for giving me their constant support and friendship throughout these years and all in all, ensuring there was never a dull moment at any point.

And finally, I would to thank my family who without I would never have reached this far: my Chachi and Chacha who have always encourage me to achieve the best in life, my Dad who is a man of very few words, but I know he is the person who is most proud of me today, and the most special person in my life, my Granny. Everything I am today, everything I've achieved is because of her encouragement and love.

*This thesis is dedicated to my Granny*

# TABLE OF CONTENTS

<b>University of Birmingham Research Archive .....</b>	<b>i</b>
<b>ABSTRACT .....</b>	<b>ii</b>
<b>DECLARATION.....</b>	<b>iii</b>
<b>ACKNOWLEDGMENTS .....</b>	<b>iv</b>
<b>TABLE OF CONTENTS.....</b>	<b>vii</b>
<b>LIST OF FIGURES .....</b>	<b>xiv</b>
<b>LIST OF TABLES .....</b>	<b>xvii</b>
<b>LIST OF ABBREIVIATIONS.....</b>	<b>xviii</b>
<b>PUBLISHED WORK ASSOCIATED WITH THESIS.....</b>	<b>xxiv</b>
<b>1 General Introduction .....</b>	<b>1</b>
1.1 <i>Mycobacterium</i> species .....	2
1.2 History of tuberculosis.....	3
1.3 Immune response to tuberculosis.....	6
1.4 Epidemiology of tuberculosis .....	9
1.5 Treatment.....	11
1.5.1 Anti-tuberculosis drugs .....	11



1.5.2	Directly Observed Treatment – Short Course .....	15
1.5.3	Drug resistance .....	16
1.6	Mycobacterial cell wall.....	17
1.6.1	Peptidoglycan (PG) .....	18
1.6.2	Arabinogalactan (AG) .....	21
1.6.3	Mycolic acids.....	23
1.6.4	Solvent-extractable free lipids .....	25
1.6.5	Trehalose dimycolate (TDM) and trehalose monomycolate (TMM).....	25
1.6.6	Sulfolipids (SL) .....	26
1.6.7	Phthiocerol dimycocerosate (PDIM) and phenolic glycolipid (PGL) .....	27
1.6.8	Lipoarabinomannan (LAM) and related biosynthetic precursors (LM and PIMs) 29	
1.7	<i>Mycobacterium smegmatis</i> as a surrogate system in tuberculosis research.....	32
1.8	Aims and objectives.....	32
<b>2</b>	<b>Identification of an inhibitor targeting glycerol kinases .....</b>	<b>34</b>
2.1	Introduction.....	35
2.1.1	TB drug discovery .....	35
2.1.2	Recent successes using whole-cell screening approaches.....	36
2.1.3	ChemBridge library .....	44
2.2	Materials and Methods.....	45

2.2.1	Bacterial strains and growth conditions .....	45
2.2.2	MIC determination .....	45
2.2.3	Generation of <i>M. smegmatis</i> spontaneous mutant resistant to AKR334 .....	46
2.2.4	Construction of Recombinant Plasmids .....	46
2.2.5	Polar and apolar lipid extraction of [ <sup>14</sup> C]-labelled inhibitor-treated cultures of <i>M. smegmatis</i> .....	47
2.3	Results and Discussion .....	48
2.3.1	Identification of AKR334 as an inhibitor of <i>M. smegmatis</i> .....	48
2.3.2	Identification of single nucleotide polymorphisms (SNPs) in a spontaneous resistant mutant.....	50
2.3.3	Over-expression of glycerol operon genes in <i>M. smegmatis</i> .....	54
2.3.4	MmpL3 protein is not the cellular target of AKR334 .....	55
2.3.5	AKR334 displays greater inhibitory activity in the presence of glycerol as a carbon source .....	56
2.4	Conclusion .....	58

### **3 The essentiality of Ppm1-encoded polyprenyl monophosphomannose synthase in lipoglycan biosynthesis in mycobacteria..... 61**

3.1	Introduction.....	62
3.1.1	Immunomodulatory properties of LM and LAM .....	62
3.1.2	Biosynthesis of PIMs, LM and LAM .....	69

3.1.3	Polyprenyl monophosphomannose synthase (PPM synthase) encoded by Ppm1	74
3.2	Materials and Methods.....	77
3.2.1	Bacterial strains and growth conditions .....	77
3.2.2	Construction of recombinant plasmids .....	77
3.2.3	Generation of knockout phage for null mutant creation using specialised transduction .....	79
3.2.4	Generation of the $\Delta$ MsPpm Conditional Mutant.....	81
3.2.5	Southern blotting .....	83
3.2.6	Conditional depletion of $\Delta$ MsPpm conditional mutant.....	83
3.2.7	Extraction of polar lipids .....	84
3.2.8	Extraction and purification of lipoglycans .....	84
3.2.9	PPM synthase assay.....	85
3.3	Results and Discussion .....	86
3.3.1	Confirming the essentiality of <i>MSMEG3859</i> in <i>M. smegmatis</i> .....	86
3.3.2	Loss of <i>MSMEG3859</i> leads to an alteration in PIM profile and cessation of LM biosynthesis .....	88
3.3.3	Effects of loss of <i>MSMEG3859</i> on membrane-associated PPM synthase activity	91
3.3.4	Potential ability of alternative <i>M. tuberculosis</i> PPM synthases to rescue viability and restore wild-type phenotype in the $\Delta$ MsPpm mutant .....	92

3.4	Conclusion .....	95
-----	------------------	----

## **4 Deletion of the serine/threonine protein kinase H alters phthiocerol dimycocerosate synthesis in *Mycobacterium tuberculosis*..... 97**

4.1	Introduction.....	98
4.1.1	Biosynthesis of phthiocerol dimycocerosates (PDIMs) .....	98
4.1.2	Serine/threonine protein kinase H (PknH).....	100
4.2	Materials and methods .....	103
4.2.1	Bacterial strains and growth conditions .....	103
4.2.2	Extraction of polar lipids and apolar lipids .....	103
4.2.3	Extraction, purification and characterisation of lipoglycans .....	104
4.2.4	Fourier transform ion cyclotron resonance (FT-ICR) MS analysis.....	105
4.2.5	Production of single-chain, fragment-variable (scFv) antibodies .....	106
4.2.6	Immunostaining and fluorescence microscopy .....	107
4.2.7	Isobaric tags for relative and absolute quantitation (iTRAQ) analysis .....	107
4.2.8	MS data analysis.....	109
4.2.9	Statistical analysis .....	110
4.3	Results and Discussion .....	110
4.3.1	The $\Delta pknH$ mutant produces low levels of PDIMs .....	110
4.3.2	Structural analysis of total lipids from the $\Delta pknH$ strain .....	115
4.3.3	Detection of PDIMs using immunofluorescence microscopy.....	119

4.3.4	Proteins involved in PDIM production are differentially regulated in the $\Delta pknH$ strain	121
4.3.5	Lipoglycan profiles of wild type, $\Delta pknH$ and $\Delta pknH::pknH$ strains	122
4.4	Conclusion	124
<b>5</b>	<b>General Conclusions</b>	<b>129</b>
<b>6</b>	<b>General Material and Methods</b>	<b>134</b>
6.1	Polymerase Chain Reaction (PCR)	135
6.2	DNA digestion	136
6.3	DNA ligation	137
6.4	Preparation of chemical competent <i>E. coli</i> cells	137
6.5	Transformation of <i>E. coli</i> competent cells	138
6.6	Plasmid extraction	138
6.7	Preparation of <i>M. smegmatis</i> electrocompetent cells	138
6.8	Electroporation of <i>M. smegmatis</i>	139
6.9	<i>M. smegmatis</i> genomic DNA extraction	139
6.10	Apolar and polar lipid extraction	140
6.11	Thin layer chromatography (TLC) analysis for lipids	140
6.12	Solvent systems for 2D-TLC analysis	141
6.13	Dialysis of lipoglycans	142

6.14 SDS-PAGE..... 142

**7 References ..... 143**

## LIST OF FIGURES

Figure 1.1. Schematic representation of granuloma formation in humans.....	8
Figure 1.2. Map showing estimated TB incidence rates in the year 2011.....	10
Figure 1.3. Map showing estimated HIV prevalence in TB cases in the year 2011.....	10
Figure 1.4. Activation of the prodrug isoniazid (INH) to form isonicotinic acyl-NADH.....	14
Figure 1.5. Conversion of pyrazinamide (PZA) to pyrazinoic acid .....	15
Figure 1.6. Representation of the <i>M. tuberculosis</i> cell wall.....	18
Figure 1.7. Structure of <i>M. tuberculosis</i> peptidoglycan .....	20
Figure 1.8. Structure of arabinogalactan in <i>M. tuberculosis</i> .....	21
Figure 1.9. Structure of mycolic acids found in <i>M. tuberculosis</i> . .....	24
Figure 1.10. Structure of and trehalose monomycolate (TMM) and trehalose dimycolate (TDM).....	26
Figure 1.11. Structure of sulfolipid – SL-1. ....	27
Figure 1.12. Structure of phthiocerol dimycocerosate (PDIM) and phenolic glycolipid (PGL) from “ <i>M. canetti</i> ” .....	28
Figure 1.13. Structures of phosphatidyl- <i>myo</i> -inositol mannosides (PIMs), lipomannan (LM) and lipoarabinomannan (LAM).....	31
Figure 2.1. Structure of TMC207. ....	37
Figure 2.2. Structure of BTZ043. The most advanced compound from the BTZ series. BTZ043 is a <i>S</i> enantiomer of BTZ038 which has a single chiral centre. ....	38
Figure 2.3. Structure of DNB1. ....	38
Figure 2.4. BTZ and DNB targeting the DPA biosynthesis pathway. ....	39
Figure 2.5. Structure of SQ109.....	40

Figure 2.6. Structure of AU1235 - 1-(2-adamantyl)-3-(2,3,4-trifluorophenyl)urea. ....	40
Figure 2.7. Structure of pyrrole derivative BM212. ....	41
Figure 2.8. Structure of THPP 1 and Spiro 2. ....	41
Figure 2.9. Structure of thiophenes TP2 and TP4. ....	42
Figure 2.10. Structure of compounds from imidazo[1,2- <i>a</i> ]pyridines (IP) series. ....	43
Figure 2.11. Compounds from the ChemBridge library active against <i>M. tuberculosis</i> . ....	49
Figure 2.12. Multiple protein sequence alignment of mmpL3 orthologues in different mycobacteria.....	52
Figure 2.13. Genetic organisation of the glycerol operon cluster in <i>M. smegmatis</i> and <i>M.</i> <i>tuberculosis</i> .....	53
Figure 2.14. 2D-TLC analysis of [1,2- <sup>14</sup> C]acetate-labelled lipids from wild-type and AKR334-resistant <i>M. smegmatis</i> strains in the presence of AKR334 inhibitor.....	56
Figure 2.15. Percentage of bacterial killing of <i>M. smegmatis</i> in liquid media containing varying concentrations of compound AKR539 with acetate or glycerol as the carbon source. .....	58
Figure 3.1. The role of ManLAM and PIMs in phagosome maturation arrest in mycobacteria. .....	64
Figure 3.2. Pathway of biogenesis of phosphatidyl- <i>myo</i> -inositol mannosides, lipomannan and lipoarabinomannan biosynthesis in <i>M. tuberculosis</i> .....	70
Figure 3.3. Genomic organisation of the <i>ppm1</i> locus in various mycobacteria and in <i>Corynebacterium glutamicum</i> . ....	75
Figure 3.4 Schematic representation of sequential events leading to the generation of the knockout plasmid.....	80
Figure 3.5 Schematic representation of CESTET. ....	82



Figure 3.6. Essentiality of <i>MSMEG3859</i> in <i>M. smegmatis</i> mc <sup>2</sup> 155. ....	88
Figure 3.7. 2D-TLC autoradiograph of [ <sup>14</sup> C]-labelled polar lipids from the $\Delta$ MsPpm conditional mutant .....	89
Figure 3.8. Lipoglycan profile of the $\Delta$ MsPpm conditional mutant .....	90
Figure 3.9. PPM synthase activity in membranes of the $\Delta$ MsPpm conditional mutant .....	92
Figure 3.10. Complementation of the $\Delta$ MsPpm conditional mutant.....	94
Figure 4.1. Structure of PDIMs .....	98
Figure 4.2. Pathway of phthiocerol dimycocerosates (PDIMs) biosynthesis.....	99
Figure 4.3. Colony morphology .....	110
Figure 4.4. Apolar lipid profile of the $\Delta$ pknH mutant strain.....	111
Figure 4.5. Polar lipid profile of the $\Delta$ pknH mutant strain.....	112
Figure 4.6 Apolar lipid profile 2D-TLC of the $\Delta$ pknH mutant strain .....	113
Figure 4.7. PDIMs production using propionate as carbon source.. .....	114
Figure 4.8. PDIMs region of FT-ICR mass spectra.....	116
Figure 4.9. Relative abundance of ion species corresponding to dimycocerosates A/B.....	117
Figure 4.10. Relative abundance of ion species corresponding to dimycocerosates C.....	118

## LIST OF TABLES

Table 1.1. List of slow-growing and fast-growing <i>Mycobacterium</i> species. ....	3
Table 1.2. Drugs used in the current drug regimen. ....	13
Table 2.1. Oligonucleotide primers used for PCR of various <i>M. smegmatis</i> and <i>M. tuberculosis</i> glycerol operon genes.. ....	47
Table 2.2. Minimum inhibitory concentration (MIC) values of compounds from ChemBridge library against <i>M. tuberculosis</i> and <i>M. smegmatis</i> .. ....	50
Table 2.3. Single nucleotide polymorphisms detected in <i>M. smegmatis</i> spontaneous mutants to AKR334.....	51
Table 3.1. Oligonucleotide primers used for PCR of various glycosyltransferases from <i>M. smegmatis</i> and <i>M. tuberculosis</i> . ....	79
Table 4.1. iTRAQ analysis of proteins encoded by the PDIM biosynthetic pathway in $\Delta pknH/pknH$ in presence or absence with 3 mM acidified nitric oxide.....	122
Table 6.1 PCR reaction components. ....	135
Table 6.2 Gradient PCR programme. ....	136
Table 6.3 Developing system of 2D- TLC analysis for lipid .....	141

## LIST OF ABBREVIATIONS

2D-TLC	2-Dimensional thin layer chromatography
ACN	Acetonitrile
AG	Arabinogalactan
AIDS	Acquired immunodeficiency syndrome
amu	Atomic mass unit
Ara	Arabinose
<i>Araf</i>	Arabinofuranose
AraLAM	Uncapped LAM
ATc	Anhydrotetracycline
BC	Before Christ
BCG	Bacille Calmette-Guérin
BSA	Bovine serum albumin
BTZ	Benzothiazione
CD 1	Cluster of differentiation 1
CESTET	Conditional expression specialised transduction essentiality test
CLR	C-type lectin receptor
cpm	Counts per minute
CR	Complement receptor
DAG	Diacyl glycerol
DAT	Diacyl trehalose
DC	Dendritic cells
DCM	Dichloromethane

DNA	Deoxyribonucleic acid
DNB	Dinitrobenzamides
DMSO	Dimethylsulfoxide
DOTS	Directly observed treatment short course
DPA	Decaprenyl-monophosphorylarabinose
DPM	Dolichol-monophosphomannose
DPR	Decaprenyl-monophosphorylribose
EEA1	Effector early endosome autoantigen 1
EMB	Ethambutol
ESI	Electrospray ionisation
ETH	Ethionamide
FCS	Fetal calf serum
FHA	Forkhead-associated domain
FT-ICR	Fourier transform ion cyclotron resonance
g	Grams
Gal $f$	Galactofuranose
GBq	Gigabecquerel
GlcNAc	<i>N</i> -acetylglucosamine
GMM	Glucose monomycolates
HIV	Human immunodeficiency virus
h	Hour
HTS	High-throughput screening
IL	Interleukin
INF- $\gamma$	Interferon gamma

INH	Isoniazid
Ins	Inositol
IP	Imidazo[1,2-a]pyridine
iTRAQ	Isobaric tags for related and absolute quantitation
kDa	Kilodalton
L	Litre
LAM	Lipoarabinomannan
LB	Luria-Bertani
LC-MS	Liquid chromatography-mass spectrometry
LM	Lipomannan
mAGP	Mycolyl-arabinogalactan-peptidoglycan complex
ManLAM	LAM with mannose caps
Manp	Mannopyranose
MAPK	Mitogen-activated protein kinase
MBP	Maltose binding protein
mDAP	<i>meso</i> -Diaminopimelic acid
MDR	Multi-drug resistant
mCi	Millicurie
mg	Milligram
MHC	Major histocompatibility complex
min	Minute
MIC	Minimum inhibitory concentration
mmol	Millimole
MmpL3	Mycobacterial membrane protein large 3

ml	Millilitre
MPI	Mannosyl-phosphatidyl- <i>myo</i> -inositol
MR	Mannose receptors
MS	Mass spectrometry
Mur	Muramic acid
ng	Nanogram
OADC	Oleic acid/albumin/dextrose/catalase
OD	Optical density
PAS	<i>para</i> -Aminosalicylic acid
PAT	Penta-acyl trehalose
PCR	Polymerase chain reaction
PDIM	Phthiocerol dimycoserolate
PG	Peptidoglycan
PGL	Phenolic glycolipids
PI	Phosphatidyl- <i>myo</i> -inositol
PILAM	LAM with phosphoinositide caps
PIM	Phosphatidyl- <i>myo</i> -inositol mannoside
PI3P	Phosphatidylinositol 3-phosphate
PKS	Polyketide synthase
PPD	Purified protein derivative
PPM	Polyprenol monophosphomannose
PZA	Pyrazinamide
Rha	$\alpha$ -L-Rhamnose
RIF	Rifampicin

RNA	Ribonucleic acid
rpm	Revolutions per minute
s	Second
SCFv	Single-chain antibodies
SDS-PAGE	Sodium dodecyl sulfate-polyacrylamide gel electrophoresis
SL	Sulfolipids
SNARE	Soluble NSF attachment protein receptor
SNP	Single nucleotide polymorphisms
SR	Scavenger receptor
STPK	Serine/threonine protein kinase
TAE	Tris-acetate EDTA
TAG	Triacyl glycerol
TAT	Triacyl trehalose
TB	Tuberculosis
TDM	Trehalose dimycolate
TLR	Toll-like receptor
TMM	Trehalose monomycolate
TNF- $\alpha$	Tumour necrosis factor- $\alpha$
TP	Thiophene
TSB	Tryptic soy broth
v/v	Volume per volume
w/v	Weight per volume
WHO	World Health Organization
XDR-TB	Extensive drug-resistant tuberculosis

$\mu\text{Ci}$	Microcurie
$\mu\text{g}$	Microgram
$\mu\text{l}$	Microlitre



## **PUBLISHED WORK ASSOCIATED WITH THESIS**

**Rana AK, Singh A, Gurcha SS, Cox LR, Bhatt A, Besra GS (2012).** Ppm1-encoded polyprenyl monophosphomannose synthase activity is essential for lipoglycan synthesis and survival in mycobacteria. *PLoS One*. [online], 7(10): e48211.

**Gómez-Velasco A, Bach H, Rana AK, Cox LR, Bhatt A, Besra GS, Av-Gay Y (2013).** Disruption of the serine/threonine protein kinase H affects phthiocerol dimycocerosates synthesis in *Mycobacterium tuberculosis*. *Microbiology* [online], 159 (Pt 4): 726-36.

**Jankute M, Grover S, Rana AK, Besra GS (2012).** Arabinogalactan and lipoarabinomannan biosynthesis: structure, biogenesis and their potential as drug targets. *Future Microbiol.* 7(1):129-47. Review.

# **1 General Introduction**

## 1.1 *Mycobacterium* species

*Mycobacterium* is a genus of Actinomycetales of which other genera include *Corynebacterium*, *Nocardia*, *Rhodococcus* and *Streptomyces* (Brennan and Nikaido, 1995). Mycobacteria are aerobic, rod-shaped, non-motile and non-sporulating with high guanine and cytosine content in their genomes. Although they do not retain the crystal violet stain very well using the Gram method, they are still classified as Gram-positive. All mycobacteria share a unique, thick, waxy, lipid-rich cell wall; however, their most defining feature is the presence of distinctive mycolic acids that contribute to the cell wall's hydrophobicity (Minnikin and Goodfellow, 1980; Dover *et al.*, 2004). Mycobacteria can be stained using concentrated dyes, particularly when combined with heat, but are resistant to decolourisation by dilute acid or ethanol-based procedures. This physical property is referred to as acid-fastness and can be detected using the Ziehl-Neelsen staining method (Harada *et al.*, 1976).

The species within the *Mycobacterium* genus have variable growth rates, allowing them to be divided into fast-growing mycobacteria and slow-growing mycobacteria (Table 1.1). Highly pathogenic bacteria, including *Mycobacterium tuberculosis*, the causative agent of tuberculosis (TB) and *Mycobacterium leprae*, the causative agent of leprosy, are characterised by their slow generation times. In comparison to *Escherichia coli*, which divides every 20 min, *M. tuberculosis* divides extremely slowly, every 15 to 20 hours, and colonies are not visible on plates for 4 to 6 weeks. *Mycobacterium smegmatis* is a faster-growing species, which can grow visible colonies in 3 to 5 days. This particular species of *Mycobacterium* is non-pathogenic and commonly used as a model for studying *M. tuberculosis*.

The *M. tuberculosis* complex is a group of closely related *Mycobacterium* species which have up to 99% similarity at the DNA level (Brosch *et al.*, 2002). Species include *M. tuberculosis*, *Mycobacterium bovis*, “*Mycobacterium canettii*” and *Mycobacterium africanum*.

Table 1.1. List of slow-growing and fast-growing *Mycobacterium* species.

Slow-growing mycobacteria	Fast-growing mycobacteria
<u><i>M. tuberculosis</i> complex</u> <ul style="list-style-type: none"> <li>• <i>M. tuberculosis</i></li> <li>• <i>M. bovis</i></li> <li>• <i>M. africanum</i></li> <li>• <i>M. canetti</i></li> <li>• <i>M. microti</i></li> </ul>	<u><i>M. chelonae</i> clade</u> <ul style="list-style-type: none"> <li>• <i>M. abscessus</i></li> <li>• <i>M. chelonae</i></li> <li>• <i>M. bolleti</i></li> </ul>
<u><i>M. avium</i> complex</u> <ul style="list-style-type: none"> <li>• <i>M. avium</i></li> <li>• <i>M. kansasii</i></li> <li>• <i>M. ulcerans</i></li> </ul>	<u><i>M. vaccae</i> clade</u> <ul style="list-style-type: none"> <li>• <i>M. faurum</i></li> <li>• <i>M. vaccae</i></li> </ul>
<u><i>M. kansasii</i> clade</u> <ul style="list-style-type: none"> <li>• <i>M. gastri</i></li> <li>• <i>M. kansasii</i></li> </ul>	<u>Ungrouped</u> <ul style="list-style-type: none"> <li>• <i>M. phei</i></li> <li>• <i>M. smegmatis</i></li> </ul>

## 1.2 History of tuberculosis

Tuberculosis (TB) is a major cause of death worldwide and has been since ancient times. The aetiological agent of TB, *M. tuberculosis* is hypothesised to have originated approximately 150 million years ago (Hayman, 1984; Daniel, 2006). Due to the low mutation rate of *M. tuberculosis*, estimations into its time of origin have concluded that early predecessor strains existed 3 million years ago in East Africa where early hominids would have been infected (Gutierrez *et al.*, 2005). Present

strains of *M. tuberculosis*, which are responsible for the majority of TB cases worldwide, are the result of an evolutionary bottleneck around 20,000 years ago (Kapur *et al.*, 1994; Brosch *et al.*, 2002; Gutierrez *et al.*, 2005). All modern members of the *M. tuberculosis* complex, including *M. africanum*, "*M. canetti*" and *M. bovis*, are derived from a common ancestor (Daniel, 2006; Supply *et al.*, 2013). The migrant human population from East Africa may have carried their diseases, including TB, to other parts of the world. Archaeological evidence of early TB has been identified using molecular and paleomicrobiological studies in Egyptian mummies dating from 3000-2400 BC (Zink *et al.*, 2001) and more recently in a 9000 year old mummy from a Neolithic settlement in the Eastern Mediterranean using PCR techniques and lipid biomarkers analysis (Hershkovitz *et al.*, 2008).

TB was first documented as the term phthisis (also known as consumption) by the ancient Greek physician Hippocrates in 460 BC who identified symptoms of chest pain and coughing, frequently with blood in the sputum amongst young adults with the disease (Coar, 1982; Daniel, 2006). Although Hippocrates recognised its prevalence and cause of fatality, at the time, it was thought of as a hereditary disease until Aristotle described it as being infectious. However, it was the renowned Greek physician Clarissimus Galen who first described phthisis as an ulceration of the lungs, accompanied by a cough, fever, and wasting away of the body (Pease, 1940). Over the following centuries, documentation of TB became sparse, that is until the 17<sup>th</sup> Century, when TB epidemics across Europe became the main cause of death and were known as the "Great White Plague". During this time, physician René Laennec, known for inventing the stethoscope, studied the pathogenesis of TB and

described the pathology of the infection as being either pulmonary or extrapulmonary (Daniel, 2004). However, the major turning point in TB research came in 1882 when Robert Koch discovered that the tubercle bacillus was the cause of the disease, work for which he was awarded a Nobel Prize in 1905 (Koch, 1932). This significant discovery proved to be key to developing new, effective therapies for treating TB. Koch attempted to develop a cure for TB by producing tuberculin, a glycerine extract of tubercle bacilli. Although tuberculin proved to be ineffective as a cure, it was later utilised by Clemens von Pirquet as a diagnostic agent for TB and eventually a purified protein derivative (PPD) was developed into the tuberculin skin test which is still used today (Daniel, 2006).

Whilst the scientific community was advancing its knowledge of TB through the discovery of tubercle bacillus as its cause, this coincided with a decrease in the mortality rates of TB patients during the mid-19<sup>th</sup> Century despite the absence of antibiotics at that time (Wilson, 1990). Although the exact cause for this reduction is unknown, it could have been aided by the idea that a regimen of rest and good nutrition was effective in treating the disease. This idea was popularised by Herman Brehmer through the formation of institutions, such as the sanatoria created in 1859, where TB patients were able to recuperate in isolation, thereby preventing the transmission of the infection (Cox, 1923; Daniel, 2006).

In an attempt to treat the diseased lungs of patients, pulmonary collapse therapy (artificial pneumothorax) and thoracoplasty procedures were employed to force compression of the lung cavities by inserting air through the pleural space (Singer,

1936). These invasive techniques, popular during the 20<sup>th</sup> Century, were used to allow the lung to heal from lesions; however, there are many risks and complications associated with these operations including tissue infection and empyema, which has discouraged the continued use of these treatments (Heaton, 1936).

The development of the BCG (Bacille Calmette-Guérin) vaccine was the first successful immunisation approach to tackling TB. The idea of vaccines was pioneered by Edward Jenner who discovered that healthy individuals could be immunised against smallpox using the pus from the hand of a milkmaid infected with cowpox (Riedel, 2005). Albert Calmette and Camille Guérin, taking inspiration from Jenner's work, produced an attenuated strain of *M. bovis*, the causative agent of bovine TB, which proved to be an effective vaccine against TB particularly when given at an early age (Sakula, 1983; Daniel, 2005). Although there is much debate concerning how the efficacy of this vaccination strategy varies according to geographical location, BCG remains the only available vaccine against TB (Fine, 1995).

### **1.3 Immune response to tuberculosis**

*M. tuberculosis* are carried in droplet nuclei particles, which can remain in the atmosphere for several hours after exhalation by an active TB sufferer. Transmission occurs when these infectious droplets are inhaled into the respiratory tract, where the majority of the bacilli become trapped in the upper airways. If the bacteria reach the lungs, they are phagocytosed by alveolar macrophages. This phagocytosis process is mediated by the expression of several host receptors including complement

receptors (CR1 and CR2), C-type lectin receptors (CLRs) and scavenger receptors (SRs) (Philips and Ernst, 2012). Bacteria contained within the phagosomes can be killed by several mechanisms including fusing with lysosomes to form a phagolysosome, and through the production of reactive oxygen and nitrogen intermediates, resulting in necrosis or apoptosis (Russell, 2001). However, from this point, *M. tuberculosis* has the ability to avoid the normal sequence of events by inhibiting the maturation process of the phagosome, by limiting acidification to pH 6.4 and blocking fusion with lysosomes (Houben *et al.*, 2006; Deretic *et al.*, 2006). This evasion process can be overcome when antigen-specific T-lymphocytes are recruited to the macrophage and further stimulate it to inhibit the growth of, or kill, mycobacteria, a response modulated by the secretion of interferon- $\gamma$  (IFN- $\gamma$ ) (Schluger and Rom, 1998).

In the majority of cases, *M. tuberculosis* infection follows a cascade of events which enables the pathogen to survive in a dormant state within host cells through granuloma formation, a characteristic feature of TB (Figure 1.1). Bacterial uptake by alveolar macrophages induces a robust proinflammatory response, which drives the recruitment of mononuclear cells from blood vessels (Russell, 2007). Lymphocytes migrate to the site of infection and begin the formation of the granuloma which comprises a core of infected macrophages, surrounded by foamy macrophages and an external layer of lymphocytes further stratified by extracellular components (Russell, 2007). This host response forms the 'containment' phase of the infection as the granuloma is usually sufficient to limit replication and keep the primary infection enclosed, preventing it from advancing to the active state. However, a subsequent



defect in cell-mediated immunity, for example by co-infection with HIV, malnutrition or old age (Russell, 2007), can lead to the failure of this containment of the infection. In this event, the granuloma can rupture to allow the release of infectious bacilli into the airways, causing reactivation of the disease.

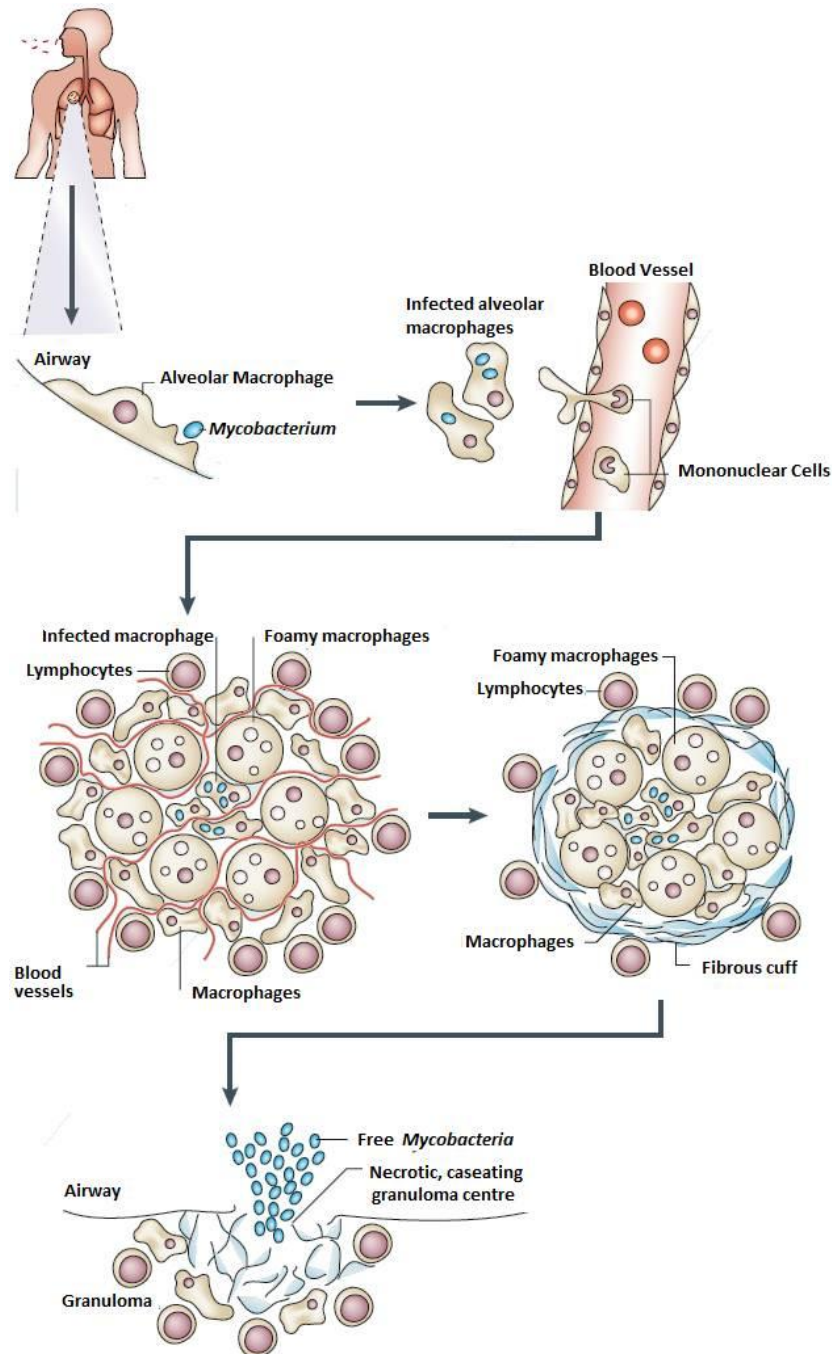


**Figure 1.1. Schematic representation of granuloma formation in humans. (Russell, 2007).**

#### 1.4 Epidemiology of tuberculosis

The steady decline of TB mortality, which began in the mid-19<sup>th</sup> Century, continued into the 20<sup>th</sup> Century due to improved healthcare provisions, BCG vaccination programmes and the development of antibiotic therapies, giving hope that the disease might be eradicated (Lienhardt *et al.*, 2012). However, a resurgence of the disease during the 1990s was aggravated by several factors, including the emergence of the HIV/AIDS pandemic and drug-resistant *M. tuberculosis* strains, and forced the World Health Organisation (WHO) to declare TB a global health emergency.

WHO estimates that a third of the world's population is currently latently infected with *M. tuberculosis*. In 2011, there were 8.7 million new cases of TB and 1.4 million deaths from TB (WHO, 2012). Heavily populated countries of Asia, including India, China, Indonesia, Bangladesh and Pakistan, together contribute to half of all new cases (Dye, 2006); however, the highest incidence of TB cases is in the Sub-Saharan region of Africa, which has been particularly impacted by the HIV/AIDS pandemic (Figures 1.2 & 1.3) (Nunn *et al.*, 2005). HIV infection has rapidly become a significant risk factor for TB as the suppression of the immune system can increase the annual risk of reactivating latent *M. tuberculosis* by 5-15% (Nunn *et al.*, 2005). In Eastern European countries, particularly those of the former Soviet Union, a rise in the incidence of TB cases has been associated with socio-economic changes and a decline of an appropriate healthcare system, leading to problems involving drug resistance (Frieden *et al.*, 2003). Overall, the recent increase in global TB cases is

largely a consequence of HIV infection and the emergence of multi-drug resistant (MDR-TB) strains.



**Figure 1.2. Map showing estimated TB incidence rates in the year 2011. (WHO, 2012).**



**Figure 1.3. Map showing estimated HIV prevalence in TB cases in the year 2011. (WHO, 2012)**

## 1.5 Treatment

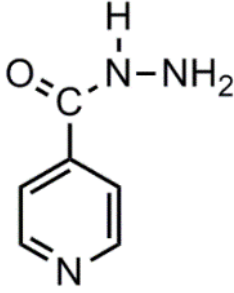
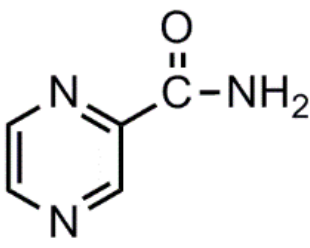
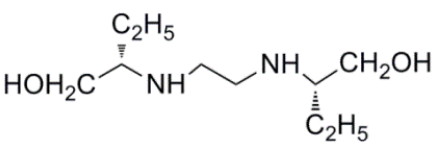
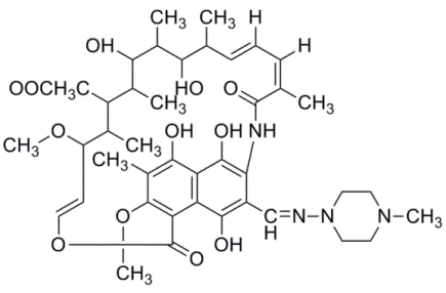
### 1.5.1 Anti-tuberculosis drugs

The discovery of streptomycin, isolated from *Streptomyces griseus* in the 1940s by Albert Schatz and Selman Waksman, as the first effective antibiotic against *M. tuberculosis*, initiated the beginning of anti-tuberculosis chemotherapy (Schatz *et al.*, 2005). Streptomycin became the first drug available for the treatment of TB until evidence of acquired resistance reduced its efficacy against inhibition of the tubercle bacillus, possibly due to administration as a single drug therapy (Wolinsky *et al.*, 1948). Post this discovery, it became evident that the use of multiple drugs in the treatment of TB was necessary to limit the generation of drug-resistant strains. In 1946, Jorgen Lehmann found that *para*-aminosalicylic acid (PAS) stimulates oxygen depletion in the tubercle bacillus (Bernheim, 1940) and PAS became another effective drug against TB (Lehmann, 1946).

A major breakthrough in TB chemotherapy came in 1952 with the introduction of isoniazid (INH), a highly active drug with no substantial side effects, which displayed a high specificity for the tubercle bacillus (Y Zhang, 2003). The 1950s and 1960s are considered to be the golden era of anti-TB drug discovery as many prominent antibiotics were developed during this time including pyrazinamide (PZA) (Malone *et al.*, 1952), ethionamide (ETH) (Liebermann *et al.*, 1956), ethambutol (EMB) (J P Thomas *et al.*, 1961), cycloserine (Kurosawa, 1952) and rifampicin (RIF) (Maggi *et al.*, 1966).

The current drug regimen administered to TB patients consists of a six-month therapy divided into two phases: an initial intensive phase for the first two months followed by a continuation phase for the remaining four months (WHO, 2012). The initial two-month intensive phase aims to kill actively growing and semi-dormant bacilli through the employment of the first-line anti-TB drugs INH, EMB, PZA and RIF (Table 1.2). These drugs can be further allocated into two groups: bactericidal drugs, which include INH and RIF, and bacteriostatic, which include EMB and PAS. In the first two weeks of treatment, INH is responsible for killing the large numbers of actively replicating bacilli. RIF and PZA kill the less active bacilli in the following weeks and rifampicin largely eliminates the remaining dormant bacilli in the continuation phase. Although the initial two-month therapy is sufficient to eliminate the tubercle bacilli, the follow-up continuation phase is vital to eliminate any remaining bacilli and is necessary to diminish the risk of failure of the treatment programme or relapse of the infection. In this second phase, INH and RIF are taken for a further four months (Maartens and Wilkinson, 2007).

Table 1.2. Drugs used in the current drug regimen.

Drug	MIC (µg/µl)	Mechanism of action	Important genes
<b>isoniazid (INH)</b> 	0.01 – 0.2	Inhibition of mycolic acid synthesis	<i>katG</i> <i>inhA</i>
<b>pyrazinamide (PZA)</b> 	20-100	Acidification of cytoplasm & decrease membrane potential	<i>pncA</i>
<b>ethambutol (EMB)</b> 	1-5	Inhibition of arabinogalactan & lipoarabinomannan synthesis	<i>embCAB</i>
<b>rifampicin (RIF)</b> 	0.05-2.5	Inhibition of RNA synthesis	<i>rpoB</i>

INH is a prodrug and is activated by a catalase-peroxidase enzyme (KatG), which is present in *M. tuberculosis* (Figure 1.4) (Zhang *et al.*, 1992). The primary mode of action of INH is to inhibit the synthesis of mycolic acids, which are vital components of the mycobacterial cell wall, by targeting the enoyl-ACP reductase (InhA) (Winder and Collins, 1970; Banerjee *et al.*, 1994). The specific mechanism of action involves coupling the isonicotinic acyl radical with NAD to form a complex which binds tightly to InhA, preventing the formation of mycolic acids (Rozwarski *et al.*, 1998).

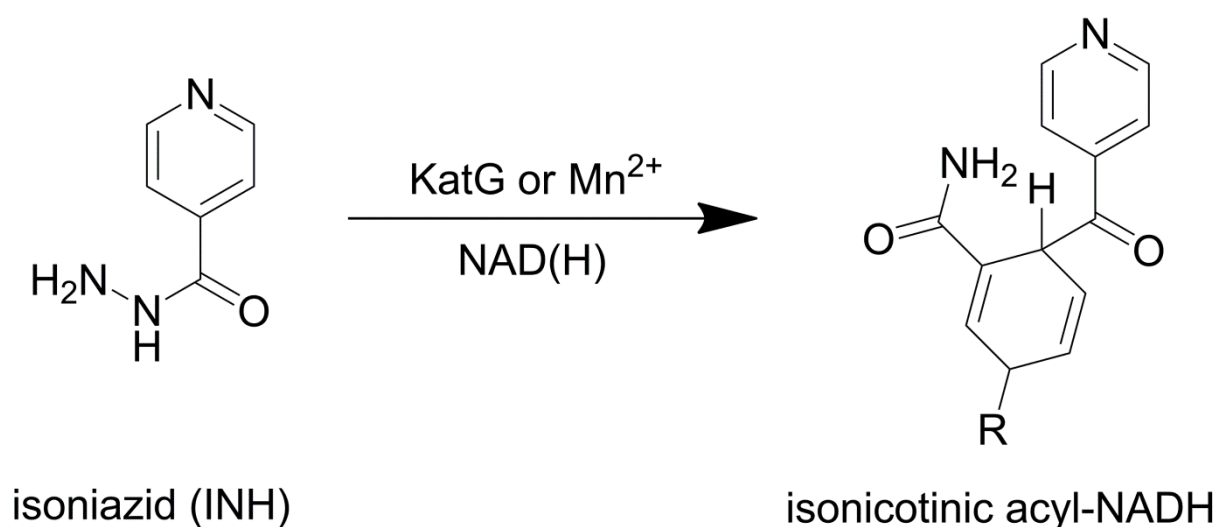


**Figure 1.4. Activation of the prodrug isoniazid (INH) to form isonicotinic acyl-NADH (Rozwarski *et al.*, 1998).**

PZA is also a prodrug and is converted into its active form, pyrazinoic acid, by a nicotinamidase encoded by *pncA* (Figure 1.5) (Zhang *et al.*, 2003). Pyrazinoic acid leads to acidification of the cytoplasm and decreasing membrane potential, which is required for membrane transport (Ying Zhang, Wade, *et al.*, 2003). EMB has been found to target the *embCAB* genes, which encode the arabinosyltransferase responsible for arabinan synthesis (Belanger *et al.*, 1996; Telenti *et al.*, 1997); therefore EMB inhibits the biosynthesis of arabinogalactan (AG) and

lipoarabinomannan (LAM) (Mikusová *et al.*, 1995). RIF targets nucleic acid synthesis by binding to the  $\beta$ -subunit of the DNA-dependent RNA polymerase encoded by *rpoB* (Blanchard, 1996).

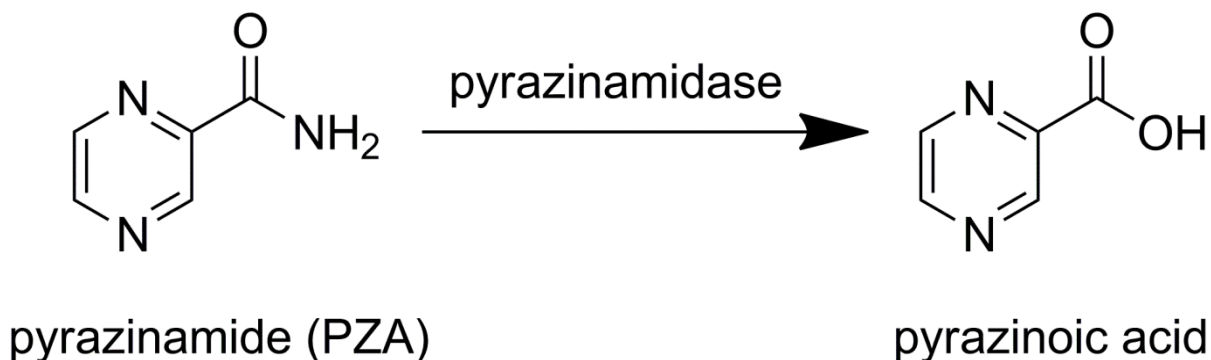


Figure 1.5. Conversion of pyrazinamide (PZA) to pyrazinoic acid (Zhang *et al.*, 2003).

### 1.5.2 Directly Observed Treatment – Short Course

Despite the best efforts to control TB, the multidrug regimen has not been successful in eradicating TB due to the emergence of drug resistance. A major reason for this is that not all patients complete the full treatment as its duration is deemed too long and burdensome to comply with (Zhang, 2005). WHO has recommended the use of the Directly Observed Treatment Short course (DOTS) as an effective method of controlling the transmission of TB and ensuring that patients adhere to the full treatment (WHO, 2012). DOTS therapy is composed of five points: political commitment, use of sputum smear microscopy in case detection, directly observed treatment for at least the first two months, efficient drug supply and monitoring of results (Maartens and Wilkinson, 2007; WHO, 2012). DOTS therapy involves a trained observer being present to monitor patients while taking each dose of medication. This system has successfully been used to obtain high rates of treatment completion, reduce the development of acquired drug resistance and prevent relapse



of infection (Frieden *et al.*, 2003). The DOTS-plus variant, which includes drug-susceptibility testing and availability of second-line drugs, was introduced in 1998 in an attempt to treat drug-resistant TB cases (Mukherjee *et al.*, 2004). In addition to this, WHO has established a new six-point Stop TB Strategy, which aims to build on the success of DOTS and raise awareness of the rising incidence of drug-resistant TB strains (Raviglione and Uplekar, 2006; WHO, 2012).

### 1.5.3 Drug resistance

Multidrug-resistant TB (MDR-TB) is caused by those TB strains that are resistant to both INH and RIF, which are two of the first-line drugs in TB treatment. Extensively drug-resistant TB (XDR-TB) is caused by those strains that are resistant to both INH and RIF, in addition to fluoroquinolones and at least one injectable second-line drug such as capreomycin, amikacin and kanamycin (Maartens and Wilkinson, 2007). TB drug resistance continues to increase: the estimated number of cases worldwide was expected to be 630,000 for MDR-TB and 40,000 for XDR-TB in 2011 (WHO, 2012).

Drug resistance can emerge by three interconnected mechanisms: i) acquired resistance, which involves the conversion of wild-type strains to drug-resistant strains; ii) amplified resistance, which occurs due to inappropriate chemotherapy; and iii) transmitted resistance, which involves the transmission of drug-resistant cases (Jassal and Bishai, 2009; Da Silva *et al.*, 2011). Although acquired and amplified resistance are the principal mechanisms by which drug resistance is produced, transmission resistance accounts largely for the recent rise in XDR-TB cases (Jassal and Bishai, 2009).

At present, it is very difficult to treat cases of MDR-TB and XDR-TB as the bacilli are resistant to the drugs commonly used in the standard regimen. Patients with drug-resistant TB are therefore currently treated with at least three drugs that the organism is fully susceptible to and which need to be taken for typically a minimum duration of 18 to 24 months (Frieden *et al.*, 2003; Jassal and Bishai, 2009). However, these reserve drugs are less efficient in eliminating the infection, more toxic than standard drugs and need to be taken daily or even several times a day (Frieden *et al.*, 2003). As a result, greater morbidity and mortality is associated with XDR-TB compared to TB cases with no drug resistance (Jassal and Bishai, 2009).

## 1.6 Mycobacterial cell wall

The cell wall of *M. tuberculosis* consists of a lipid-rich, hydrophobic barrier, which is responsible for its acid-fastness and hydrophobic properties (Kaur *et al.*, 2007). The complexity of the cell wall also makes it difficult for antibiotics to enter the bacterium (Minnikin *et al.*, 2002). The cell-wall structure is comprised of a mycolyl-arabinogalactan-peptidoglycan (mAGP) complex, consisting of a peptidoglycan (PG) layer that is covalently attached to arabinogalactan (AG), which is further esterified to complex lipids known as mycolic acids. Non-covalently linked biosynthetically related glycolipids and lipoglycans, including phosphatidyl-*myo*-inositol mannosides (PIMs), lipomannan (LM) and lipoarabinomannan (LAM) are also embedded in the cell wall (Figure 1.6) (Brennan, 2003). Mycolic acids are  $\alpha$ -alkyl  $\beta$ -hydroxylated fatty acids composed of 60 to 90 carbon residues and form part of the hydrophobic external layer of the cell wall (Chatterjee *et al.*, 1993). The outer membrane segment is further

decorated with solvent-extractable lipids, including dimycolyltrehalose (TDM), phthiocerol dimycocerosates (PDIM), phenolic glycolipids (PGL) and sulfolipids (SL).

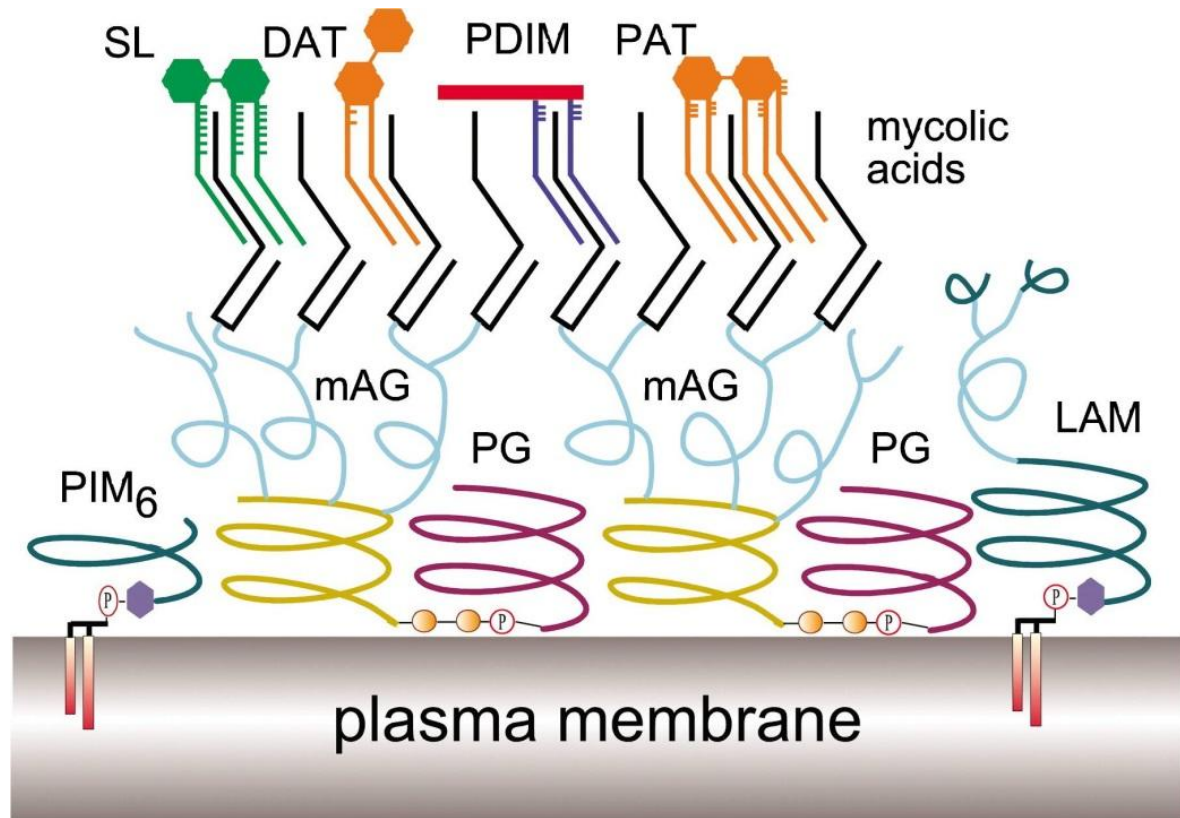


**Figure 1.6. Representation of the *M. tuberculosis* cell wall.** The cell-wall structure consists of a peptidoglycan layer covalently attached to arabinogalactan, which is further esterified to mycolic acids. Non-covalently linked biosynthetically related glycolipids, including PIMs, LM and LAM are embedded in the cell wall. The outer membrane is further decorated with solvent-extractable lipids. AG, Arabinogalactan; DAT, Diacyl trehalose; LAM, Lipoarabinomannan; mAG, mycolyl arabinogalactan; PAT, Penta-acyl Trehalose; PDIM, Phthiocerol dimycocerosate; PG, Peptidoglycan; PIM<sub>6</sub>, Phosphatidylinositol hexamannoside. Adapted from Minnikin *et al.*, 2002.

### 1.6.1 Peptidoglycan (PG)

The PG layer forms the backbone of the mAGP complex, forming a rigid layer external to the plasma membrane to provide cellular shape and resistance to osmotic pressure. Categorized as A1 $\gamma$  in accordance with the Schleifer and Kandler

classification system (Schleifer and Kandler, 1972), the structure of mycobacterial PG shares similarity with other Gram-negative bacteria, including *E. coli* and *Bacillus* species (Figure 1.7). However, the PG *M. tuberculosis* and *M. smegmatis* is distinct from that found in other species as it is composed of linear chains of repeating  $\beta(1\rightarrow4)$ -*N*-acetylglucosamine (GlcNAc) and *N*-glycolyl muramic acid (Mur) residues, where the *N*-acetyl group is oxidised to *N*-glycolyl (Azuma *et al.*, 1970; Mahapatra *et al.*, 2005). Tetrapeptide side chains consisting of L/D-alanine, D-isoglutamine and *meso*-diaminopimelic acid (mDAP) components are attached to Mur components, which are cross-linked to AG (Wietzerbin *et al.*, 1974; Lederer *et al.*, 1975). The peptide chains are more heavily cross-linked in mycobacteria at 70-80% than in other species, such as *E. coli*, where cross-linking between peptides is around 50% (Vollmer and Holtje, 2004). This increased cross-linking adds to the structural integrity of the bacterium. While two-thirds of the cross-links are formed between the carboxyl group of a terminal D-alanine and the amino group of DAP, commonly found in most bacterial species, one-third of the peptide links occurs between two DAP residues in mycobacterial PG (Wietzerbin *et al.*, 1974). In addition, PG is connected to the galactan domain of AG *via* a 'linker unit', whereby the carbon-6 position of Mur residues forms a phosphodiester bond with the carbon-1 position of GlcNAc, which is (1 $\rightarrow$ 3) linked to an  $\alpha$ -L-rhamnose (Rha) residue (McNeil *et al.*, 1991). Although the synthesis of *M. tuberculosis* PG is poorly understood, the process is considered to be similar to the *E. coli* PG biosynthetic pathway (van Heijenoort, 2001).

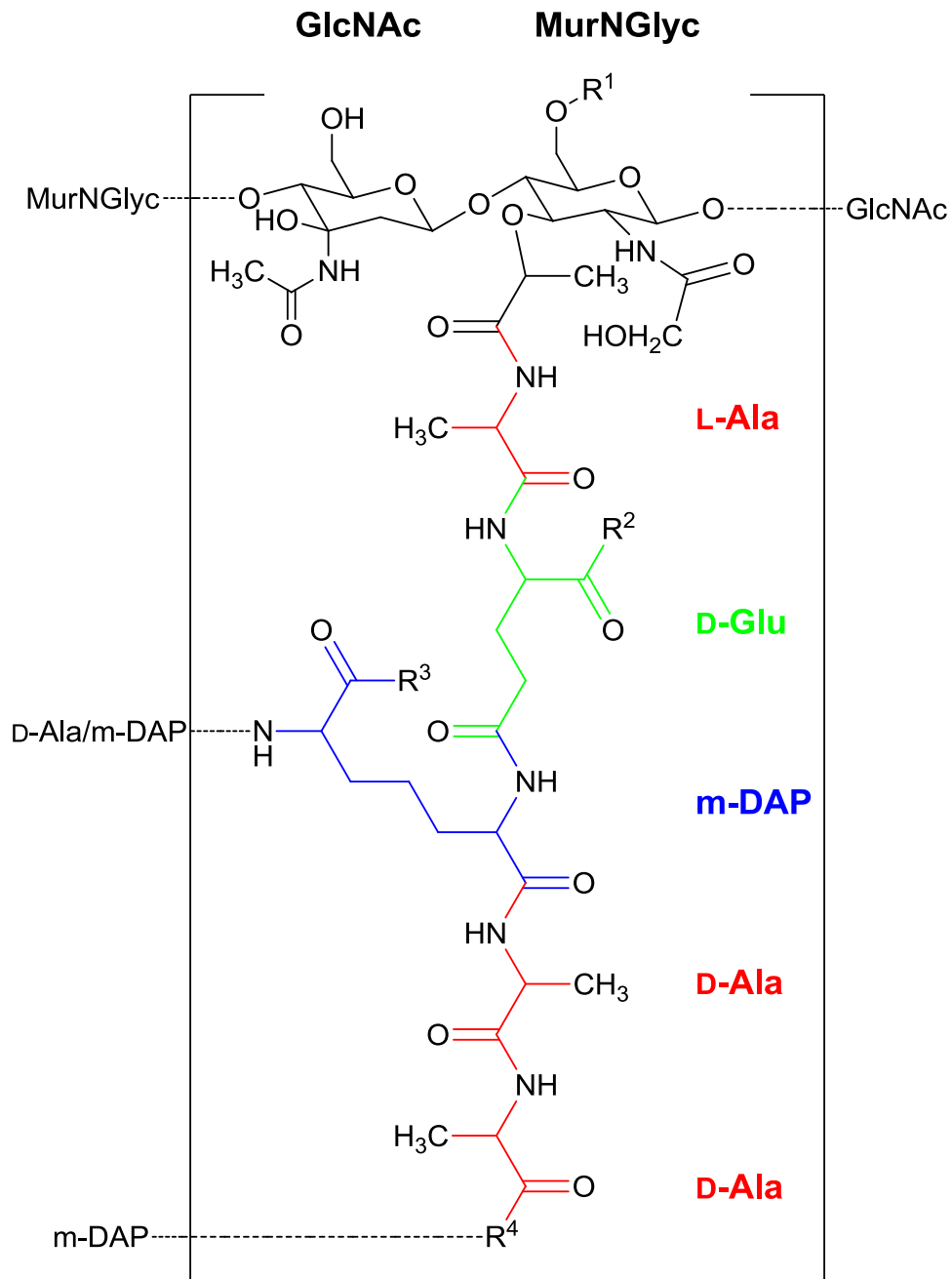


**Figure 1.7. Structure of *M. tuberculosis* peptidoglycan.** Broken lines designate cross-links to arabinogalactan or to the sugar and peptide stems of neighbouring monomeric units. R<sup>1</sup>, H or the linker unit of AG; R<sup>2</sup>, OH, NH<sub>2</sub> or glycine; R<sup>3</sup>, OH or NH<sub>2</sub>; R<sup>4</sup>, OH or amidated cross-link to m-DAP. Ala, Alanine; Glu, Glutamate; GlcNAc, N-acetylglucosamine; mDAP, meso-diaminopimelic acid; MurNGlyc, N-glycolyl muramic acid.

### 1.6.2 Arabinogalactan (AG)

AG forms a major part of the *M. tuberculosis* cell wall, accounting for approximately 35% of the overall mycobacterial mass. This unique polysaccharide is predominantly composed of arabinose (Ara) and galactose (Gal) residues, which are both present in their furanose ring form as arabinofuranose (Araf) and galactofuranose (Gal<sub>f</sub>) (Figure 1.8) (McNeil *et al.*, 1987).

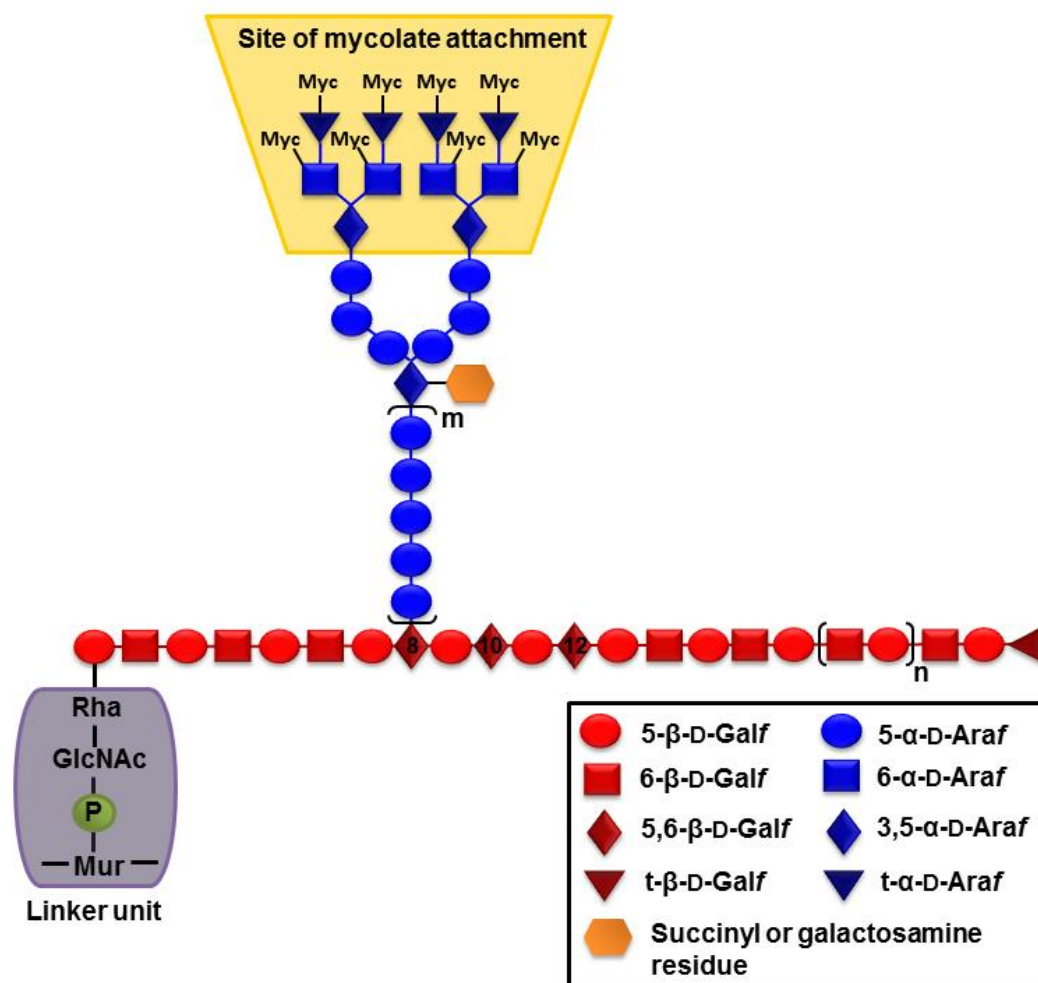


**Figure 1.8. Structure of arabinogalactan in *M. tuberculosis*.** The galactan component, composed of 30 Gal<sub>f</sub> residues, is attached to the peptidoglycan *via* a phosphodiester linker unit. Three arabinan chains are connected to the galactan strand *via* attachment to positions 8, 10 and 12 (Alderwick *et al.*, 2006). The branched arabinan structure is covalently attached to mycolic acids through a distinct hexa-arabinofuranosyl (Ara<sub>6</sub>) motif. A succinyl (Bhamidi *et al.*, 2008) or galactosamine (Lee *et al.*, 2006) residue is attached to the 3,5-α-D-Araf units. Araf, Arabinofuranose; Gal<sub>f</sub>, Galactofuranose; GlcNAc, β(1→4)-N-acetylglucosamine; Myc, Mycolic acid; Mur, Muramic acid; Rha, α-L-rhamnose. Adapted from Jankute *et al.*, (2012).

As described previously, PG is covalently attached through a phosphodiester linker unit to the galactan component reducing end of AG, whereas mycolic acids are linked to the non-reducing end of AG which is composed of the Ara residues (Nikaido *et al.*, 1993). The lack of repeating units of sugar residues makes the structure of mycobacterial AG dissimilar to other bacterial species; however, its structure consists of several distinct structural motifs (Daffé *et al.*, 1990). The galactan region of AG is composed of a linear chain of 30 units of alternating 5- and 6-linked  $\beta$ -D-Galf residues. The highly branched arabinan chains, each containing approximately 30 Araf residues, are attached to the carbon-5 position of some 6-linked Galf residues (Daffé *et al.*, 1990); three arabinan chains can be linked to one galactan strand *via* attachment to the 8<sup>th</sup>, 10<sup>th</sup> and 12<sup>th</sup> galactosyl residues (Alderwick *et al.*, 2006). These arabinan chains are mostly comprised of 5-linked  $\alpha$ -D-Araf residues where branching is introduced at the carbon-3 hydroxyl position to form 3,5- $\alpha$ -D-Araf residues (Daffé *et al.*, 1990). The arabinan structure at the non-reducing termini of AG consists of a characteristic hexa-arabinofuranosyl (Ara<sub>6</sub>) motif [ $\beta$ -D-Araf-(1 $\rightarrow$ 2)- $\alpha$ -D-Araf]<sub>2</sub>-3,5- $\alpha$ -D-Araf-(1 $\rightarrow$ 5)- $\alpha$ -D-Araf, where mycolic acids are located in clusters of four attached to the position 5 of the  $\beta$ -D-Araf unit and the penultimate 2- $\alpha$ -D-Araf residue (McNeil *et al.*, 1991); however only two-thirds of these motifs are mycolated (McNeil *et al.*, 1991). The attachment of a succinyl ester (Bhamidi *et al.*, 2008) or galactosamine residue (Lee *et al.*, 2006) to the inner 3,5- $\alpha$ -D-Araf units completes the AG structure.

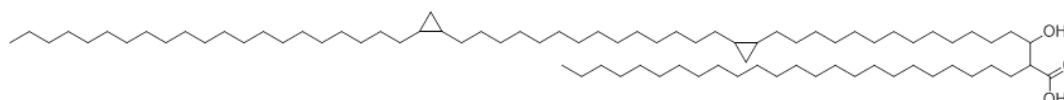
### 1.6.3 Mycolic acids

Mycolic acids are a major component of mycobacteria, accounting for approximately 60% of the dry mass of the bacterium. They are predominantly esterified to AG and present as solvent-extractable free lipids such as trehalose monomycolates (TMM), trehalose dimycolates (TDM) and glucose monomycolates (GMM) (Minnikin *et al.*, 2002). In mycobacteria, mycolic acids are composed of 70-90 carbon residues and as such, are the largest amongst the bacteria (Goodfellow and Minnikin, 1981). Mycolic acids are very hydrophobic  $\alpha$ -alkyl branched,  $\beta$ -hydroxylated fatty acids. They consist of a meromycolate moiety with carbon chain lengths of up to C<sub>56</sub>, and long saturated  $\alpha$ -branch ranges from C<sub>20</sub> to C<sub>24</sub> in length and possess at least two stereogenic centres at the positions  $\alpha$  and  $\beta$  to the carboxylic acid (Brennan and Nikaido, 1995). Although the generic mycolate structure is well conserved, various classes of mycolic acids can be defined by the presence of modifications at two mid-chain positions with functional groups in *M. tuberculosis* including *cis* and *trans* cyclopropane rings, *cis* and *trans* double bonds and keto-, methoxy-, epoxy- and wax-ester functionality (Barry *et al.*, 1998). The key mycolic acid structures found in *M. tuberculosis* are classified into three groups:  $\alpha$ -mycolates, keto-mycolates and methoxy-mycolates (Figure 1.9) (Minnikin *et al.*, 1982; Minnikin *et al.*, 2002; Watanabe *et al.*, 2002). The most abundant type of mycolic acid containing no oxygen functional groups at the proximal or distal positions of the meromycolate chain and two *cis* cyclopropane rings are known as  $\alpha$ -mycolates (Minnikin *et al.*, 1982; Minnikin *et al.*, 2002; Watanabe *et al.*, 2002). Keto-mycolates and methoxy-mycolates are oxygenated species comprising of one *cis* cyclopropane ring or one *trans* cyclopropane ring with and adjacent methyl branch, respectively.

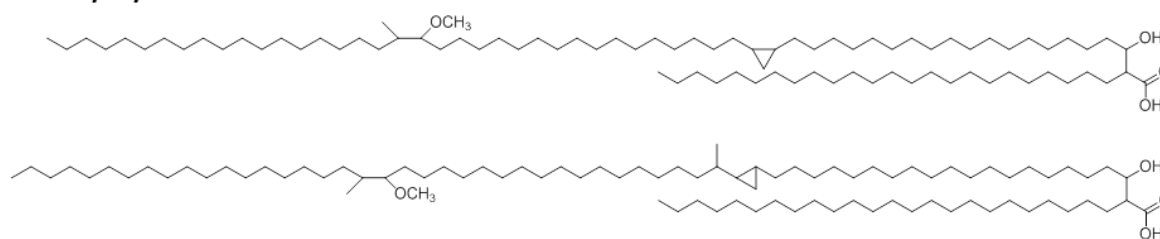


Mycolic acid biosynthesis is vital for the survival and pathogenesis of *M. tuberculosis*. The presence of mycolic acids in the cell wall of *M. tuberculosis* gives rise to important characteristics including increased resistance to chemical damage and dehydration, low permeability to hydrophobic antibiotics all of which allow persistence of the bacterium within the host. Specific modifications of the mycolic acid structures are possibly linked to these unique characteristics. For example, the incorporation of cyclopropane residues in the chain contributes to the structural integrity of the cell wall structure (George *et al.*, 1995) and is also reportedly essential for cord formation in mycobacteria (Glickman *et al.*, 2001). In addition, a *cis*-cyclopropane modification allows the bacterium to grow readily inside macrophages, effectively hiding it from the host's immune system (Rao *et al.*, 2005) whereas the *trans*-cyclopropane modification causes suppressive effects on *M. tuberculosis*-induced inflammation and virulence (Rao *et al.*, 2006).

#### $\alpha$ -mycolates



#### methoxy-mycolates



#### keto-mycolates

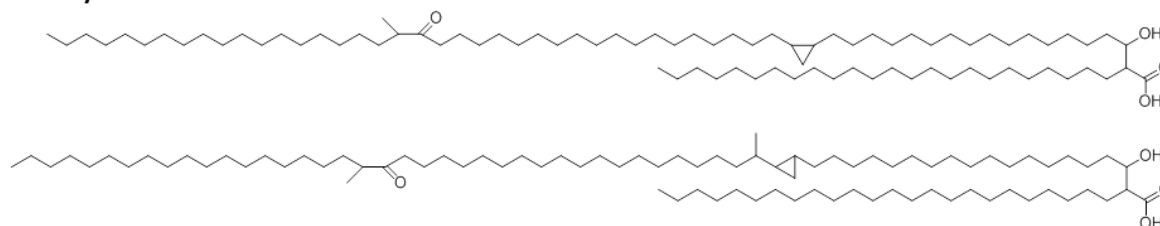


**Figure 1.9. Structure of mycolic acids found in *M. tuberculosis*.**

#### 1.6.4 Solvent-extractable free lipids

As previously mentioned, the outer part of the membrane is intercalated with various solvent-extractable 'free' lipids such as cord factor or TDM, PDIM, PGL and SL. These complex lipids are attached to the mAGP complex through hydrophobic interactions and some are specific to mycobacteria.

#### 1.6.5 Trehalose dimycolate (TDM) and trehalose monomycolate (TMM)

Of the many glycosylated forms of mycolic acids, present in the outer layer of the mycobacterial cell envelope, the most widely studied is trehalose-6,6' dimycolate (TDM), also known as 'cord factor' due to the characteristic cord-like structure of *M. tuberculosis* strains (Figure 1.10). Virulent *M. tuberculosis* strains subjected to petroleum ether extractions, which removes these lipids, have been shown to remain viable; however, they displayed a loss of virulence and were unable to form cord-like structures (Bloch, 1950). Non-virulent bacilli adsorbed with TDMs were able to inhibit leukocyte migration, which is only observed in virulent bacilli (Noll *et al.*, 1956) and administration in small doses was toxic to laboratory animals (Bloch, 1950). TDM molecules comprise a trehalose sugar acylated with two mycolic acid residues. Trehalose monomycolate (TMM) possesses a single mycolate residue and is transported across the cell membrane for TDM biosynthesis or to form part of the mycolic acids that are esterified to the AG complex (Belisle, 1997). TDM is the most abundant of the non-covalently bound, surface-exposed lipids and is a virulence factor in mycobacteria. It is involved in many important immunological interactions such as the recruitment of cells for granuloma formation (Hunter *et al.*, 2006) and in modulating the expression and production of cytokines (Lima *et al.*, 2001).

Macrophages have been represented as a major target of the immune-stimulating effects of TDM; they possibly aid the entry of bacilli to inactivate macrophages (Porcelli and Besra, 2002). Besides, TDM shows diverse immunological activities including adjuvant and anti-tumour properties (Silva *et al.*, 1985).

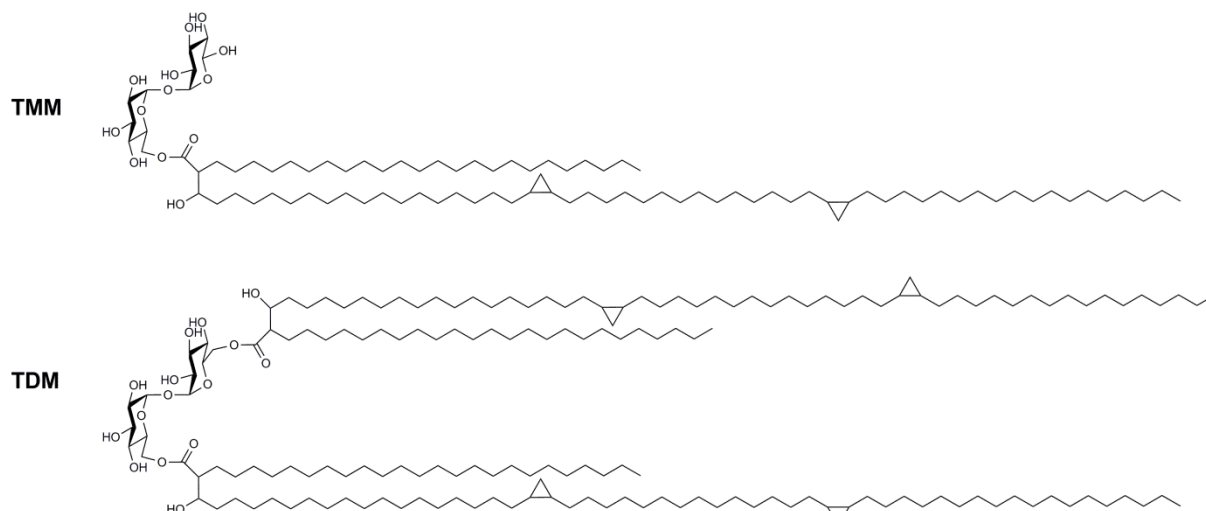


**Figure 1.10. Structure of and trehalose monomycolate (TMM) and trehalose dimycolate (TDM).**

### 1.6.6 Sulfolipids (SL)

Sulfolipids (SLs) are a class of glycolipids found in virulent *M. tuberculosis* strains. They are composed of a trehalose 2-sulfate core, which is acylated with four fatty acyl substituents (Figure 1.11) (Goren *et al.*, 1976). Studies have identified a clear correlation between the presence of SLs and virulence of TB in guinea pigs, which has led to the proposal that SLs play a prominent role in pathogenesis (Goren *et al.*, 1976). More recently, it has been shown that SLs block the release of tumour necrosis factor- $\alpha$  (TNF- $\alpha$ ), induced by TDMs in macrophages, resulting in inhibition of granuloma formation in mice (Okamoto *et al.*, 2006). Although mutant strains of *M. tuberculosis* devoid of SL did not significantly affect the replication, persistence and

pathogenicity of bacilli in guinea pig and cultured macrophages (Rousseau *et al.*, 2003), strains with disruption in the sulfolipid transporter MmpL8 were highly attenuated for the growth in the mouse model of TB (Converse *et al.*, 2003).

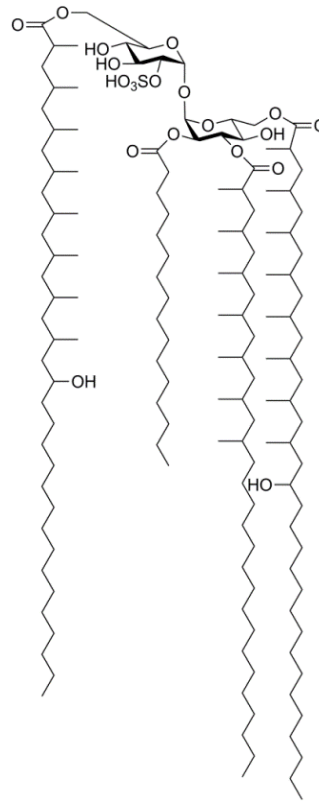


**Figure 1.11. Structure of sulfolipid – SL-1.**

### 1.6.7 Phthiocerol dimycocerosate (PDIM) and phenolic glycolipid (PGL)

Phthiocerol dimycocerosates (PDIMs) are highly non-polar waxes (Figure 1.12) found in the *M. tuberculosis* cell wall. They are composed of two mycocerosic acids (long-chain polymethyl-branched fatty acids) which are linked to a lipid core backbone of  $C_{34}$  and  $C_{34}$  long-chain  $\beta$ -diols known as phthiocerols (Minnikin *et al.*, 2002). PDIM deficiency has been shown to be responsible for attenuation of virulent strains of *M. tuberculosis* in mice lungs which identified genes involved in the PDIM biosynthesis as being involved in TB pathogenesis (Cox *et al.*, 1999; Camacho *et al.*, 2001).

Further studies have shown that PDIMs participate in the early stages of *M. tuberculosis* infection by protecting the bacilli against reactive nitrogen intermediates and modulating the early immune response to infection (Rousseau *et al.*, 2004). PDIMs have been demonstrated to control the invasion of macrophages by *M. tuberculosis* by modifying the organisation of lipids, thereby providing a protective niche for bacilli by preventing phagosome acidification (Astarie-Dequeker *et al.*, 2009).

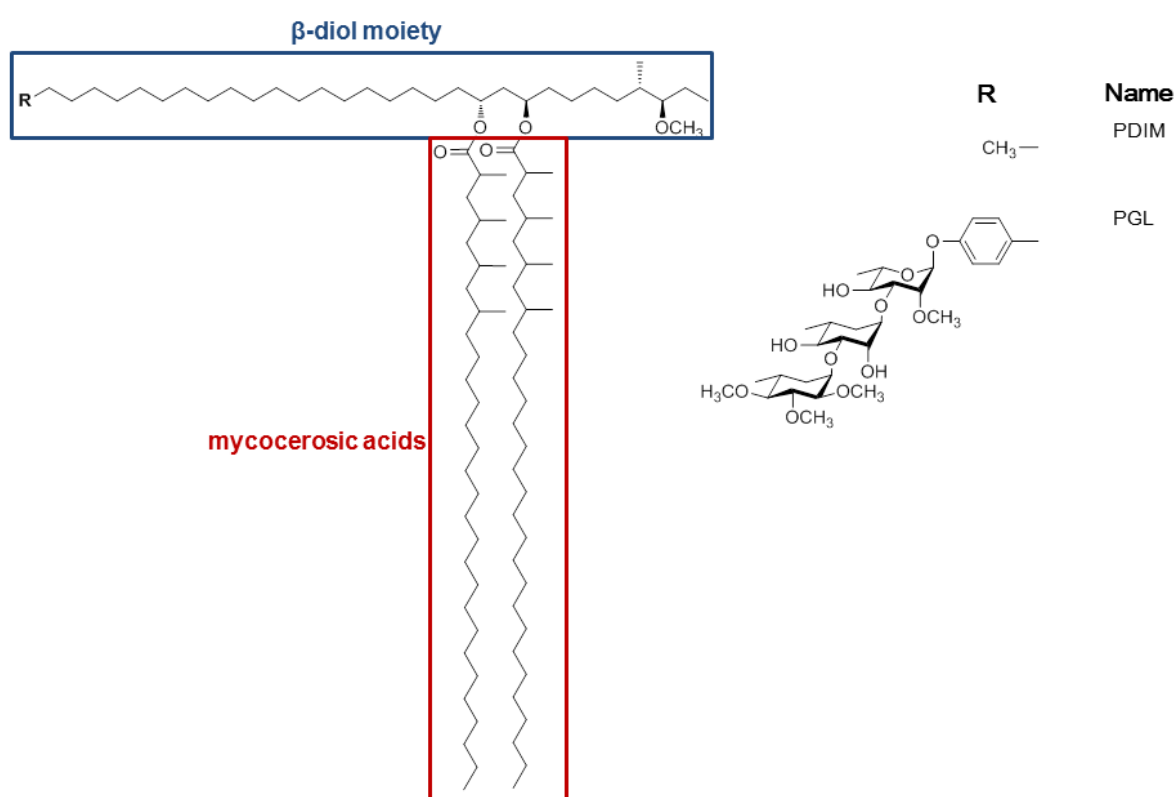


**Figure 1.12. Structure of phthiocerol dimycocerosate (PDIM) and phenolic glycolipid (PGL) from “*M. canetti*”.** PDIMs and PGLs have long chain  $\beta$ -diol backbones known as phthiocerols that are esterified with polymethyl-branched fatty acids known as mycocerosates.

Phenolic glycolipids (PGLs) are structurally similar to PDIMs; however, they possess a glycosylated phenolic moiety at the end of the phthiocerol chain (Figure 1.12) (Daffé *et al.*, 1987). These lipids are only found in slow-growing pathogenic bacteria such as *M. kansasii*, *M. gastri*, *M. ulcerans*, *M. leprae*, *M. marinum*, *M. bovis*, *M.*

*tuberculosis* (strain Canetti) (Daffé *et al.*, 1987; Daffé and Lanélaelle, 1988). Studies have identified PGL as being involved in immunomodulatory responses such as inhibiting the release of proinflammatory chemokines and cytokines in Beijing lineages of *M. tuberculosis* (Reed *et al.*, 2004).

### **1.6.8 Lipoarabinomannan (LAM) and related biosynthetic precursors (LM and PIMs)**

Lipoglycans including LAM, its truncated form LM, and their biosynthetic precursor PIMs are another dominant feature of the *M. tuberculosis* cell wall and are embedded within the mAGP structure. The fully mature mycobacterial LAM comprises three distinct regions: a lipidated reducing end known as the phosphatidyl-*myo*-inositol (PI) anchor, the mannan core and the arabinan domain, which is capped with species-specific motifs (Figure 1.13) (Hunter and Brennan, 1990; Chatterjee *et al.*, 1992). The PI anchor, based on an *sn*-glycero-3-phosphate (1-D-*myo*-inositol), covalently attaches the lipoglycan to the cell wall (Hunter and Brennan, 1990). The current model of lipoglycan biosynthesis involves a series of steps where the PI anchor is further glycosylated as shown in the simplified linear pathway: from PI→PIM<sub>2</sub>→LM→LAM (Mishra *et al.*, 2011).

PIMs are synthesised by the addition of mannopyranose (*Manp*) units to the *myo*-inositol ring of the PI precursor (Ballou and Lee, 1964). The smallest PIM residue is PIM<sub>2</sub> in which PI is substituted with *Manp* residues at the 2 and 6 positions of the inositol moiety (Lee and Ballou, 1964). The PI unit can be elongated with up to five *Manp* residues to give rise to PIM<sub>6</sub> (Briken *et al.*, 2004). Two forms of acylated PIMs

are present in mycobacteria:  $Ac_1PIM_V$  with the acyl group at the 3-OH of the *myo*-inositol ring or 6-OH of the *Manp* residue and  $Ac_2PIM_V$ , which is acylated at both, the 3-OH of the *myo*-inositol ring and 6-OH of the *Manp* residue (Figure 1.13) (Khoo *et al.*, 1995). Higher order PIMs, as well as LM are derived from  $Ac_1PIM_2$ , which is further glycosylated with a branched arabinan domain leading to the formation of LAM. The mannan core consists of approximately 30 *Manp* residues which form a linear  $\alpha(1\rightarrow6)$ -*Manp* backbone with  $\alpha(1\rightarrow2)$ -*Manp* side-chains. This linear polymannoside is linked to the branched D-arabinan domain comprising approximately 70 arabinofuranose (*Araf*) residues (Dinadayala *et al.*, 2006; Birch *et al.*, 2010; Mishra *et al.*, 2011). The capping moieties of the arabinan domain vary between species; slow-growers such as *M. tuberculosis* display various degrees of short  $\alpha(1\rightarrow2)$  *Manp* chains (ManLAM) (Chatterjee *et al.*, 1993), whereas caps of inositol phosphate are present in fast-growers such as *M. smegmatis* (PILAM) (Khoo *et al.*, 1995) and non-capped LAM in *M. chelonae* (Guerardel *et al.*, 2002). PIMs, LM and LAM are not only essential for mycobacterial growth and survival but they also exhibit a broad spectrum of immunomodulatory activities. For example, ManLAM can inhibit IFN- $\gamma$ -mediated activation of macrophages and the production of the Th1 proinflammatory cytokines IL-12 and TNF- $\alpha$  (Mishra *et al.*, 2011), as well as induce apoptosis in macrophages (Nigou *et al.*, 2001). PILAM, in contrast, can induce a proinflammatory response in both macrophages and dendritic cells in a Toll-like receptor-2 (TLR-2) dependent manner (Vignal *et al.*, 2003). Both PIMs and LAM enable mycobacteria to persist in phagosomes by preventing phagosome maturation (Vergne *et al.*, 2003; Welin *et al.*, 2008).

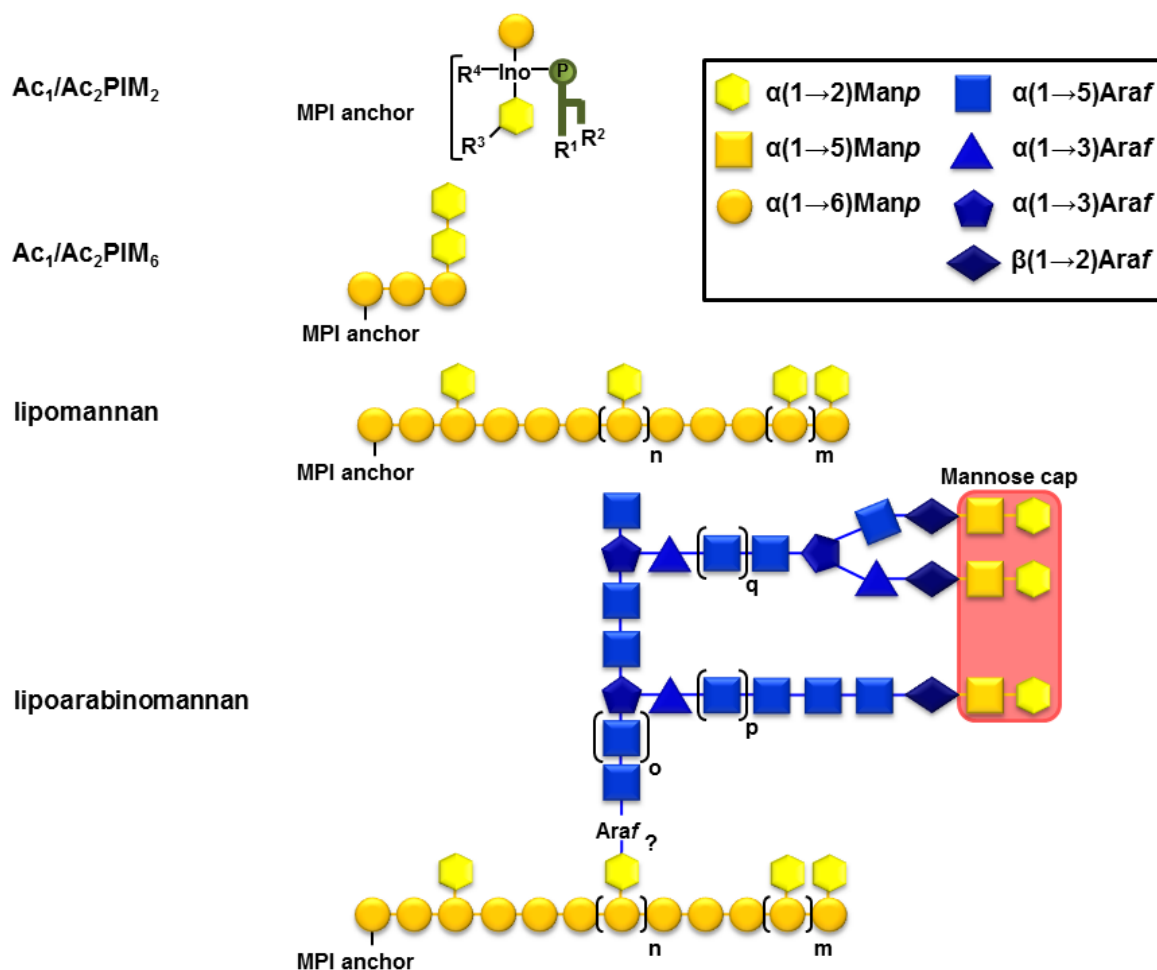


**Figure 1.13. Structures of phosphatidyl-*myo*-inositol mannosides (PIMs), lipomannan (LM) and lipoarabinomannan (LAM).** PI is glycosylated with Man<sub>p</sub> residues at the 2 and 6 positions of the inositol moiety and acylated at position 3-OH of the *myo*-inositol ring or 6-OH of the Man<sub>p</sub> residue to generate Ac<sub>1</sub>PIM<sub>2</sub> or acylated at both positions to generate Ac<sub>2</sub>PIM<sub>2</sub>. Ac<sub>1</sub>/Ac<sub>2</sub>PIM<sub>2</sub> is further glycosylated with two α(1→6)-Man<sub>p</sub> residues and two α(1→6)-Man<sub>p</sub> residues to produce Ac<sub>1</sub>/Ac<sub>2</sub>PIM<sub>6</sub>. LM and LAM share a common mannan core composed of approximately 30 Man<sub>p</sub> residues which form a linear α(1→6)-Man<sub>p</sub> backbone with α(1→2)-Man<sub>p</sub> side chains. A branched D-arabinan domain comprising approximately 70 Araf residues is attached to the mannan core to generate LAM. In *M. tuberculosis*, the non-reducing termini arabinan is capped with mannan residues; however, capping moieties differ according to species. Here R<sup>1</sup>, R<sup>2</sup>, R<sup>3</sup> and R<sup>4</sup> represent potential acylation sites within the MPI anchor. The letters m, n, o and p depict different amount of glycosylations in LAM according to species. Araf, Arabinofuranose; Ino, Inositol; Man<sub>p</sub>, mannopyranose; MPI, Mannosyl phosphate inositol.



### **1.7 *Mycobacterium smegmatis* as a surrogate system in tuberculosis research**

The major hurdles involved with carrying out research with *M. tuberculosis* are its highly infectious nature, which poses risks for researchers and makes it necessary to work in a high containment Bio-Safety Level-3 (BSL-3) environment. Moreover, due to the long generation time of approximately 24 hours, experiments with *M. tuberculosis* take significantly longer compared to those involving fast-growing organisms. *M. smegmatis* overcomes these two major problems and is therefore extensively used in *M. tuberculosis* research; it is non-pathogenic and has an average generation time of 4 to 5 hours.

*M. smegmatis* shares the same cell-wall structure of *M. tuberculosis* although it does generate some lipids that are different. However, the major cell wall components including PG, AG and mycolic acids are fairly well conserved between both species. Genome analysis shows that *M. smegmatis*, which has a genome the size of 7.0 Mb, shares more than 2000 homologues with *M. tuberculosis*. *M. smegmatis* is more tolerant than *M. tuberculosis* to alterations in cell-wall biosynthesis and some genes essential in *M. tuberculosis* are non-essential in *M. smegmatis*, making it an attractive model for TB research.

### **1.8 Aims and objectives**

The recent emergence of MDR- and XDR-TB cases has worsened the global problem of TB, increasing the need to discover novel drug targets in *M. tuberculosis*. The main objective of this thesis was to identify and characterise novel drug targets

against TB focusing specifically on the mycobacterial cell wall. In addition, we wanted to biochemically characterise selected mutants which had disruptions in the biosynthesis of glycolipids. The aims are as follows:

- ❖ To generate spontaneous mutants against chemical compounds from selected ChemBridge compounds and identify their drug targets.
- ❖ To test the essentiality of a polyprenol monophosphomannose (PPM) synthase in lipoglycan biosynthesis of mycobacteria.
- ❖ To biochemically characterise the *pknH* deletion mutant and analyse the composition of LM and LAM.

## **2 Identification of an inhibitor targeting glycerol kinases**

## 2.1 Introduction

### 2.1.1 TB drug discovery

While there has been limited success in the development of new anti-TB drugs in the past 40 years, the emergence of drug resistance has reduced the efficacy of current front-line anti-TB agents. As a result, there is an urgent requirement for more effective compounds that are active against MDR and XDR-TB strains, and which act on novel drug targets and have no cross-resistance to existing drugs. Furthermore, to achieve global control of this epidemic, the next generation of TB drugs needs to overcome the limitations of current therapies. This includes drugs that can shorten the duration of treatment, lower the dosage frequency, be administered alongside HIV medications and reduce adverse side-effects.

There is no clear consensus on the best method for TB drug discovery. Techniques range from the target-based approach, which relies on knowledge of essentiality and function of the protein to be screened against, to the whole cell-based approach, which involves screening against the whole bacterium. The availability of the *M. tuberculosis* genome sequence and the recent development of High-Throughput Screening (HTS) technologies have increased the potential to allow rational discovery and optimisation of new lead compounds, making target-based screening a particularly attractive strategy; however, to date, this approach has been largely unsuccessful in yielding novel drug targets. Reasons for the failure of this approach to identify new inhibitors include a lack of target validation, difficulty in predicting the biological effect of target inhibition on the whole bacterium and that essentiality of a target is not sufficient to ensure 'druggability', where the target can bind with high

affinity to the drug. The whole cell-based screening approach using HTS of compound libraries has been more successful. The major advantages of this strategy include the ability to identify inhibitors with complex and pleiotropic modes of action causing cellular death and the ability to recognise potential holistic interactions of a drug target with one or more components of the bacterium. Disadvantages of this approach include a lack of upfront knowledge regarding the mechanism of action of the drug and the need to identify the right *in vitro* growth conditions relevant for *in vivo* infections as metabolic targets behave differently depending on the composition of the growth medium. Several anti-mycobacterial compounds, which are currently in clinical development, have been discovered through whole cell-based screening methods.

## **2.1.2 Recent successes using whole-cell screening approaches**

### **2.1.2.1 TMC207**

A whole-cell assay testing for inhibition of *M. smegmatis* and *M. tuberculosis* led to the discovery of a promising new diarylquinoline compound, TMC207, which acts on a novel target (Figure 2.1) (Andries *et al.*, 2005). This compound displays high potency against *M. tuberculosis* and other mycobacterial species *in vitro*, but little activity against other bacteria and shows similar *in vitro* efficacy against drug-sensitive and drug-resistant TB. The mechanism of action of TMC207 is different to that of fluoroquinolones and other quinolone classes, which target DNA gyrase (Andries *et al.*, 2005). Comparative analysis of *M. smegmatis* and *M. tuberculosis* mutant strain sequences, resistant to TMC207 and the wild-type genome sequence, identified two point mutations (D32V and A63P) in the *atpE* encoding gene indicating

that the proton pump of ATP synthase is the target of TMC207 (Andries *et al.*, 2005; Koul *et al.*, 2007). Recent studies in Phase II clinical trials conducted with patients with MDR-TB taking TMC207 plus a standard background regimen have shown that the drug is safe and well tolerated (Matteelli *et al.*, 2010); therefore TMC207 has the potential to be used as a front-line anti-TB agent.

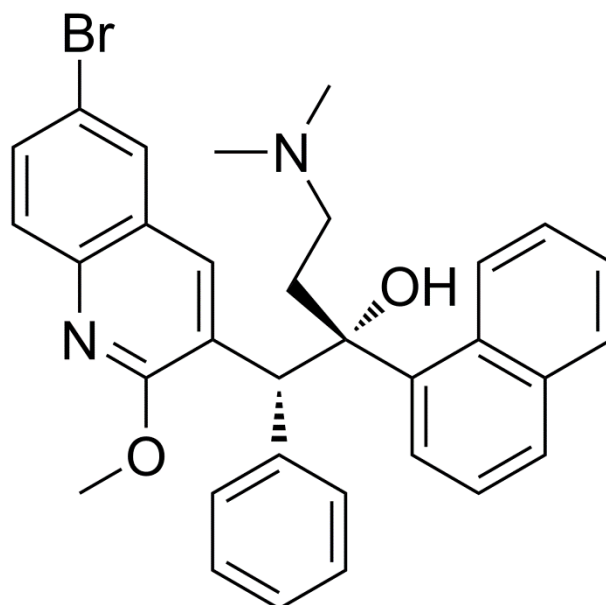
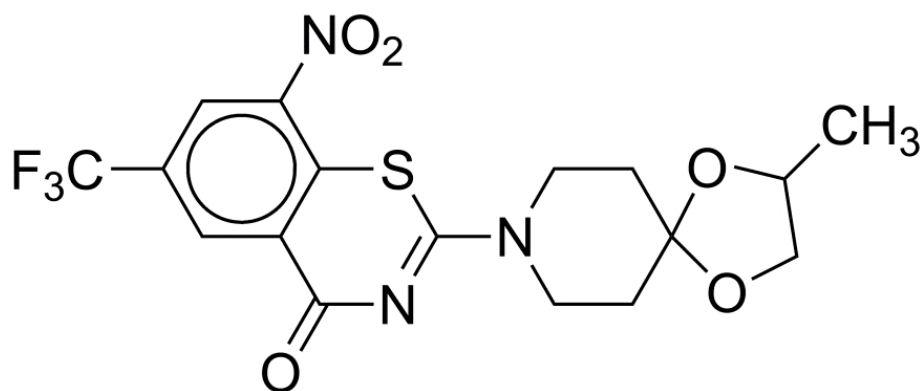


Figure 2.1. Structure of TMC207.

#### 2.1.2.2 DprE1 – the cellular target of benzothiaziones (BTZ) and dinitrobenzamides (DNB)

Testing of sulfur-containing heterocycles for antibacterial activity led to the discovery of benzothiaziones (BTZ) (Figure 2.2) (Makarov *et al.*, 2006). These highly potent compounds have very low MICs for *M. tuberculosis* and *M. smegmatis* and display high potency against MDR-TB strains (Pasca *et al.*, 2010). Spontaneous mutant strains of *M. smegmatis* and *M. tuberculosis* with high-level resistance to BTZ were isolated and allowed comparative analysis against the wild-type genome sequence. This analysis identified MSMEG\_6382 and Rv3790 as the drug target for *M.*

*smegmatis* and *M. tuberculosis*, respectively (Makarov, 2009). Rv3790 (*dprE1*) and its adjacent gene Rv3791 (*dprE2*) encode proteins which catalyse the epimerisation of decaprenyl-monophosphorylribose (DPR) into decaprenyl-monophosphorylarabinose (DPA) (Figure 2.4) (Mikusová *et al.*, 2005).



**Figure 2.2. Structure of BTZ043.** The most advanced compound from the BTZ series. BTZ043 is a *S* enantiomer of BTZ038 which has a single chiral centre.

An alternative whole-cell screening of compounds using high-throughput, fluorescence microscopy identified dinitrobenzamides (DNB) (Figure 2.3) as potent anti-TB inhibitors that also target DprE1 (Figure 2.4) (Christophe *et al.*, 2009).

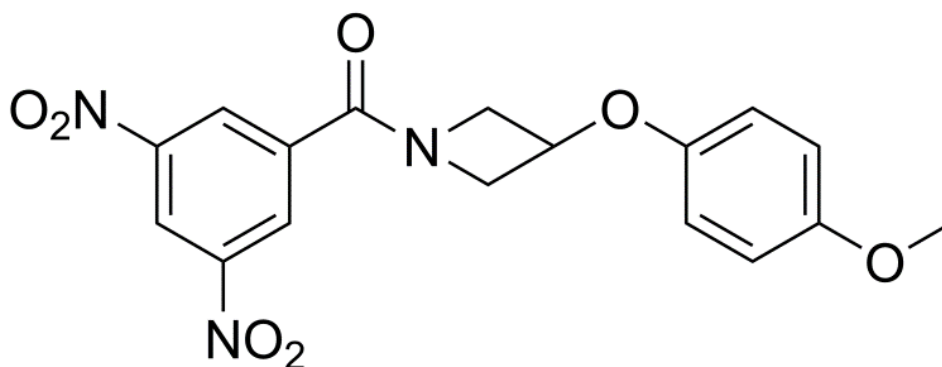


**Figure 2.3. Structure of DNB1.**

The production of DPA is vital for arabinan synthesis as it is the only known precursor of polymerised *Araf* residues in mycobacteria and is therefore necessary for the formation of the complete cell wall (Mikusová *et al.*, 2005; Wolucka, 2008). In addition, recent studies have identified DprE1, which is highly conserved in various actinobacteria including *Corynebacterium glutamicum* (Meniche *et al.*, 2008), as an essential enzyme in *M. smegmatis*, suggesting it is essential across mycobacteria (Crellin *et al.*, 2011) further validating DprE1 as a novel target for treatment of TB.

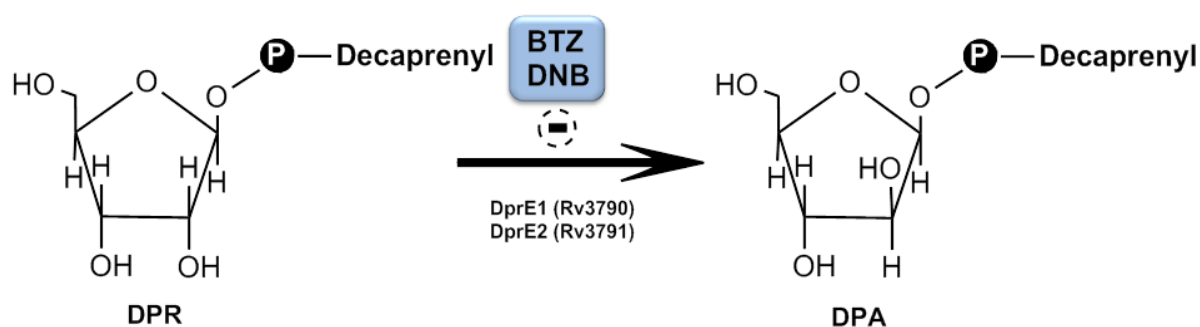


**Figure 2.4. BTZ and DNB targeting the DPA biosynthesis pathway.**

### 2.1.2.3 MmpL3 membrane protein

Mycobacterial membrane protein large 3 (MmpL3) is an essential membrane transporter involved in the export of TMM and vital for formation of the cell wall (Varela *et al.*, 2012). It has been identified as a common drug target of several chemically unrelated small molecules using comparative genomic analysis of spontaneous resistant mutants. These inhibitors include SQ109 (Tahlan *et al.*, 2012), adamantyl urea (Grzegorzewicz *et al.*, 2012), BM212 (La Rosa *et al.*, 2012), THPP and spiro analogues (Remuiñán *et al.*, 2013). A 1,2-diamine SQ109 (Figure 2.5), was discovered during an investigation of EMB derivatives and exhibits very high anti-mycobacterial activity and potency against MDR-TB strains (Lee *et al.*, 2003;



Protopopova *et al.*, 2005). Recent success in Phase I and early Phase II clinical trials, where this compound was found to be safe and well tolerated, has highlighted SQ109 as a promising candidate as a future anti-TB agent (Sacksteder *et al.*, 2012).

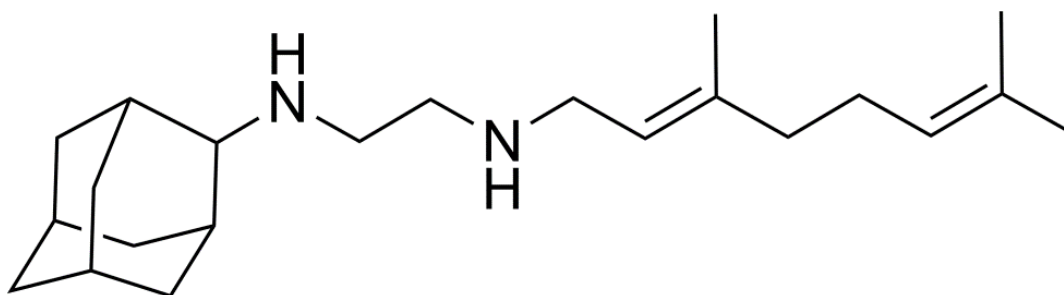


Figure 2.5. Structure of SQ109.

AU1235 (Figure 2.6) is a recently identified adamantyl urea displaying activity against *M. tuberculosis* (Grzegorzewicz *et al.*, 2012). MmpL3 was identified as its cellular target when resistant mutants were found to harbour a single mutation in *mmpL3* (G758A) (Grzegorzewicz *et al.*, 2012). Similarly, pyrrole derivative BM212 (Figure 2.7) was shown to target the MmpL3 protein as all of the characterised mutants of *M. smegmatis*, *M. bovis* BCG, and *M. tuberculosis* H37Rv mutants harboured mutations in the *mmpL3* gene (La Rosa *et al.*, 2012).

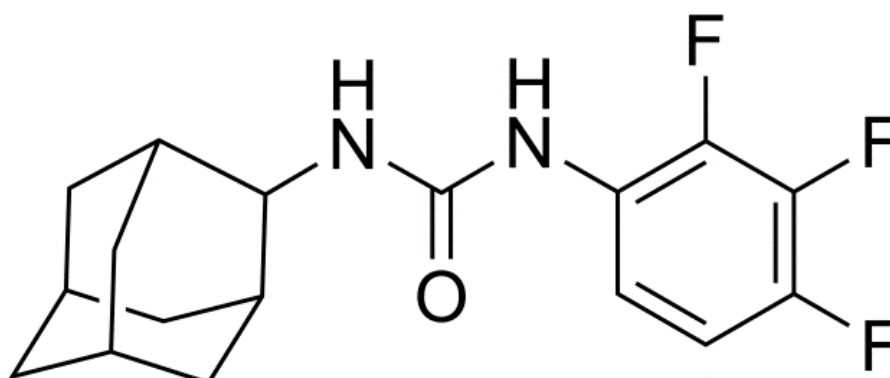
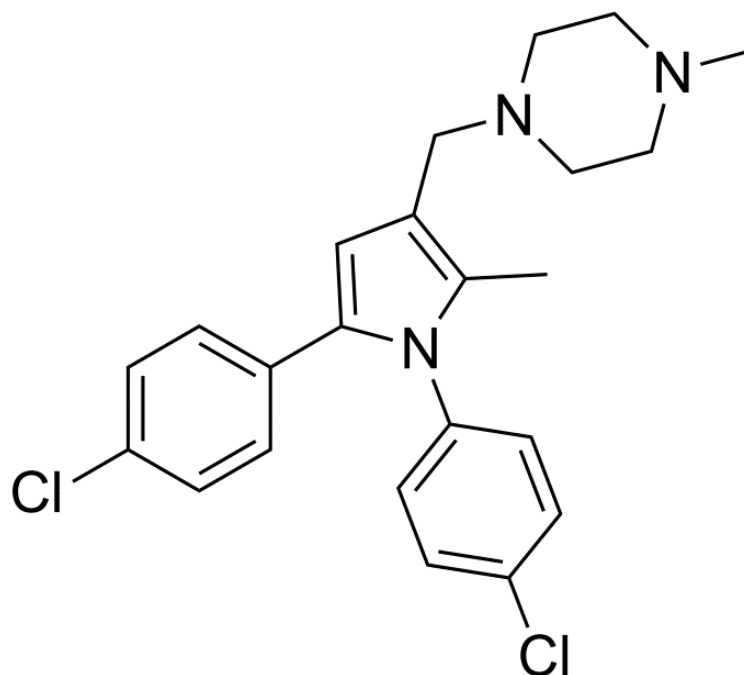
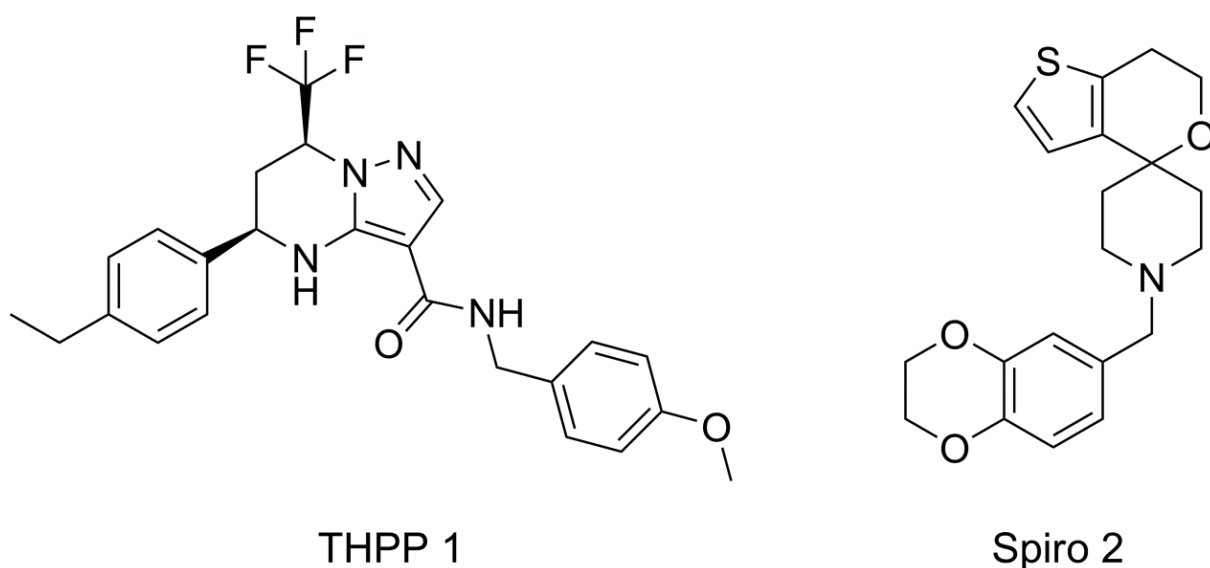


Figure 2.6. Structure of AU1235 - 1-(2-adamantyl)-3-(2,3,4-trifluorophenyl)urea.



**Figure 2.7. Structure of pyrrole derivative BM212.**

A recent study has identified THPP and spiro analogues (Figure 2.8) as inhibitors against *M. tuberculosis* and *M. bovis* BCG through a high-throughput whole-cell screening campaign (Remuiñán *et al.*, 2013).



**Figure 2.8. Structure of THPP 1 and Spiro 2.**

Subsequent whole genome sequencing of several *M. tuberculosis* resistant mutants identified single mutations in the *mmpL3* gene (Remuiñán *et al.*, 2013). Furthermore, experimental data has shown that treatment of *M. bovis* BCG with THPP and spiro resulted in the accumulation of TMM, thereby confirming MmpL3 protein as the cellular target for these compounds (Remuiñán *et al.*, 2013).

#### 2.1.2.4 Pks13 – Cellular target of Thiophenes (TP)

Recent studies have identified a class of compounds known as thiophenes (TP) (Figure 2.9) which cause mycobacterial cell death through the inhibition of *M. tuberculosis* polyketide synthase 13 (Pks13) a member of the type I polyketide synthase gene family (Wilson *et al.*, 2013).

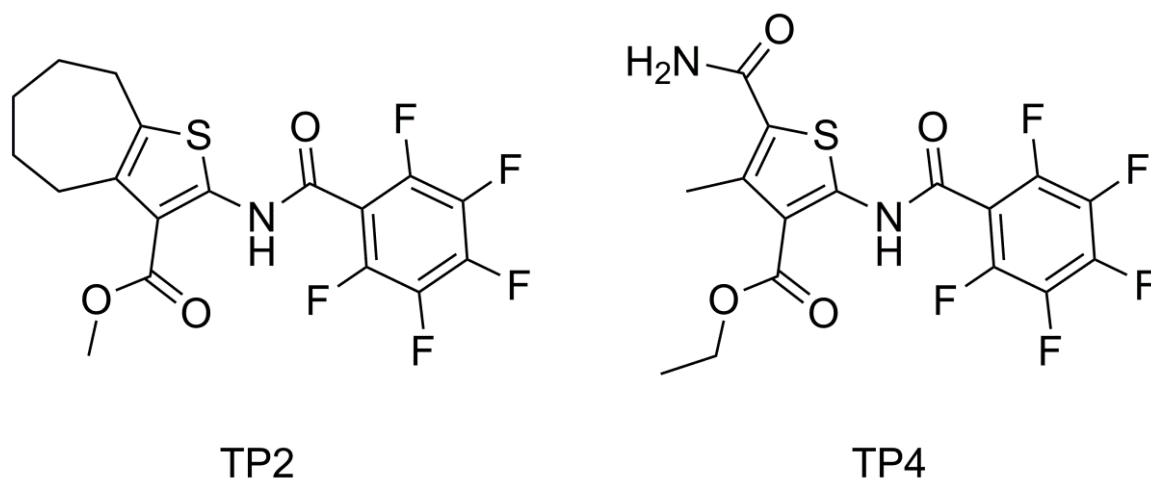


Figure 2.9. Structure of thiophenes TP2 and TP4.

Isolated TP-resistant mutants were found to carry a single mutation (F79S) in close proximity to the catalytic Ser55 domain site in *M. tuberculosis* Pks13, which plays a critical role in the final condensation step in the assembly of mycolic acids (Portevin *et al.*, 2004; Gande *et al.*, 2004; Wilson *et al.*, 2013). *In vitro* studies demonstrate TP inhibits the fatty acyl-AMP loading onto Pks13, preventing mycolic acids from being

fully synthesised (Wilson *et al.*, 2013). The essentiality of Pks13 has been previously demonstrated in *M. smegmatis*, whilst in *C. glutamicum*, the pks13 deletion mutant is deficient in mycolic acids, but can still produce fatty acid precursors (Portevin *et al.*, 2004). Inhibiting Pks13 presents a new mechanism for mycolic acid synthesis inhibition that rapidly leads to mycobacterial cell death and therefore seems to be a promising target for developing future anti-TB drugs.

#### 2.1.2.5 QcrB – Cellular target of imidazo[1,2-a]pyridines (IP)

More recently, high throughput whole-cell screening of an extensive compound library identified imidazo[1,2-a]pyridine (IP) compounds (Figure 2.10) as potent lead molecules active against *M. tuberculosis* and *M. bovis* BCG (Abrahams *et al.*, 2012).

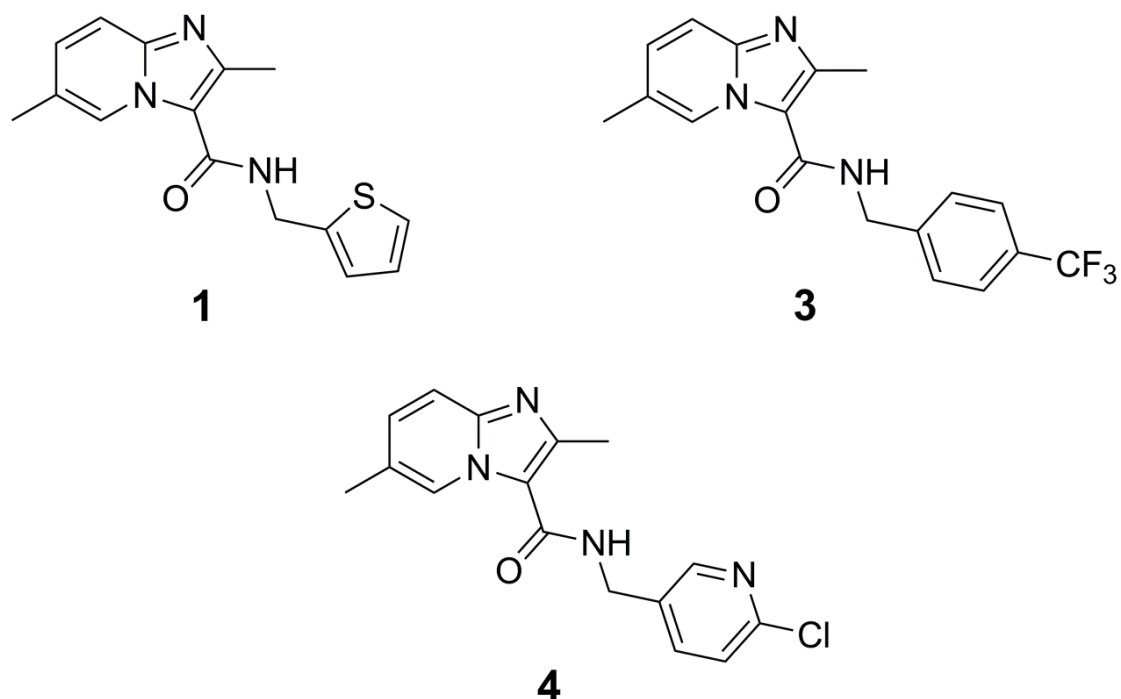


Figure 2.10. Structure of compounds from imidazo[1,2-a]pyridines (IP) series.

Spontaneous resistant mutants of *M. bovis* BCG were generated against IP 1, 3, and 4 and subsequent whole genome sequencing identified a single nucleotide polymorphism (T313A) in the *qcrB* gene, which encodes the *b* subunit of the cytochrome *bc*<sub>1</sub> complex (Abrahams *et al.*, 2012). The cytochrome *bc*<sub>1</sub> complex is an integral membrane protein in the electron transport chain and is an important component of the bacterial respiratory system; therefore, the IP inhibitor family is a promising anti-TB agent (Abrahams *et al.*, 2012).

### 2.1.3 ChemBridge library

The Tuberculosis Antimicrobial Acquisition and Coordination Facility (TAACF) has been formed to help researchers to develop new anti-TB drugs (Goldman and Laughon, 2009). One approach, which the Facility has initiated, is the development of high-throughput screening (HTS) systems, which have provided researchers with a powerful method for identifying in a short period of time, new lead compounds from a 90,000 compound library from ChemBridge and consequently new drug targets (Ananthan *et al.*, 2009). This information has been made available to researchers worldwide and provides an important basis for identifying active compounds as potential new leads as anti-tubercular drugs (Ananthan *et al.*, 2009). Chemical compounds from the ChemBridge library (Ananthan *et al.*, 2009) have been tested for anti-tubercular activity and their Minimum Inhibitory Concentration (MIC) to growing *M. tuberculosis* identified. A HTS approach was adopted to identify the cellular target of a compound from this library and the findings are presented in this Chapter.

## 2.2 Materials and Methods

### 2.2.1 Bacterial strains and growth conditions

Liquid cultures of *M. smegmatis* mc<sup>2</sup>155 strain were grown in Tryptic Soy Broth (TSB), soybean-casein digest medium (BD Difco) or Middlebrook 7H9 medium (BD, Difco) with 10% (v/v) oleic acid/albumin/dextrose/catalase (OADC) enrichment (BD, Difco), supplemented with 0.05% (v/v) Tween-80 (Sigma-Aldrich) in a shaking incubator overnight at 37 °C. Liquid cultures grown in Middlebrook 7H9 medium contained either 0.25% (v/v) glycerol or 10 µM sodium acetate. For growth on plates, solid media were made with TSB, soybean-casein digest medium (BD, Difco) with addition of 1.5% (w/v) agar. Liquid cultures of *E. coli* were grown in Luria-Bertani (LB) broth in a shaking incubator overnight at 37 °C. For growth on plates, solid media were made with using Luria agar (Fisher Bioreagents). The concentration of the antibiotics used was 50 µg/ml kanamycin (Sigma-Aldrich) for *E. coli* and 25 µg/ml kanamycin for *M. smegmatis*.

### 2.2.2 MIC determination

Compounds AKR334, AKR849, AKR745, AKR986, AKR715 and AKR766 (ChemBridge) were dissolved in 1 ml of dimethyl sulfoxide (DMSO). *M. smegmatis* culture was spread onto TSB plates containing 1 µg/ml, 2.5 µg/ml, 5 µg/ml, 10 µg/ml and 20 µg/ml concentrations of the each inhibitor. MIC was determined as the concentration of drug that reduced the number of colony-forming units (cfu) ml<sup>-1</sup> by 99%.

### 2.2.3 Generation of *M. smegmatis* spontaneous mutant resistant to AKR334

*M. smegmatis*, grown to mid-log phase, was spread onto TSB plates containing the MIC of the AKR334 compound. Resistant colonies were picked after incubating for 48 h at 37 °C and subsequently inoculated into liquid media in the absence of inhibitor. Putative mutants were grown to mid-log phase and selected on solid media containing 5× MIC of AKR334 to confirm the presence of a mutation conferring resistance to the inhibitor. Following validation of the mutant, the *M. smegmatis* spontaneous mutant and the *M. smegmatis* wild-type strains were inoculated in parallel into 50 ml TSB liquid media containing the MIC of the AKR334 compound (no compound for the wild-type), grown to late log phase and harvested by centrifugation for 10 min at 4000 rpm. Genomic DNA was extracted using the method described in Section 6.9. Purified genomic DNA from each *M. smegmatis* spontaneous mutant and the *M. smegmatis* wild-type was sent for whole-genome high-throughput sequencing using GS FLX Titanium Series (Roche) at the University of Birmingham.

### 2.2.4 Construction of Recombinant Plasmids

For overexpression of various *M. smegmatis* and *M. tuberculosis* glycerol operon genes in *M. smegmatis*, genes were amplified by PCR using Phusion High-Fidelity DNA polymerase (New England Labs) from *M. smegmatis* mc<sup>2</sup>155 and *M. tuberculosis* H37Rv genomic DNA using the oligonucleotide primers generated by Eurofins MWG Operon (Ebersberg, Germany) shown in Table 2.1. The PCR-amplified DNA fragments of *glpk1*, *glpk2*, *MSMEG\_6757*, *MSMEG\_6758* and *RvglpK* were cloned into the pMV261 vector containing a kanamycin resistance selection marker (Stover *et al.*, 1991) using primer-incorporated restriction sites (restriction

endonucleases, New England Biolabs; T4 DNA ligase; New England Biolabs). All constructs were verified by DNA sequencing performed by Eurofins MWG Operon (Ebersberg, Germany). The constructs generated along with the empty pMV261 vector were electroporated into *M. smegmatis*.

**Table 2.1. Oligonucleotide primers used for PCR of various *M. smegmatis* and *M. tuberculosis* glycerol operon genes.** Restriction site is underlined.

Oligonucleotide	Restriction site	Sequence (5' → 3')
glpk1 forward	BamHI	ATTGCG <u>GATCC</u> AGTGACCGAGCGC
glpk1 reverse	Clal	TCGACATCGATT <u>CACAC</u> GGTTTCG
glpk2 forward	EcoRI	GCAGAAT <u>TCAT</u> GGCTGACTTCGTC
glpk2 reverse	HindIII	ATA <u>AAGCTT</u> CTCACTGGACGTCCAC
MSMEG_6757 forward	BamHI	ATTGCG <u>GATCC</u> AGTGCCAGGCACT
MSMEG_6757 reverse	HindIII	ATA <u>AAGCTT</u> CTCACAGTTCCCGCCC
MSMEG_6758 forward	BamHI	ATTGCG <u>GATCC</u> AATGTCACGACGA
MSMEG_6758 reverse	HindIII	ATA <u>AAGCTT</u> CTCAGACCGCGGATGC
RvglpK forward	EcoRI	GCAGAAT <u>TCGT</u> GTCGACGCCATC
RvglpK reverse	HindIII	ATA <u>AAGCTT</u> CCTAGGACACGTCAAC

### 2.2.5 Polar and apolar lipid extraction of [<sup>14</sup>C]-labelled inhibitor-treated cultures of *M. smegmatis*

A 10 ml culture of *M. smegmatis* (wild-type and resistant mutant) was grown until mid-log phase (OD<sub>600</sub> 0.6). AKR334 was added to separate cultures at 0.5× MIC and



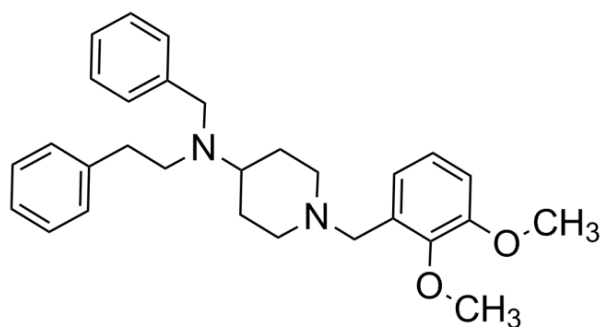
1× MIC and the culture grown for a further 4 hours at 37 °C. Cells were labelled with 10 µCi ml<sup>-1</sup> [1,2-<sup>14</sup>C]acetate (57 mCi mmol<sup>-1</sup>, GE Healthcare, Amersham Bioscience), and incubated at 37 °C overnight. The [1,2-<sup>14</sup>C]-labelled cells were harvested by centrifugation followed by washing with 2 ml phosphate buffer saline (PBS). Polar and apolar lipids were extracted using the method described in Section 6.10. Incorporation of [1,2-<sup>14</sup>C]acetate was quantified by liquid scintillation counting using 5 % of the lipid fractions in 5 ml EcoScint A (National Diagnostics). The polar lipid extracts were examined by two dimensional thin-layer chromatography (2D-TLC) on aluminium-backed plates of silica gel 60 F254 (Merck 5554) by spotting equal counts of polar lipid extracts (50,000 cpm), which were then developed using solvent system D for polar lipids: CHCl<sub>3</sub>: MeOH: H<sub>2</sub>O (100:14:0.8) in the first direction and CHCl<sub>3</sub>: acetone: MeOH: H<sub>2</sub>O (50:60:2.5:3) in the second direction (Dobson *et al.*, 1985). Polar lipids were visualised by 48 h exposure on X-ray films by autoradiography (Kodak Biomax MR film).

## 2.3 Results and Discussion

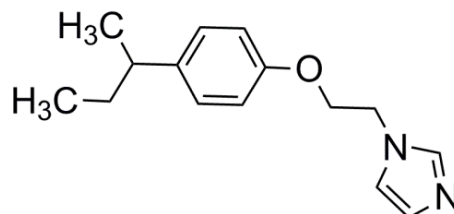
### 2.3.1 Identification of AKR334 as an inhibitor of *M. smegmatis*

A number of chemical families from the ChemBridge library were screened for anti-tubercular activity using an Alamar blue assay as part of a HTS campaign to discover new anti-mycobacterial agents (Ananthan *et al.*, 2009; Maddry *et al.*, 2009). We selected several compounds from the library (Figure 2.11) and tested for their MIC against *M. smegmatis*, as stated in Table 2.2. Amongst the compounds, *N*-benzyl-1-(2,3-dimethoxybenzyl)-*N*-(2-phenylethyl)-4-piperidinamine oxalate (AKR334)

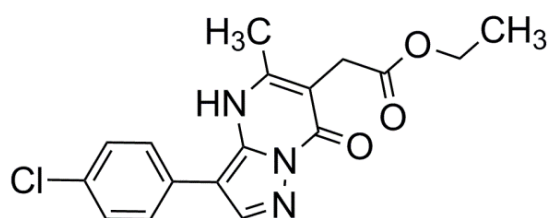
exhibited encouraging MIC values against *M. smegmatis* and thus was selected for use in strategies towards the identification of its target (Table 2.2).



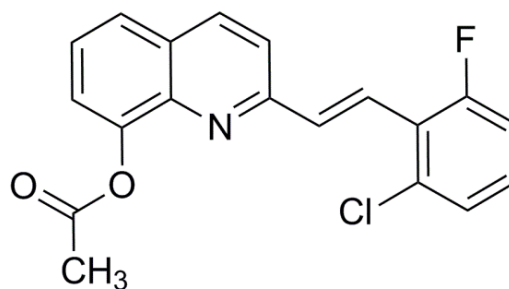
AKR334



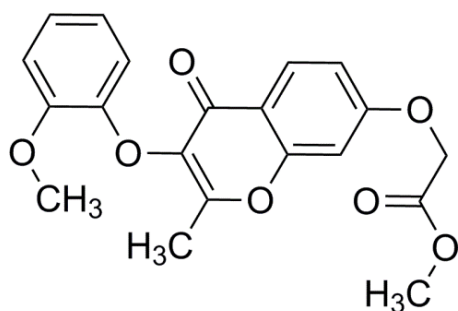
AKR849



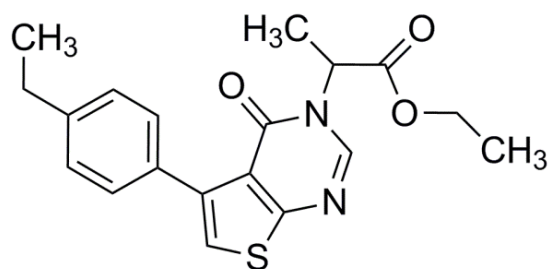
AKR745



AKR986



AKR715



AKR766

**Figure 2.11. Compounds from the ChemBridge library active against *M. tuberculosis*.**

AKR334 had a MIC value of 5  $\mu\text{g/ml}$  against *M. smegmatis*, which was very similar to its MIC against *M. tuberculosis*, reported as 6.32  $\mu\text{g/ml}$  (Ananthan *et al.*, 2009).

Antibacterial activity of this general chemical structure has not been previously reported in the scientific literature.

**Table 2.2. Minimum inhibitory concentration (MIC) values of compounds from ChemBridge library against *M. tuberculosis* and *M. smegmatis*.** MIC against *M. tuberculosis* were tested previously (Ananthan, 2009; Maddry, 2009).

Compound	MIC ( $\mu\text{g/ml}$ )	
	<i>M. tuberculosis</i> H37Rv	<i>M. smegmatis</i> mc <sup>2</sup> 155
AKR334	6.32	5
AKR849	3.02	>20
AKR745	1.95	15
AKR986	0.94	>20
AKR715	5.13	>20
AKR766	6.63	>20

### 2.3.2 Identification of single nucleotide polymorphisms (SNPs) in a spontaneous resistant mutant

As AKR334 had an encouraging MIC value against *M. smegmatis*, this bacterium was established as a suitable model for target identification. *M. smegmatis* spontaneous resistant mutants were generated against the MIC of the compound. Selected mutant colonies continued to show growth on plates containing 15  $\mu\text{g/ml}$ , 20  $\mu\text{g/ml}$  and 50  $\mu\text{g/ml}$  concentrations of the molecule, which showed they were highly resistant to AKR334. A resistant mutant was selected and sent for whole-genome sequencing to identify any mutations within the genes which might allow the resistant bacteria to survive in the presence of the inhibitor. The genome sequence of the

resistant mutant was aligned with the genome sequence of the wild-type to identify the Single Nucleotide Polymorphisms (SNPs) potentially responsible for drug resistance, which were filtered to exclude indels and low frequency variants. The remaining SNPs are shown in Table 2.3.

**Table 2.3. Single nucleotide polymorphisms detected in *M. smegmatis* spontaneous mutants resistant to AKR334.**

Gene position	Gene product	Nucleotide base change	Amino acid change
281479	mmpL3	A to G	F649L
282457	mmpL3	C to T	V323I
6802897	None*	G to T*	None*

\*Base substitution is located in the non-coding region.

Whole-genome sequencing revealed two base change mutations in the *mmpL3* gene, which encodes for the MmpL3 protein. These mutations were at codon 649 (AAG>GAG) and at codon 323 (CAG>IAG). The identified point mutations would result in the following changes in the protein sequence: phenylalanine at position 649 to leucine and valine at position 323 to isoleucine. Multiple protein sequence alignment of *mmpL3* orthologues shows that both these point mutations occur in amino acid residues conserved across various mycobacteria (Figure 2.12). As mentioned above, MmpL3 protein has recently been established as the cellular target of several drugs (La Rosa *et al.*, 2012; Tahlan *et al.*, 2012; Grzegorzewicz *et al.*, 2012; Remuiñán *et al.*, 2013).

```

MSMEG_mmpL3      1 MFAWWGRTVYQFRYIVIGVMVALCLGGGVYGISLGNHVTQSGFYDEGSQVAASLIGDEVYGRDRTSHVVAILTFPDDKK
Mtb_mmpL3        1 MFAWWGRTVYRYRFIVIGVMVALCLGGGVFGLSLGKHVTQSGFYDDGSQSVQASVLGDQVYGRDRSGHIVAI FQAPAGKT
Mb_mmpL3         1 MFAWWGRTVYRYRFIVIGVMVALCLGGGVFGLSLGKHVTQSGFYDDGSQSVQASVLGDQVYGRDRSGHIVAI FQAPAGKT
ML2620          1 MFAWWGRTVYRYRFIVIGITVALCLCGGVFGLSLGKHVTQSGFYDDSSQSVKASILGDQVYGRDRSGHIVAI FHPADGKT

MSMEG_mmpL3      81 VTDKAWQKKVTEELDQVVKDHEDQIVGWVWGLKAPDITDPTVSAMKTQDLRHTFISIPLQGGDDDDDEILKNYQVVEPELQQ
Mtb_mmpL3        81 VDDPAWSKKVDELNRFQQDHPDQVGLWAGYLRASQAT-----GMATADKKYTFVSIPLKGGDDDDTILNNYKAIAADLQR
Mb_mmpL3         81 VDDPAWSKKVDELNRFQQDHPDQVGLWAGYLRASQAT-----GMATADKKYTFVSIPLKGGDDDDTILNNYKAIAADLQR
ML2620          81 VNDPAWAKKITDELNQFQRNNSNKVTGWAGYLRASDTTNTVVQGMATPKDKYTFVSIPLKGGDDDDTILNNYKAIAADLQR

MSMEG_mmpL3      161 VNGGDIRLAGLNFELASELTGTIGEDQKRAEVAIPLVAVVLFVFGTVIAAALPAIIGGLAIAGALGIMRLVAEFTPVHF
Mtb_mmpL3        156 LDGGTVKLAGLQPVAEALGTIATDQRRMEVLALPLVAVVLFVFGGVIAAGLPVMVGGGLCIAGALGIMRFLAIFGPVHY
Mb_mmpL3         156 LDGGTVKLAGLQPVAEALGTIATDQRRMEVLALPLVAVVLFVFGGVIAAGLPVMVGGGLCIAGALGIMRFLAIFGPVHY
ML2620          161 LDGGTVQLAGLDPIANALSTIATDQRRMEVLALPLVAVVLFVFGGVIAACLPMVGGGLSIAGALGILRFIALFGPVHF

MSMEG_mmpL3      241 FAQPVVTLIGLGAIDYGLFIVSRFREEIAEGYDTEAAVRRVTMTSGRTVVSFAVIVVASSVPLLLFPQGFLKSITYAII
Mtb_mmpL3        236 FAQPVVSLIGLGAIDYGLFIVSRFREEIAEGYDTEAVRRVTITAGRTVTFSAVLIVASAIGLLLPQGFGLKSLTYATI
Mb_mmpL3         236 FAQPVVSLIGLGAIDYGLFIVSRFREEIAEGYDTEAVRRVTITAGRTVTFSAVLIVASAIGLLLPQGFGLKSLTYATI
ML2620          241 FAQPVVSLIGLGAIDYGLFVVSRRFREEIAEGYDTEAAVRRVTMTAGRTVTFSAVLIASAASGASLLLPQGFVKSITYALI

MSMEG_mmpL3      321 ASVMLAAILSITVLAALAALILGPRVDALGVITLLKI PFLANWQFSRRIIDWFAEKTKTKTREEEVERGFWRLVNVVMKR
Mtb_mmpL3        316 ASVMLSAILSITVLPACLGLGKHVDALGVRTLFRV PFLANWKISAAYLNWLADRLQRTKTRREEVAGFWGLVNRVMKR
Mb_mmpL3         316 ASVMLSAILSITVLPACLGLGKHVDALGVRTLFRV PFLANWKISAAYLNWLADRLQRTKTRREEVAGIWKLVNRVMKR
ML2620          321 AAVTLAALLSITLPACLAIALAKHVDALGVRTLFRV PFLRNWRMSHACLNWLADRLQRTKTRREEVAGFWGLVNVFMKR

MSMEG_mmpL3      401 PIAFAAPILVVMVLLIIPLGQLSLGGISEKYLPPDNAVRQSQE QFDKLPFGFRTEPLTLVMKREDGEPITDAQIADMRAK
Mtb_mmpL3        396 PVLFAAPIVIIMILLIIPVGKLSLGGISEKYLPPNTSVRQAQEE FDKLPFGYRTNPLTLVIQTSNHQFVTDQIADIRSK
Mb_mmpL3         396 PVLFAAPIVIIMILLIIPVGKLSLGGISEKYLPPNTSVRQAQEE FDKLPFGYRTNPLTLVIQTSNHQFVTEAQIADIRSK
ML2620          401 PLVFAPIVIGMILLIIPLGNLSFGGSEKYLPPNNAVRQSQEH FDKLPFGYRTNPLTLVIQTSNHQFVTDQIADIRSK

MSMEG_mmpL3      481 ALTVSGFTDPDNDPEKMWKERPANDSGSKDPSVRVVIQNGLENRNDAAKKIDELRALQPPHGGIEVFGVGTPALEQDSIHSI
Mtb_mmpL3        476 AMAIGGFIEPDNDPANMWQERAYAVGASKDPSVRVLQNGLINPADASKKTELRAITPPKGITVLVGGTPALELDSIHGL
Mb_mmpL3         476 AMAIGGFIEPDNDPANMWQERAYAVGASKDPSVRVLQNGLINPADASKKTELRAITPPKGITVLVGGTPALELDSIHGL
ML2620          481 AMAISGFIEPDNNVNMWQERTVAPGASKDPSVRVLQNGLINPNDASKKINELRSITPPKGLTVSVGGTPALEQDSIHSI

MSMEG_mmpL3      561 FDKLPLMALILIVTTTIVLMFLAFGVSVLPKKAALMSALTLGSTMGILTWMFVDGHSGLMNYTQPPLMAPMIGLIIAVIV
Mtb_mmpL3        556 FAKMPLMVVILLITTTIVLMFLAFGVSVLPKATLMSALTLGSTMGILTWIFVDGHSFKWLNFTPTPLTAPVIGLIIALVF
Mb_mmpL3         556 FAKMPLMVVILLITTTIVLMFLAFGVSVLPKATLMSALTLGSTMGILTWIFVDGHSFKWLNFTPTPLTAPVIGLIIALVF
ML2620          561 VAQAPLMVIMLITTTMLLMFLAFGVSFLPIKAAVMSALTLGSTMGILTWIFVDGHSKWLNFPTPLMVVIAALVAVGY

MSMEG_mmpL3      641 GLSTDYEVFLVSRMVEARERGMSTAEAIRIGTATTGRLITGAALI LAVVAGAFVFSDLVMMKYLAFLGLIALLLDATIIR
Mtb_mmpL3        636 GLSTDYEVFLVSRMVEARERGMSTQEAIRIGTAAATGRIIITAAALIVAVVAGAFVFSDLVMMKYLAFLGLMAALLLDATVVR
Mb_mmpL3         636 GLSTDYEVFLVSRMVEARERGMSTQEAIRIGTAAATGRIIITAAALIVAVVAGAFVFSDLVMMKYLAFLGLMAALLLDATVVR
ML2620          641 GLATDYEVFLVSRMVEARAEASMTQEAIVRIGTASTGRLITAAALVLAVVAGS VFSDLVMMKYLAFLGLMAALLLDATVVR

MSMEG_mmpL3      721 MFLVPAVMKLLGDDCWAPRWKRVQEKLGLETLPDERKRFTV--RESETDQRA-LVGVGAPPPPPRPHDPTHAP-E
Mtb_mmpL3        716 MFLVPSVMKLLGDDCWAPRWARRLQTRIGLGEIHL PDERKREVSNGRPARPPVTAGLVAARAAGDPRPHDPTHPLA-E
Mb_mmpL3         716 MFLVPSVMKLLGDDCWAPRWARRLQTRIGLGEIHL PDERKREVSNGRPARPPVTAGLVAARAAGDPRPHDPTHPLA-E
ML2620          721 MFLVPSVMKLLGDDCWAPRWARRLQNRIGLGEIHL PDERRRFTV--SGRPFVRFV--TAASLAAPASRVPRGPTHATLE

MSMEG_mmpL3      797 FV-----RPMPPMRSNAPSAAGTARISTFPQPFPQPAQAQAGD--EPATTRFAMARNAVNRNAVNSAVHGGAGSA
Mtb_mmpL3        795 SP-----RPARSSPASSPELTPALEATAAPAAPS GASTTRMQIGSSTEPPTTRLAAGRVSQ-----
Mb_mmpL3         795 SP-----RPARSSPASSPELTPALEATAAPAAPS GASTTRMQIGSSTEPPTTRLAAGRVSQ-----
ML2620          798 PSQRARSGLASRPQIKRFQELPSGASTARIQ-----MRPSQSV---EATITRLSVFGNAPTFTA---AVSSSQGVQ

MSMEG_mmpL3      866 AAPTERAPRPGGPAQPPAPPQREEREIESWL GALRGPAPAKNVFPQPAQFQRPSDTITRAMPPQGRPPAGPADRGNENAP
Mtb_mmpL3        852 -----SPASTPPTPTPPSAPSAGQTRAMPL-----AANRSTDA--
Mb_mmpL3         852 -----SPASTPPTPTPPSAPSAGQTRAMPL-----AANRSTDA--
ML2620          862 AVP-----LAATHRPLETPS-----PASGQTRAMPV-----PANRSSDNAS

MSMEG_mmpL3      946 TTAFSAQRPPNGAPADATTAIPT--PPQREQEPSTEKLNTR EDAPEDPETKRR--GGGMSAQDLLRREGRL
Mtb_mmpL3        887 -----GDPAEFTAALPIIRSDGDDSEAAATEQLN ARGTS DKTRQRRRG--GGALSAQDLLRREGRL
Mb_mmpL3         887 -----GDPAEFTAALPIIRSDGDDSEAAATEQLN ARGTS DKTRQRRRG--GGALSAQDLLRREGRL
ML2620          898 ET-----AEFTTALPIMRPQDNDSEVATEKLNALG QGDNSRQHRRATGGGISAQDLLRREGRL

```

**Figure 2.12. Multiple protein sequence alignment of mmpL3 orthologues in different mycobacteria.** Numbers indicate the amino acid co-ordinates of each protein. Conserved residues are highlighted in light blue. Dash indicates gap in amino acid sequence. Red arrows indicate position of SNP detected in the AKR334-resistant *M. smegmatis* mutant.

A single base change mutation (A to G) was also detected at the genomic position 6802897. The sequence in this region does not encode amino acids; however, this region is the promoter sequence for the glycerol operon (Figure 2.13), a cluster of genes which are involved in glycerol uptake and metabolism.

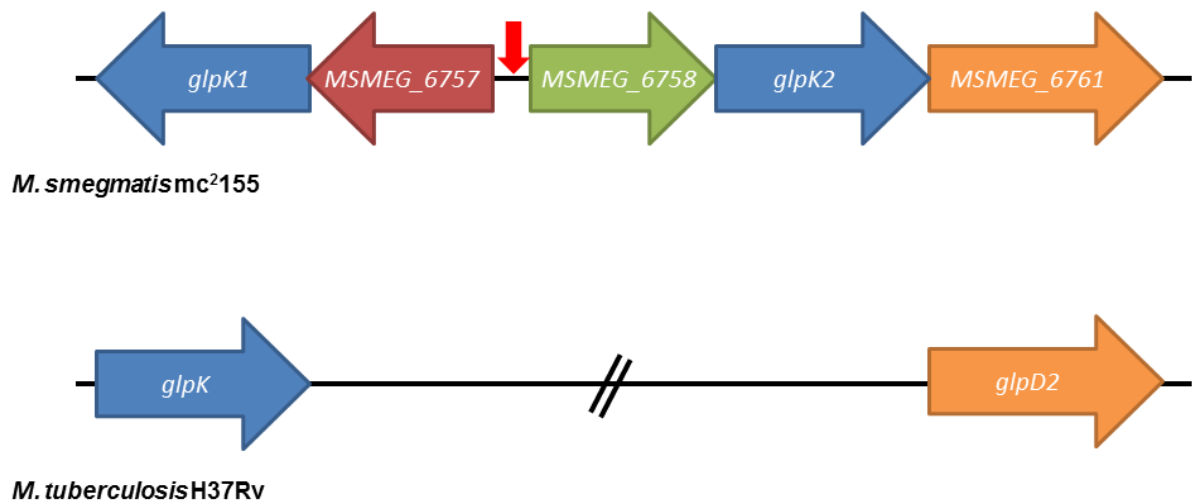


**Figure 2.13. Genetic organisation of the glycerol operon cluster in *M. smegmatis* and *M. tuberculosis*.** Red arrow indicates position of SNP in the AKR334-resistant *M. smegmatis* mutant.

In *M. smegmatis*, MSMEG\_6756 (*glpK1*) and MSMEG\_6759 (*glpK2*) genes encode glycerol kinases. These enzymes convert incoming glycerol into glycerol-3-phosphate via the transfer of a phosphate from ATP to glycerol, thus catalysing the following reaction:  $\text{ATP} + \text{glycerol} \rightleftharpoons \text{ADP} + \text{sn-glycerol 3-phosphate}$  (Titgemeyer *et al.*, 2007). While *M. smegmatis* possesses two glycerol kinases, by contrast, *M. tuberculosis* has just one glycerol kinase encoded by Rv3696c (*RvglpK*), which shows high similarity to those in *M. smegmatis* (55% protein identity for MSMEG\_6756 and 77% protein identity for MSMEG\_6759). In *M. smegmatis*,

*MSMEG\_6761*, part of the glycerol operon gene cluster, codes for a glycerol-3-phosphate dehydrogenase. This shares 56% protein identity with glycerol-3-phosphate dehydrogenase encoded by *glpD2*. The *M. smegmatis* glycerol operon also includes *MSMEG\_6757* and *MSMEG\_6758* genes, which encode a glycerol operon regulatory protein and a glycerol transport protein, respectively. However, a BLAST search did not identify any similar proteins in *M. tuberculosis*.

### 2.3.3 Over-expression of glycerol operon genes in *M. smegmatis*

To identify whether or not any of the proteins, which comprise part of the *M. smegmatis* glycerol operon were the cellular target of AKR334, the glycerol kinase (*MSMEG\_6756* and *MSMEG\_6759*), the glycerol operon regulatory protein (*MSMEG\_6757*), glycerol transport protein (*MSMEG\_6758*) and glycerol kinase (*Rv3696c*) from *M. tuberculosis* were overexpressed in *M. smegmatis* using the expression plasmid vector pMV261 (containing a kanamycin resistance selection marker) and the MIC of AKR334 inhibitor was reassessed. The pMV261 vector exerts approximately 5 times copy number. Additionally, when an empty pMV261 vector was electroporated into *M. smegmatis* and tested against AKR334, the MIC increased from 5 µg/ml to 8 µg/ml; therefore, the presence of kanamycin increases the MIC of AKR334 inhibitor in *M. smegmatis*. All constructs were successfully electroporated into *M. smegmatis*, except for pMV261-*MSMEG\_6758* which did not yield any colonies. Successful transformants of the remaining constructs were grown in liquid culture and spotted onto plates containing the MIC of AKR334 inhibitor in the presence of kanamycin. However, none of the recombinant strains was able to grow at the MIC value. Over-expression of the glycerol operon genes did not increase the

MIC of AKR334 inhibitor; as a result we could not determine that whether or not these genes were the drug target.

#### **2.3.4 MmpL3 protein is not the cellular target of AKR334**

As previously described, spontaneous mutants resistant to SQ109 (Tahlan *et al.*, 2012), adamantyl ureas (Grzegorzewicz *et al.*, 2012) and pyrrole BM212 (La Rosa *et al.*, 2012), compounds with known anti-TB activities, were shown to contain mutations in the *mmpL3* gene. Studies have shown that MmpL3 protein is involved in the transport of TMMs across the cell wall where they are then converted to TDMs (Varela *et al.*, 2012). Experiments where bacilli were exposed to SQ109 and adamantyl ureas led to the accumulation of TMM, thus proving MmpL3 protein is the cellular target of these inhibitors (La Rosa *et al.*, 2012; Tahlan *et al.*, 2012). Recent studies have used this method to show that THPP and spiro analogues target the MmpL3 protein (Remuiñán *et al.*, 2013). To address the putative role of MmpL3 in TMM export, we assessed the effects of increasing concentrations of AKR334 on lipid metabolism in *M. smegmatis*. Cultures of the wild-type and AKR334-resistant *M. smegmatis* strains were grown in broth in the presence (0.5× MIC and 1× MIC) or absence of inhibitor for 4 hours, then labelled with [1,2-<sup>14</sup>C]acetate overnight and then subjected to a lipid extraction procedure. In wild-type *M. smegmatis* [1,2-<sup>14</sup>C]acetate-labelled cultures, TMM levels remained the same in cultures grown in the absence of inhibitor and cultures grown in increasing concentrations of AKR334 inhibitor, suggesting MmpL3 protein is not the cellular target (Figure 2.14). However, AKR334-resistant [<sup>14</sup>C]-labelled cultures, grown in increasing concentrations of AKR334 inhibitor, showed an accumulation of TDM.



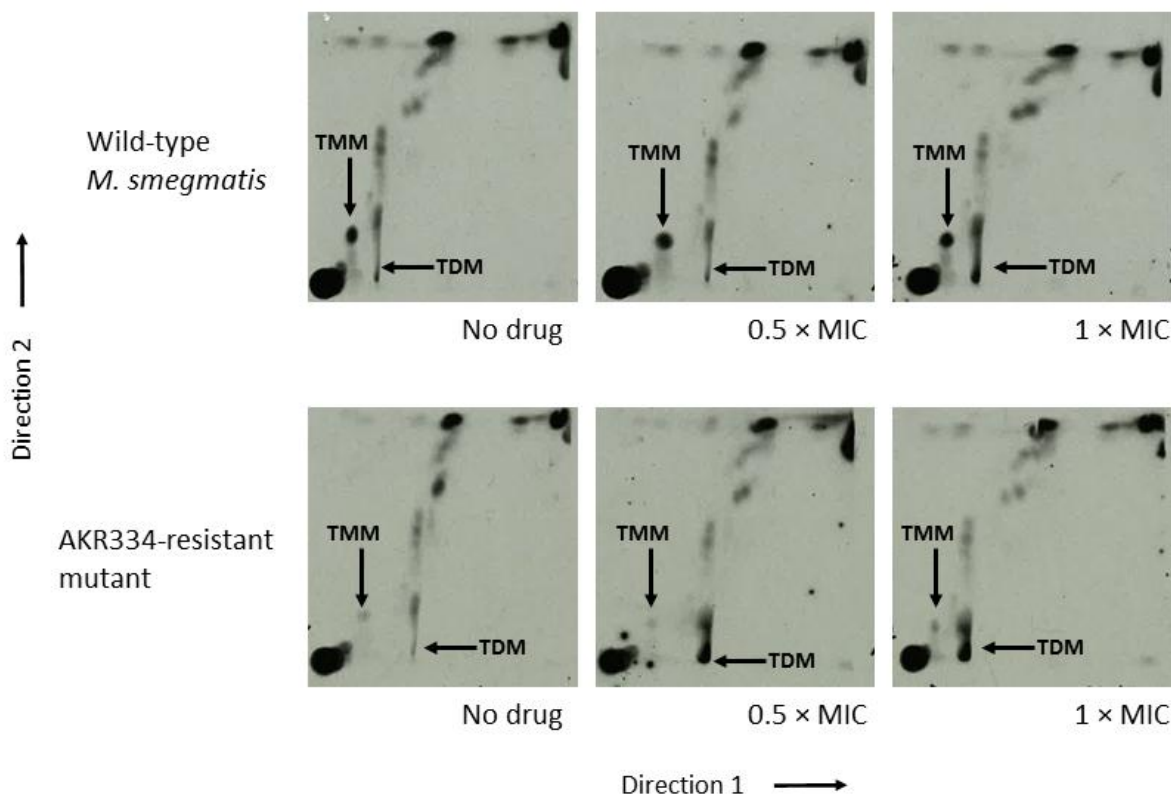


**Figure 2.14. 2D-TLC analysis of [1,2-<sup>14</sup>C]acetate-labelled lipids from wild-type and AKR334-resistant *M. smegmatis* strains in the presence of AKR334 inhibitor.** Cultures were grown in the absence and presence of AKR334 inhibitor (0.5 × MIC and 1 × MIC) for 4 hours, and then and labelled using [1,2-<sup>14</sup>C]acetate overnight. Equal counts of polar lipid extracts (50,000 cpm) were applied to TLC plates which were developed using solvent system D for polar lipids: CHCl<sub>3</sub>:CH<sub>3</sub>OH:H<sub>2</sub>O (100:14:0.8) in the first direction and CHCl<sub>3</sub>:acetone: MeOH: H<sub>2</sub>O (50:60:2.5:3) in the second direction. Polar lipids were visualised by 48 h exposure on X-ray films by autoradiography (Kodak Biomax MR film).

### 2.3.5 AKR334 displays greater inhibitory activity in the presence of glycerol as a carbon source

Recent studies have identified frame-shift mutations in *glpK* in spontaneous mutants of inhibitors against *M. tuberculosis*, indicating their mechanism of action is linked to glycerol metabolism (Pethe *et al.*, 2010; Stanley *et al.*, 2012). Pyrimidine-imidazoles (PI) are a novel class of compounds which kill bacilli by inducing self-poisoning of *M. tuberculosis* through accumulation of glycerol phosphate and rapid ATP depletion (Pethe *et al.*, 2010). However, these compounds have shown no efficacy in animal

models of TB (Petthe *et al.*, 2010). The A039 compound ((1-(4-ethoxyphenyl)-2-(4-methoxyphenyl)-6,7,8,9-tetrahydro-5H-imidazo[1,2-a]azepin-1-ium chloride) was shown to have greater inhibitory activity against *M. tuberculosis* grown on media containing glycerol as a sole carbon source compared to media containing acetate. To confirm that the observed activity of AKR334 against *M. smegmatis* is dependent upon growth in glycerol-containing media, we compared the activity of AKR334 against *M. smegmatis* grown in liquid media containing glycerol or acetate as the sole carbon source. *M. smegmatis* was grown in the following concentrations of AKR334 inhibitor: 8 µg/ml, 10 µg/ml and 14 µg/ml. Cultures were incubated at 37 °C and the OD<sub>600</sub> was measured after 24 hours. The OD<sub>600</sub> of *M. smegmatis* culture grown in the absence of the inhibitor was also measured and this was used to calculate the percentage of bacterial killing at each drug concentration (Figure 2.15). The inhibitory activity of AKR334 was higher in *M. smegmatis* cultures grown in the presence of glycerol compared to those cultures grown in the presence of acetate. The activity of AKR334 inhibitor was dependent on the presence of glycerol as a sole carbon source.

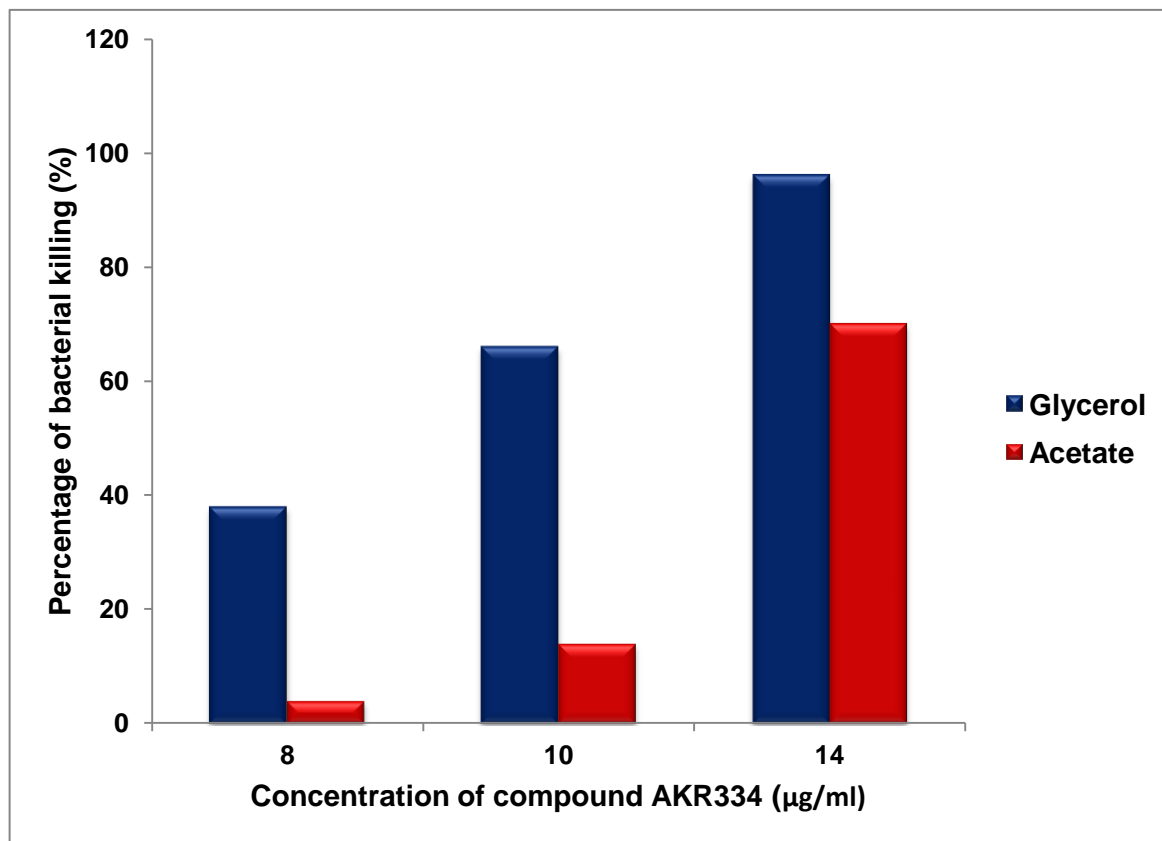


**Figure 2.15. Percentage of bacterial killing of *M. smegmatis* in liquid media containing varying concentrations of compound AKR539 with acetate or glycerol as the carbon source.** *M. smegmatis* cultures were grown in varying concentrations of AKR334 inhibitor with liquid media containing glycerol or acetate as the sole carbon source and incubated at 37 °C. OD<sub>600</sub> was measured after 24 hours. The OD<sub>600</sub> of *M. smegmatis* culture grown in the absence of the inhibitor was also measured and this was used to calculate the percentage of bacterial killing at each drug concentration.

## 2.4 Conclusion

In this Chapter, compounds, which have previously been identified to possess inhibitory activity against *M. tuberculosis* were screened against *M. smegmatis* which has a comparatively faster generation time and can be handled without BSL-3 facilities. Spontaneous resistant mutants were generated against AKR334, a compound which displayed an encouraging MIC value against *M. smegmatis*. Through the alignment of the whole-cell genomic sequence of parental and AKR334-

resistant *M. smegmatis* strains, SNPs were found in the *mmpL3* gene and the promoter sequence of the *glpK* genes.

Previous studies have demonstrated that MmpL3 specifically plays an essential role in mycolic acid transport and that depleting the *mmpL3* gene in a conditional mutant resulted in the intracellular accumulation of TMM (Varela *et al.*, 2012). These results are supported by *mmpL3*-inhibitor related studies where it was observed that inhibition of *mmpL3* resulted in TMM accumulation (La Rosa *et al.*, 2012; Tahlan *et al.*, 2012; Remuiñán *et al.*, 2013). However, in our study, when cells were treated with AKR334, there was no difference in the levels of TMM compared to untreated cells whereas. This ruled out the MmpL3 protein as the cellular target of AKR334.

In a parallel experiment, genes from the glycerol operon cluster in *M. smegmatis* and the *glpK* gene from *M. tuberculosis* were overexpressed in *M. smegmatis* using the mycobacterial vector pMV261, which exerts approximately 5 times copy number. However, overexpression of these genes did not lead to any change in tolerance to AKR334. Therefore, from this experiment, we were unable to determine whether the *glpK* genes were the drug target of AKR334.

We also tested the hypothesis that the mechanism of action of AKR334 is related to the metabolism of different carbon sources. When *M. smegmatis* cells were treated with AKR334 in the presence of glycerol, there was a higher percentage of bacterial killing after 24 hours compared to those cells grown in the presence of acetate. This indicates that the mode of action of AKR334 is possibly associated with glycerol

metabolism. Recently, the mechanisms of action of inhibitors against *M. tuberculosis* have been shown to be linked to glycerol metabolism (Pethe *et al.*, 2010; Stanley *et al.*, 2012). PI inhibitors were demonstrated to induce self-poisoning in *M. tuberculosis* by stimulating the accumulation of glycerol phosphate and leading to rapid depletion of ATP, which leads to poisoning of the cells, have been identified (Pethe *et al.*, 2010). Therefore, further work using experiments to analyse glycerol phosphate levels in AKR334-treated cells could be done to determine whether AKR334 works in the same way as PI inhibitors. In addition to this, we could conduct a comparative analysis of the transcription of the *glpK* genes in the parental and AKR-resistant mutant strains using Reverse Transcription PCR. This would allow us to examine whether there is a difference in the expression of these genes and help identify the mode of action of AKR334.

In conclusion, this Chapter sums up the identification of a new inhibitor which possibly causes killing of *M. smegmatis* via toxic poisoning through the accumulation of glycerol phosphate and ATP depletion. Further studies are needed to confirm the mechanism of action of AKR334.

**3 The essentiality of Ppm1-encoded  
polyprenyl  
monophosphomannose synthase  
in lipoglycan biosynthesis in  
mycobacteria**

### 3.1 Introduction

#### 3.1.1 Immunomodulatory properties of LM and LAM

LAM and related lipoglycans are not only essential for mycobacterial growth and survival (Haites *et al.*, 2005; Kovacevic *et al.*, 2006), but are also thought to play important roles in the modulation of the host response during infection. During the last decade, investigators have isolated LAM and LM from a range of mycobacteria with various capping motifs to investigate the broad spectrum of immunomodulatory activities displayed by these complex polysaccharides and to gain insight into the nature of these host-pathogen interactions.

The ability of mycobacteria to survive within the hostile environment of host macrophages is central to the disease and is made possible through several strategies. These include manipulation of the phagosome to prevent maturation (Armstrong and Hart, 1971; Russell, 2001; Nguyen and Pieters, 2005) and suppression of the cell-mediated host immune response after infection. Several studies have demonstrated that lipoglycans have a major role in both of these phenomena. The nature of these immunomodulatory responses is determined by the accessibility of lipoglycans with different receptors of the immune system, such as TLR-2 and C-type lectins.

##### 3.1.1.1 Phagosome maturation arrest

As described before (section 1.3), *M. tuberculosis* bacilli are able to persist within macrophages by preventing the fusion of phagosomes with lysosomes, a process

that would normally lead to killing and digestion of the pathogen in an acidic environment (Armstrong and Hart, 1971; Russell, 2001; Nguyen and Pieters, 2005). ManLAM has been demonstrated to play a role in the inhibition of phagosome maturation (Figure 3.1) (Vergne *et al.*, 2003). During infection, the phagosome-lysosome fusion process is initiated through an increase in concentration of cytosolic  $\text{Ca}^{2+}$ . ManLAM inhibits this uptake of  $\text{Ca}^{2+}$ , thus blocking the successive steps of PI3-hVPS34 kinase activity at the phagosomal membrane (Malik *et al.*, 2001; Vergne *et al.*, 2004; Vergne *et al.*, 2004; Chua and Deretic, 2004). Normally in this process, PI3-kinase alongside its modulatory subunit p150 will lead to the production of the membrane-trafficking lipid phosphatidylinositol 3-phosphate (PI3P) which subsequently mediates the recruitment of Rab 5 effector early endosome autoantigen 1 (EEA1) to the phagosome (Vergne, Chua, *et al.*, 2004). EEA1 is necessary for the delivery of cathepsins (lysosomal hydrolases) and  $\text{V}_0\text{H}^+$  ATPase from the *trans*-Golgi network to the phagosome *via* interaction with syntaxin-6, soluble NSF attachment protein receptor (SNARE) protein (Simonsen *et al.*, 1999).

The exact mechanism by which ManLAM modulates  $\text{Ca}^{2+}$  fluxes is unknown. It has been suggested that ManLAM activates the macrophage phosphatase SHP-1 leading to the impairment of  $\text{Ca}^{2+}$  signalling (Vergne, Chua, *et al.*, 2004). It has also been reported that ManLAM may cause phagosome maturation arrest by activating p38 mitogen-activated protein kinase (p38 MAPK), a mechanism distinct from blocking the rise of cytosolic  $\text{Ca}^{2+}$ . Furthermore, ManLAM has been implicated as a trigger for an increase in p38 MAPK activation, leading to modulation of EEA1 recruitment (Fratti, Chua, and Deretic, 2003). However, recent experiments have



shown that isolated ManLAM does not influence p38 MAPK activation (Welin *et al.*, 2008).

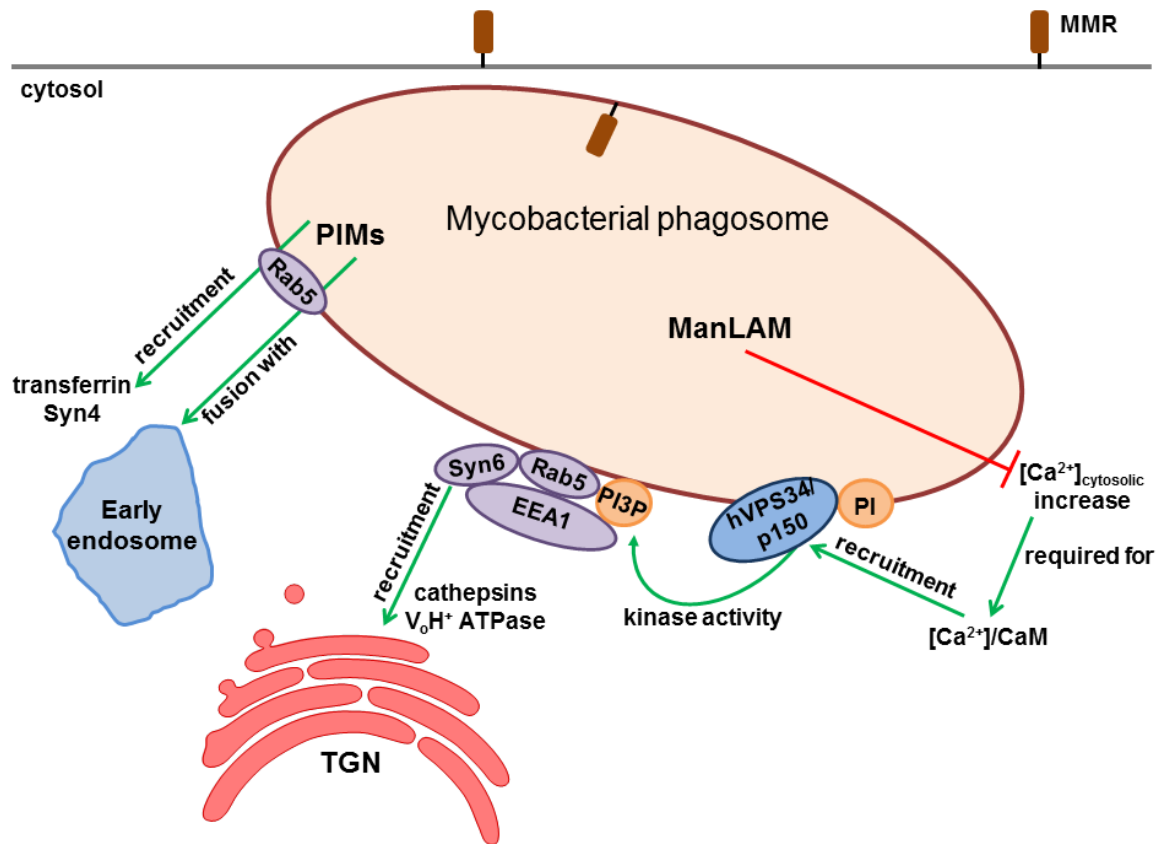


**Figure 3.1. The role of ManLAM and PIMs in phagosome maturation arrest in mycobacteria.** ManLAM inhibits lysosomal fusion and acidification by inhibiting cytosolic- $\text{Ca}^{2+}$  increase and thereby blocks the successive steps of hVPS34 kinase activity, the recruitment of Rab5, EEA1 and Syn6, and the delivery of cathepsins and  $\text{VoH}^+$  ATPase to the phagosome. PIMs induce the fusion of the phagosome with early endosomes to promote delivery of nutrients to the bacteria; this mechanism is dependent on Rab5. CaM, Calmodulin; EEA1, Early endosome autoantigen; MMR, Macrophage mannose receptor; PI3P, Phosphatidylinositol 3-phosphate; Syn, Syntaxin; TGN, trans-Golgi network. Adapted from Mishra *et al.*, (2011).

As well as ManLAM, PIMs and LM have also been investigated for their possible role in affecting phagosome maturation. LM does not interfere with phagolysosomal development (Kang *et al.*, 2005). However, similarly to LAM, PIMs appear to be involved in this process *via* incorporation into lipid rafts (Vergne *et al.*, 2004), which are cholesterol and glycosphingolipid-rich domains that are associated with cell

signalling processes, thereby competitively inhibiting insertion of LAM (Welin *et al.*, 2008). PIMs appear to stimulate the fusion of phagosomes with early endosomes to provide nutrients to mycobacteria residing in the phagosome (Figure 3.1) (Kelley and Schorey, 2003; Vergne *et al.*, 2004). Although PIMs seem to have the opposite to the effect of LAM, which prevents endosomal fusion, they are also involved in the inhibition of phagosome acidification by inducing recruitment of syntaxin-4 and the transferrin receptor (involved in iron delivery) (Fratti *et al.*, 2003; Vergne *et al.*, 2004; Vergne, *et al.*, 2004).

Despite their differences in the influence of phagosome maturation, both ManLAM and PIMs may be involved in recognition by the mannose receptor (MR) (Vergne *et al.*, 2004). Recent studies have demonstrated that MR has a higher affinity to higher-order PIMs (e.g. PIM<sub>5</sub> and PIM<sub>6</sub>) than to lower-order PIMs (i.e. PIM<sub>2</sub>), which are not recognised (Torrelles *et al.*, 2006).

### **3.1.1.2 Cluster of differentiation (CD)1 glycoproteins**

Cluster of differentiation (CD)1 glycoproteins are related to major histocompatibility complex (MHC) class I and II molecules, which are important antigen-presenting molecules of the immune system. While MHC class I and II molecules are responsible for presenting peptide antigens to T-cells, CD1 glycoproteins have been identified to present glycolipids to CD1-restricted T cells (Young and Moody, 2006; De Libero and Mori, 2010). Therefore, in mycobacterial infection, exposure to unique

glycolipids of the mycobacterial cell wall differentially elicits CD1-restricted innate and adaptive T-cell responses (Porcelli *et al.*, 1998; Barral and Brenner, 2007).

The CD1 family can be categorised into three groups: group 1 includes CD1a, CD1b and CD1c; group 2 includes CD1d; and group 3 includes CD1e (Barral and Brenner, 2007). From these CD1 molecules, CD1b and CD1d have been identified as binding and presenting PIMs and related lipoglycans. While CD1b can bind to PIM<sub>2</sub> and ManLAM (Fischer *et al.*, 2004; Zajonc *et al.*, 2006), CD1d can only bind to lower-order PIMs, including PIM<sub>2</sub> and PIM<sub>4</sub>, but not LM or ManLAM (Sieling *et al.*, 1995; Prigozy *et al.*, 1997; Ernst *et al.*, 1998).

Recent studies have shown that mycobacteria have the ability to impair the function and expression of CD1 molecules and in doing so, provide a way to evade the host immune response (Gagliardi *et al.*, 2007; Gagliardi *et al.*, 2009). For example,  $\alpha$ -glucan has been demonstrated to induce monocyte differentiation into dendritic cells, thereby blocking the expression of CD1 molecules and preventing them from presenting lipid antigens to CD1-restricted T-cell clones (Gagliardi *et al.*, 2007).

### **3.1.1.3 Toll-like receptors (TLR)**

TLRs have been demonstrated to play a role in the recognition of mycobacterial pathogens (Quesniaux, Fremont, *et al.*, 2004; Jo, 2008). Although lipoproteins are the major ligands for TLR2 (Brightbill *et al.*, 1999), MPI-anchored mannosylated lipoglycans can also signal *via* TLR2, depending on their degree of acylation and mannosylation (Gilleron *et al.*, 2006; Doz *et al.*, 2007; Nigou *et al.*, 2008). For

example, there is a positive correlation between mannan chain length and the ability of the lipoglycan to activate TLR2 (Nigou *et al.*, 2008). LM, has been shown to be a potent inducer of TLR2-signalling (Quesniaux *et al.*, 2004); however, this activity is limited to the tri- and tetra-acylated forms (Ac<sub>3</sub>LM and Ac<sub>4</sub>LM, respectively) (Gilleron *et al.*, 2006; Doz *et al.*, 2007). Studies have reported that in comparison to Ac<sub>1</sub>/Ac<sub>2</sub>PIM<sub>6</sub> and LM, Ac<sub>1</sub>/Ac<sub>2</sub>LAM, PILAM and AraLAM were shown to be poor inducers of TLR2 (Nigou *et al.*, 2008). Recently, this was demonstrated in an experiment where LAM comprising a truncated arabinan domain from a *M. smegmatis* AftC knock-out mutant showed enhanced TLR2-signalling compared to wild-type LAM (Birch *et al.*, 2010). This indicates the arabinan domain prevents proper interaction of LAM with TLR2 (Vignal *et al.*, 2003).

#### 3.1.1.4 DC-SIGN

The interaction of mycobacteria and dendritic cells (DC) is largely mediated by a C-type lectin receptor called dendritic cell-specific intercellular adhesion molecule-3 (ICAM-3) grabbing nonintegrin (DC-SIGN) (Tailleux *et al.*, 2003). While the exact role of DC-SIGN in mycobacterial infection is unclear, it has been reported that ManLAM interacts with DC-SIGN to prevent DC maturation, thereby suppressing the immune response (Geijtenbeek *et al.*, 2003).

As well as only recognising LAM that is mannose-capped (Geijtenbeek *et al.*, 2003; Maeda *et al.*, 2003), DC-SIGN has a stronger affinity to increasing  $\alpha(1\rightarrow2)$ -linked Man<sub>p</sub> residue chain length (Koppel *et al.*, 2004). Thus, higher-order PIMs, including

PIM<sub>5</sub> and PIM<sub>6</sub>, are recognised by DC-SIGN with a higher affinity than are lower-order PIMs (Boonyarattanakalin *et al.*, 2008; Driessen *et al.*, 2009).

Although DC-SIGN is thought to be a vital uptake receptor to infect DCs, recent studies have demonstrated that ManLAM binding to lipopolysaccharide-activated DCs leads to a rise in the secretion of proinflammatory IL-12 and IL-6 as well as IL-10 (Gringhuis *et al.*, 2009). Therefore, it may be possible that DC-SIGN signalling may function primarily in the protection of the host (Ehlers, 2010).

#### **3.1.1.5 Mannose receptor (MR)**

In addition to complement receptors, mannose receptors (MR), a type I transmembrane monomeric C-type lectin, are important mediators for phagocytic uptake of mycobacteria by macrophages (Schlesinger, 1993). For example, a recent study has shown that binding of ManLAM to MR during phagosomal development is a key step in inhibition of fusion with lysosomes (Kang *et al.*, 2005). That MR only binds ManLAM and not AraLAM or PILAM, shows that the presence of a mannose cap on ManLAM is essential for the recognition by the MR (Schlesinger *et al.*, 1994). This observation further demonstrates that the macrophage MR is necessary for blocking phagosome maturation, a step which is more prevalent in virulent strains of mycobacteria (Kang *et al.*, 2005). Unsurprisingly, MR binds PIM<sub>5</sub> and PIM<sub>6</sub>, with a preference for the tri-acylated species rather than the tetra-acylated, but not to lower-order PIM<sub>2</sub>, LM and AraLAM or PILAM (Schlesinger *et al.*, 1994; Villeneuve *et al.*, 2005; Torrelles *et al.*, 2006). The macrophage MR has also been implicated in the

delivery of LAM to the late endosomal compartments for loading on to CD1b molecules, thus inducing T-cell immune response (Prigozy *et al.*, 1997).

### 3.1.2 Biosynthesis of PIMs, LM and LAM

Deciphering the biosynthetic pathway of PIMs, LM and LAM has been central to biochemical and genetic studies in recent times. These studies have proposed the following model for PIM biosynthesis: PI→PIM<sub>2</sub>→PIM<sub>4</sub>→PIM<sub>6</sub>. Glycosylation of PI is sequentially catalysed by the  $\alpha$ -mannopyranosyltransferases PimA, PimB', PimC and PimE and occurs on the cytosolic face of the plasma membrane (Figure 3.2) (Besra and Brennan, 1997; Morita *et al.*, 2006; Mishra *et al.*, 2011). In the first step of the pathway, PimA (Rv2610c), an enzyme of the GT-B superfamily, catalyses the addition of a Man<sub>p</sub> residue, using GDP-mannose as the donor to position O-2 of PI to generate PIM<sub>1</sub> (Korduláková *et al.*, 2002; Guerin *et al.*, 2007) which is subsequently acylated by Rv2611c at the 6-position of the Man<sub>p</sub> residue (Korduláková *et al.*, 2003). The acyltransferase role of Rv2611c was determined in a study where a Rv2611c mutant of *M. smegmatis* exhibited severe growth defects and accumulated non-acylated PIM<sub>1</sub> and PIM<sub>2</sub> (Korduláková *et al.*, 2003). A second mannosylation step, catalysed by PimB' (Rv2188c), introduces another Man<sub>p</sub> residue at position O-6 of PI to produce Ac<sub>1</sub>/Ac<sub>2</sub>PIM<sub>2</sub> (Mishra *et al.*, 2008). Initially, this reaction was thought to be performed by PimB (Rv0557c) (Schaeffer *et al.*, 1999); however, it was subsequently shown that disruption of this gene had no effect on Ac<sub>1</sub>PIM<sub>2</sub> biosynthesis in *M. tuberculosis* (Torrelles *et al.*, 2009). However, deletion of PimB' in *C. glutamicum* resulted in a mutant devoid of Ac<sub>1</sub>/Ac<sub>2</sub>PIM<sub>2</sub> and accumulation of

Ac<sub>1</sub>PIM<sub>1</sub>, thereby confirming the α-D-mannose-α(1→6)-phosphatidyl-*myo*-inositol-mannopyranosyltransferase activity of PimB' (Mishra *et al.*, 2008).

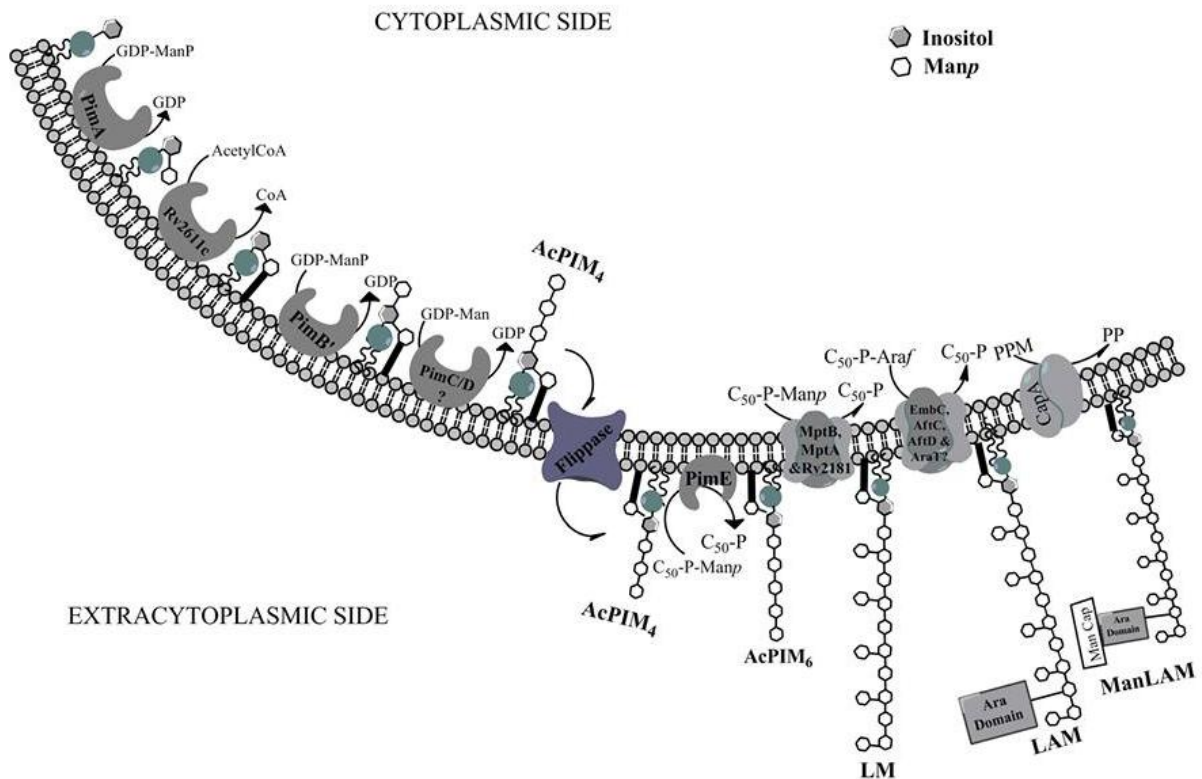


**Figure 3.2. Pathway of biogenesis of phosphatidyl-*myo*-inositol mannosides, lipomannan and lipoarabinomannan biosynthesis in *M. tuberculosis*.** PI is glycosylated by PimA, PimB' (Guerin *et al.*, 2007; Guerin *et al.*, 2009) and acylated by Rv2611c to form AcPIM<sub>2</sub> (Korduláková *et al.*, 2003), which is further mannosylated by PimC or possibly PimD to form AcPIM<sub>4</sub> (Mishra *et al.*, 2011). AcPIM<sub>4</sub> is probably transported to the extracytoplasmic side by an unidentified flippase and further mannosylated by PimE and/or another unidentified enzyme to form AcPIM<sub>6</sub> (Morita *et al.*, 2006). AcPIM<sub>4</sub> is sequentially extended by MptB, MptA and MptC resulting in lipomannan (Mishra *et al.*, 2007; Mishra, Alderwick, *et al.*, 2008; Mishra, Krumbach, *et al.*, 2011). Lipomannan is then primed by an unidentified arabinofuranosyltransferase, which is extended by EmbC, AftD and AftC to form Ara-4 or branched Ara-6 (Birch *et al.*, 2008; Skovierová *et al.*, 2009; Birch *et al.*, 2010), while AftB terminates the chain to form LAM (Seidel *et al.*, 2007). LAM is capped by CapA and Rv2181 (MptC) to form ManLAM (Dinadayala *et al.*, 2006). GDP, Guanosine diphosphate; LAM; Lipoarabinomannan; LM, Lipomannan; ManLAM, Mannosyl-lipoarabinomannan; PI, Phosphatidylinositol; PIM, Phosphatidyl-*myo*-inositol. Manp, Mannopyranose; Araf, Arabinofuranose. Adapted from Jankute *et al.*, (2012).

Biochemical studies of the *M. tuberculosis* CDC1551 strain led to the identification of RvD2-ORF1 as the mannosyltransferase PimC with Ac<sub>1</sub>PIM<sub>2</sub>: α-D-mannose-α(1→6)-phosphatidyl-*myo*-inositol-mannopyranosyltransferase activity, responsible for the

addition of a Man<sub>p</sub> residue to the 6-OH of mannose at the non-reducing end of Ac<sub>1</sub>/Ac<sub>2</sub>PIM<sub>2</sub>, to form Ac<sub>1</sub>/Ac<sub>2</sub>PIM<sub>3</sub> (Kremer *et al.*, 2002). This was demonstrated in a study in which a cell-free assay containing GDP-[<sup>14</sup>C] mannose, amphomycin (an antibiotic that inhibits the PPM synthase) and membranes from *M. smegmatis* overexpressing PimC led to the synthesis of Ac<sub>1</sub>/Ac<sub>2</sub>PIM<sub>3</sub> (Kremer *et al.*, 2002). The addition of a Man<sub>p</sub> residue from GDP-mannose to the 6-OH of mannose at the non-reducing end of Ac<sub>1</sub>/Ac<sub>2</sub>PIM<sub>3</sub> to generate Ac<sub>1</sub>/Ac<sub>2</sub>PIM<sub>4</sub> is catalysed by either an unknown α(1→6)-mannopyranosyltransferase (PimD) or PimC itself (Mishra *et al.*, 2011). While mannosyltransferases utilising nucleotide-derived sugar donors are employed in the mannosylation steps leading to this point, from here on mannosyltransferases from the GT-C superfamily utilising polyprenylphosphate-based mannosyl donors are used for elongation and branching of LM and LAM (Liu and Mushegian, 2003; Guerin *et al.*, 2010).

From Ac<sub>1</sub>/Ac<sub>2</sub>PIM<sub>4</sub>, the biosynthetic pathway diverges into two branches: one leads to the formation of Ac<sub>1</sub>/Ac<sub>2</sub>PIM<sub>6</sub>, whereas the other leads to the formation of LM and LAM. PimE (Rv1159), a recently identified α(1→2)-mannopyranosyltransferase, utilises the polyprenylphosphate sugars PPM/C<sub>50</sub>-P-Man as a donor to add an α(1→2)-Man<sub>p</sub> residue to Ac<sub>1</sub>/Ac<sub>2</sub>PIM<sub>4</sub> in the synthesis of Ac<sub>1</sub>/Ac<sub>2</sub>PIM<sub>5</sub> (Morita *et al.*, 2006). A successive α(1→2)-Man<sub>p</sub> residue is added on to Ac<sub>1</sub>/Ac<sub>2</sub>PIM<sub>5</sub> to produce Ac<sub>1</sub>/Ac<sub>2</sub>PIM<sub>6</sub>. Although the putative glycosyltransferase responsible for this last reaction is currently uncharacterised, it is thought to be encoded by Rv0051 or Rv0541 (Liu and Mushegian, 2003; Berg *et al.*, 2007). While PimE directs Ac<sub>1</sub>/Ac<sub>2</sub>PIM<sub>4</sub> towards Ac<sub>1</sub>/Ac<sub>2</sub>PIM<sub>6</sub> production, the LpqW channel, which *M.*



*smegmatis* regulates the amount of higher PIMs and lipoglycans, is thought to channel  $Ac_1/Ac_2PIM_4$  towards LM synthesis (Kovacevic *et al.*, 2006; Crellin *et al.*, 2008). It has also been hypothesised that  $Ac_1/Ac_2PIM_4$  is transported across the plasma membrane, by unidentified flippases to become available for further mannosylation by PimE (Liu and Mushegian, 2003; Mishra *et al.*, 2008).

In the second branch of the pathway,  $Ac_1/Ac_2PIM_4$  is hypermannosylated by glycosyltransferases of the GT-C superfamily leading to synthesis of LM. Recent studies have demonstrated that MptA (Rv2174) and MptB (Rv1459c), orthologue of two  $\alpha(1\rightarrow6)$ -mannopyranosyltransferases in *C. glutamicum*, are involved in the synthesis of the mannan backbone (Mishra *et al.*, 2007; Kaur *et al.*, 2007). While MptA synthesises the distal end of the  $\alpha(1\rightarrow6)$  mannan core of LM, MptB catalyses the synthesis of the proximal end through the addition of 12–15 Man<sub>p</sub> residues to the backbone (Mishra *et al.*, 2007; Kaur *et al.*, 2007). A decrease in  $\alpha(1\rightarrow6)$ -mannopyranosyltransferase activity and the absence of LM and LAM, was observed in a MptB-deletion mutant in *C. glutamicum*. Furthermore, cell-free *C. glutamicum* assays using C<sub>50</sub>-P-Man<sub>p</sub> and expressing Rv1459c and/or its *M. smegmatis* homologue MSMEG\_3120 further indicated that these enzymes possess  $\alpha(1\rightarrow6)$ -mannopyranosyltransferase activity. MptC (Rv2181) is responsible for further decorating the  $\alpha(1\rightarrow6)$ -mannan core with a single  $\alpha(1\rightarrow2)$ -Man<sub>p</sub> residue to the side chains of LM (Mishra *et al.*, 2011).

The transition of LM and LAM is thought to involve the initial priming of LM by a few Ara<sub>f</sub> units from the sugar donor decaprenylphosphate arabinan (DPA) in a similar

fashion to how the galactan portion of AG is primed by AftA (Alderwick *et al.*, 2006; Wolucka, 2008). However, the enzyme responsible for this function is uncharacterised. EmbC (Rv3793) is then responsible for further extension of the primed Araf-LM, namely the addition of 12-16  $\alpha(1\rightarrow5)$ -Araf residues (Zhang *et al.*, 2003; Birch *et al.*, 2010). AftC (Rv2673) has been demonstrated to catalyse the addition of the  $\alpha(1\rightarrow3)$ -Araf branch points in LAM (Birch *et al.*, 2010), in a similar manner to AG (Birch *et al.*, 2008). More recently, studies have proposed a second  $\alpha(1\rightarrow3)$ -arabinofuranosyltransferase called AftD (Rv0236c) through experiments based on artificial chemical acceptors on crude membrane extracts from *M. smegmatis* (Skovierová *et al.*, 2009); however, as a viable deletion mutant of this enzyme with a clear phenotype could not be generated, the role of AftD is debatable (Skovierová *et al.*, 2009). AftB (Rv3805c) is likely to be responsible for terminating the arabinan domain in LAM synthesis (Seidel *et al.*, 2007). Although AftB has also been shown to have  $\beta(1\rightarrow2)$ -arabinofuranosyltransferase activity in the synthesis of AG (Seidel *et al.*, 2007), it is possible as observed with AftC that this enzyme has dual functionalities in both AG (Birch *et al.*, 2008) and LAM (Birch *et al.*, 2010).

The homologue of Rv1635c in *M. tuberculosis* CDC1551 was identified as a glycosyltransferase possibly involved in ManLAM capping (Dinadayala *et al.*, 2006). Deletion mutants of homologues of Rv1635c in *M. marinum* and *M. bovis* BCG identified this gene as a PPM-dependent  $\alpha(1\rightarrow5)$ -mannopyranosyltransferase termed CapA, which adds the first Man<sub>p</sub> residue on to the non-reducing arabinan termini of

LAM (B.J. Appelmelk *et al.*, 2008). In *M. tuberculosis*, MptC (Rv2181) has been characterised as a PPM-dependent  $\alpha(1\rightarrow2)$ -mannosyltransferase that plays a bi-functional role in LAM biosynthesis; while it is involved in branching LM, it is also involved in the capping of LAM with  $\alpha(1\rightarrow2)$ -Manp residues at the non-reducing end of LAM (Mishra *et al.*, 2011).

### 3.1.3 Polyprenyl monophosphomannose synthase (PPM synthase) encoded by Ppm1

Comparative studies with known dolichol-monophosphomannose (DPM) synthases led to the identification of Mt-Ppm1 (Rv2051c) in *M. tuberculosis* (Gurcha *et al.*, 2002). Experimental studies conducted *in vitro* have demonstrated that Mt-Ppm1 generates a key PPM sugar donor that utilises GDP-Man and C<sub>50</sub>/C<sub>35</sub>-polyprenol phosphates as substrates, similar to DPM synthase (Gurcha *et al.*, 2002). Although highly conserved within bacterial species, studies have identified subtle alterations in the organisation of the *ppm1* locus across mycobacteria (Gurcha *et al.*, 2002). In *M. tuberculosis*, the well characterised *Mt-ppm1* encodes a large polypeptide comprising of two unique domains: *Mt-ppm1/D1*, which is membrane-anchored *via* six transmembrane segments and *Mt-ppm1/D2* which is sufficient for DPM synthase activity (Gurcha *et al.*, 2002; Baulard *et al.*, 2003). Conversely, in *M. smegmatis*, these two domains are encoded by two separate ORFs arranged in an operon: *MSMEG3860* (Domain 1, Ms-ppm2) and *MSMEG3859* (Domain 2, Ms-ppm1) (Figure 3.3) (Gurcha *et al.*, 2002). This organisation is also found in *M. leprae*, *M. avium* and the related *C. glutamicum* (Gurcha *et al.*, 2002; Gibson *et al.*, 2003). Studies conducted using bacterial two-hybrid systems has demonstrated the interaction

between MSMEG3859 and MSMEG3860 (Baulard *et al.*, 2003) While MSMEG3859 was sufficient for PPM synthase activity, interacting with MSMEG3860 ensured the stability of the synthase (Gurcha *et al.*, 2002; Baulard *et al.*, 2003).

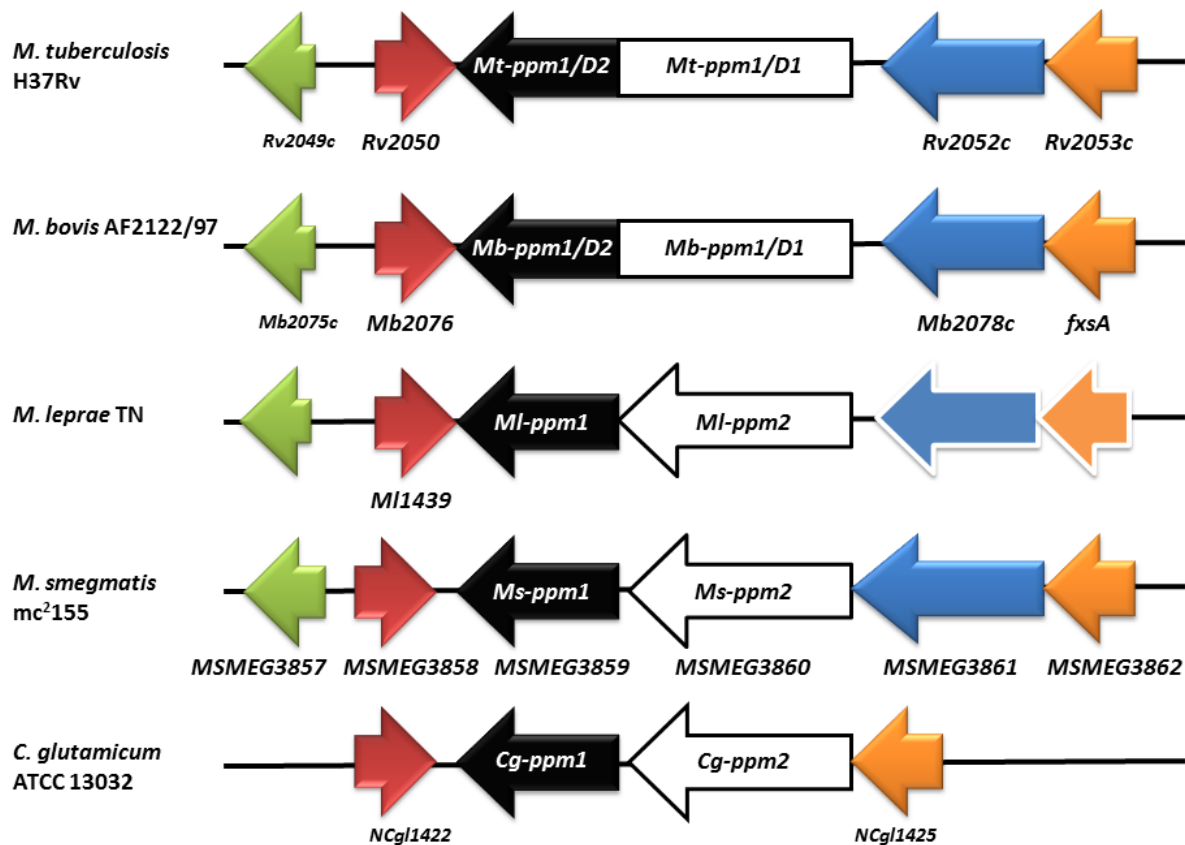


**Figure 3.3. Genomic organisation of the *ppm1* locus in various mycobacteria and in *Corynebacterium glutamicum*.** Homologous genes are indicated by similar coloured arrows and pseudogenes in *M. leprae* are indicated by arrows with white borders. While the *ppm1*-encoded protein consists of two domains fused together in *M. tuberculosis* and *M. bovis*, in *M. leprae*, *M. smegmatis* and *C. glutamicum*, these two domains are encoded by two distinct ORFs.

It was similarly observed in *M. tuberculosis* that a recombinant protein consisting only of the C-terminal domain (*Mt-Ppm1/D2*) was sufficient for production of PPM activity (Gurcha *et al.*, 2002). However, whilst *in vitro* data has established that Mt-Ppm1 (and MSMEG3859) has PPM synthase activity, there have been no genetic studies that determine that Mt-Ppm1 is the sole PPM generating enzyme encoded by the *M.*

*tuberculosis* genome. If this was the case and in light of the crucial role of PPM for biosynthesis of LM/LAM, *Mt-ppm1* would be expected to be an essential gene and thus genetic studies could only be conducted *via* the generation of a conditional knockout strain.

Recently, the report of conflicting results that another membrane-associated glycosyltransferase, Rv3779 functions as a PPM synthase in *M. tuberculosis* (Scherman *et al.*, 2009), and as a glycosyltransferase that uses polyprenyl-P-D-GalNAc as a D-GalNp (or D-GalNAc) donor for transfer to 3,5-branched D-Araf residues of AG (Skovierová *et al.*, 2010), has further necessitated the need to study the *in vivo* role of ppm1 by generation of a conditional mutant strain. Furthermore, a recently published report also describes Rv3631 (*ppgS*) and Rv3632 as genes encoding a polyprenyl-P-D-GalN synthase and a small integral membrane protein, respectively, analogous to Mt-Ppm1/D2 and Mt-Ppm1/D1. While PpgS is a GT-2 family glycosyltransferase, involved in the generation of polyprenyl-phospho-N-acetylgalactosamine (polyprenyl-P-GalNAc) from polyprenyl-P and UDP-GalNAc, it could function as a secondary, prospective PPM synthase.

In order to confirm the *in vivo* function of Mt-Ppm1/D2 in the biogenesis of LM/LAM, we aimed to test the essentiality of PPM glycosyltransferase activity in *M. smegmatis* by using conditional expression specialised transduction essentiality test (CESTET), a genetic tool for determining gene essentiality in *M. smegmatis*. As there are no homologues of *PpgS* or *Rv3779* in *M. smegmatis*, it also provided us with a valuable

surrogate to investigate the *in vivo* role and potential essentiality of *MSMEG3859* in the loss of any potential functional redundancy caused by an alternative PPM synthase. In addition, mutant or conditional mutant strains of *M. smegmatis* could consequently be used as a host strain to test functional complementation of PPM synthase activity using recombinant *PpgS* or *Rv3779*.

## 3.2 Materials and Methods

### 3.2.1 Bacterial strains and growth conditions

Liquid cultures of *M. smegmatis* mc<sup>2</sup>155 strain were grown in Tryptic Soy Broth (TSB), soybean-casein digest medium (BD Difco) supplemented with 0.05% (v/v) Tween-80 (Sigma-Aldrich) in a shaking incubator overnight at 37 °C. For growth on plates, solid media were made with TSB, soybean-casein digest medium (BD, Difco) with addition of 1.5% (w/v) agar. Liquid cultures of *E. coli* were grown in Luria-Bertani (LB) broth in a shaking incubator overnight at 37 °C. For growth on plates, solid media were made with using Luria agar (Fisher Bioreagents). The concentration of the antibiotics used was 50 µg/ml kanamycin for *E. coli*, 25 µg/ml kanamycin for *M. smegmatis*, 50 µg/ml apramycin for *E. coli*, 25 µg/ml apramycin for *M. smegmatis* and 50 ng/ml for *M. smegmatis*.

### 3.2.2 Construction of recombinant plasmids

For producing an integrative vector containing *MSMEG3859*, the ORF was PCR amplified using Phusion High-Fidelity DNA polymerase (New England Labs) from *M. smegmatis* mc<sup>2</sup>155 (Snapper *et al.*, 1990) genomic DNA using the primers F3859

and R3859, cloned downstream of the tetracycline promoter in the integrative vector pTIC6a vector containing a kanamycin resistance selection marker (gift from A. Baughn and W.R. Jacobs Jr., Albert Einstein College of Medicine, NY) and termed pTIC6a-*MSMEG3859*. For subsequent complementation/rescue experiments, the plasmid pMV261Apra, a derivative of pMV261 containing an apramycin resistance selection marker (Stover *et al.*, 1991), was used for cloning various GTFs using Phusion High-Fidelity DNA polymerase (New England Labs). *MSMEG3859* was amplified using primer pairs F3859A and R3859; the C-terminal domain of *Rv2051c* (*Mt-ppm1/D2*) using primer pairs F2051C and R2051C; *Rv3779* using F3779 and R3779; *Rv3631* (*ppgS*) using F3631 and R3631. The-PCR amplified DNA fragments of *MSMEG3859*, *Mt-ppm1/D2*, *Rv3779* and *ppgS* were cloned into pMV261Apra using primer-incorporated restriction sites and the resultant plasmids were named pAKR-*MSMEG3859*, pAKR-*Mt-ppm1/D2*, pAKR-*Rv3779* and pAKR-*ppgS*, respectively. Table 3.1 outlines the sequence and restriction site incorporated in oligonucleotide primers used in the construction of recombinant plasmids. The production of all oligonucleotide primers and the sequencing of generated constructs were performed by Eurofins MWG Operon (Ebersberg, Germany).

**Table 3.1. Oligonucleotide primers used for PCR of various glycosyltransferases from *M. smegmatis* and *M. tuberculosis*. Restriction site is underlined.**

Oligonucleotide	Restriction site	Sequence (5' → 3')
<b>F3859</b>	EcoRI	TCGGA <u>ATTC</u> ATGAGCGTCCCCGGTGAACG
<b>R3859</b>	Clal	GCTATCGA <u>TT</u> CAGCGGACCACGCCCTGG
<b>F3859A</b>	PvuII	GCGGT <u>CAGCT</u> GATGAGCGTCCCCG
<b>F2051C</b>	MscI	GCTGCTGG <u>CCA</u> ACCACCGGCCAGC
<b>R2051C</b>	HindIII	ATA <u>AGCTT</u> CTCATTCCGGTCACGTC
<b>F3779</b>	MscI	GATGG <u>CC</u> AGTGGGCCTGTGGTTCCG
<b>R3779</b>	HindIII	ATA <u>AGCTT</u> CCTAGGAGTGTGTTGC
<b>F3631</b>	MscI	GCTCGTGG <u>CCA</u> ATGGCCTCGAAAA
<b>R3631</b>	Clal	TCGACATCGA <u>TT</u> CATCGTGGCATC

### 3.2.3 Generation of knockout phage for null mutant creation using specialised transduction

Approximately 1 kb sequences of the upstream and downstream regions of the *MSMEG3859-MSMEG3860* genes were PCR-amplified from *M. smegmatis* mc<sup>2</sup>155 genomic DNA using the following primer pairs: RL-3859 (5'-TTTTTTTTCCATAGATTGGTACTCCGTGCTGGTCGAGATG-3') and RR-3859 (5'-TTTTTTTTCCATCTTTTGGCGAGGAGTTTCGACGTAG-3'). Figure 3.4 shows the sequential procedures involved in generation of the knockout phage.



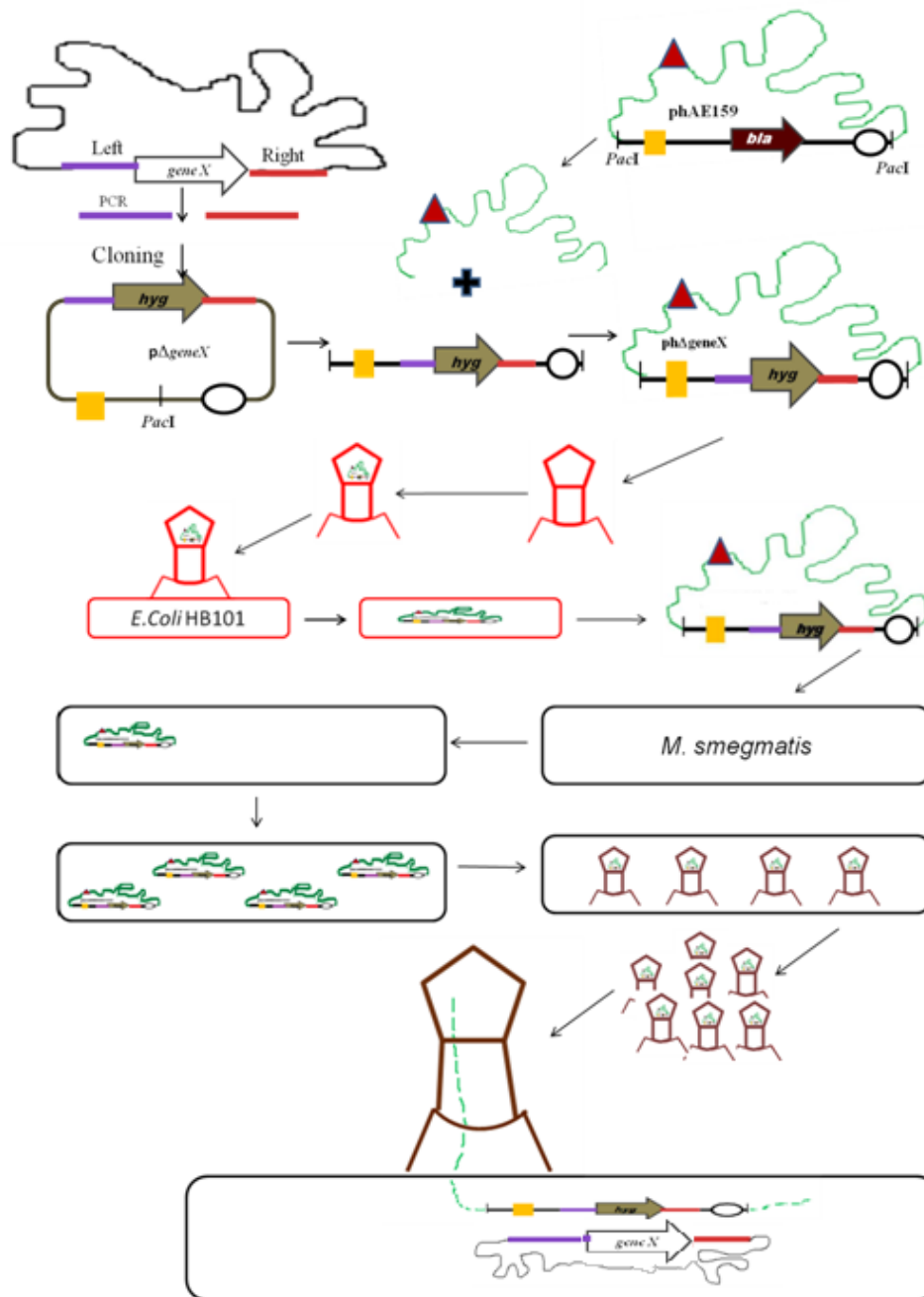


**Figure 3.4. Schematic representation of sequential events leading to the generation of the knockout plasmid.** These steps lead to the generation of a recombinant phage which is used to replace the targeted gene by specialized transduction. Adapted from Bhatt *et al.*, 2009.

The PCR products were purified and the primer incorporated *Van91I* sites were digested with *Van91I*, following which the digested PCR fragments were cloned into *Van91I*-digested p0004S to generate the allelic exchange plasmid ph $\Delta$ MsPpm. One positive plasmid was *PacI* digested and ligated to *PacI* digested phAE159 DNA. The ligation mix was then packaged into empty  $\lambda$ -phage heads and transduced into *E. coli* HB101. Cells containing phasmid DNA were selected for on LB agar containing hygromycin at 37 °C. Packaging of ph $\Delta$ MsPpm into phAE159 was confirmed by *PacI* digestion. The positive phasmids were transformed by electroporation into *M. smegmatis* at 1800V and recovered at 30 °C for ~4 hours in TSB. The recovered cells were then harvested and resuspended in 200  $\mu$ l of MP buffer (50 mM Tris pH 7.8, 150 mM NaCl, 10 mM MgCl<sub>2</sub>, 2 mM CaCl<sub>2</sub>). This was mixed with 200  $\mu$ l of freshly growing *M. smegmatis* and 5 ml molten soft agar (50 °C) and poured on 7H9 basal agar plates and incubated at 30°C for 2 -3 days and allowed to form plaques. The plates were soaked in minimum amount of MP buffer for 5-6 hours and the solution containing phages was filtered and stored at 4 °C. This generated the recombinant phage – ph $\Delta$ MsPpm designed to substitute the *MSMEG3859-MSMEG3860* genes with a hygromycin resistance marker.

#### 3.2.4 Generation of the $\Delta$ MsPpm Conditional Mutant

The *M. smegmatis* conditional mutant  $\Delta$ MsPpm was generated using CESTET (Figure 3.5) (Bhatt *et al.*, 2005). Briefly, the integrative vector pTIC6a-*MSMEG3859* was introduced by electroporation into *M. smegmatis* mc<sup>2</sup>155 to generate a merodiploid strain named mc<sup>2</sup>155::pTIC6a-*MSMEG3859* (Bhatt *et al.*, 2005). Subsequently, the merodiploid strain was subjected to specialised transduction, as

previously described (Bardarov *et al.*, 2002), using a temperature-sensitive, recombinant phage  $\phi\Delta MsPpm$  designed to substitute *MSMEG3859-MSMEG3860* with a hygromycin resistance marker. Transductants were selected at the non-permissive temperature of 37 °C on selective plates containing 25  $\mu\text{g/ml}$  kanamycin, 100  $\mu\text{g/ml}$  hygromycin B and 50 ng/ml anhydrotetracycline (ATc). After replacement of the gene was confirmed by Southern blot, one such transductant was termed the  $\Delta MsPpm$  conditional mutant and was selected for further analysis.

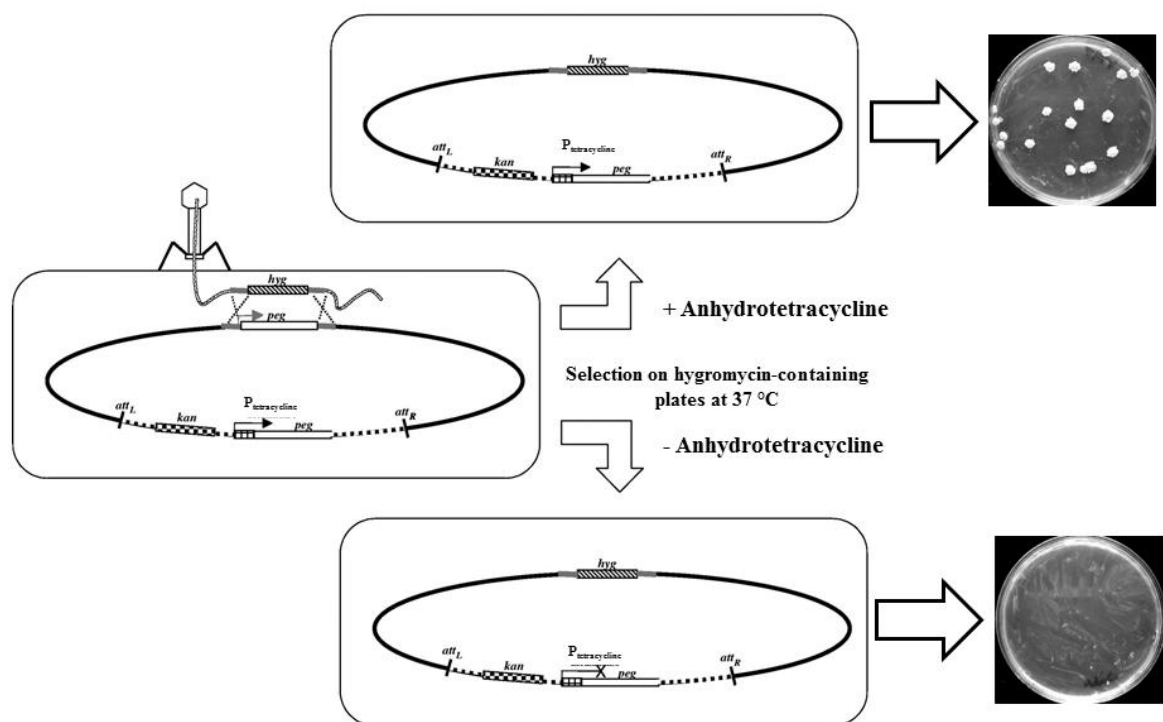


**Figure 3.5. Schematic representation of CESTET.** After specialised transduction using a phage delivery system to replace the putative essential (*peg*) on the bacterial chromosome with a chromosome marker, cells are spread onto plates containing hygromycin with or without anhydrotetracycline. The tetracycline promoter will induce the expression of *peg* in the presence of anhydrotetracycline leading to the growth of bacterial colonies. *kan*, kanamycin resistance cassette; *hyg*, hygromycin resistance cassette; Hyg, hygromycin;  $P_{\text{tetracycline}}$ , inducible tetracycline promoter. The interrupted arc represents the integrative vector, the solid arc represents the  $mc^2155$  chromosome, and the dotted strand represents phage DNA. Adapted from Bhatt *et al.*, 2005.

### 3.2.5 Southern blotting

Genomic DNA was extracted from wild-type *M. smegmatis* and the  $\Delta$ MsPpm conditional mutant strains using the method described in Section 6.9 and digested with *Sma*I. The agarose gel was depurinated in 0.25 M HCl for 10 min, followed by denaturation (1.5 M NaCl, 0.5 M NaOH) for 10 -15 minutes and finally neutralised for 15-20 minutes (0.5 M Tris-HCl pH 7.2, 1 M NaCl ). The DNA on the gel was then transferred onto a nylon membrane (Nylon Membrane, positively charged, No-11209299001, Roche) by capillary transfer with 20 $\times$  SSC (3 M NaCl, 0.3 M sodium citrate, pH 7.0), overnight. DNA was fixed to the membrane by UV cross-linking. After cross-linking, the membrane was rinsed with distilled water and used for hybridisation, labelling and detection. The procedure was performed as described in DIG High Prime DNA Labelling and Detection Starter Kit II (cat no – 11585614910, Roche). This kit uses digoxigenin, a steroid to label DNA probes by random priming. The hybridised probes are then immunodetected by anti-digoxigenin-AP (Fab fragments), which are visualised by chemiluminescence. The expected gene sizes were 1.7 kb and 3.3 kb for the wild-type *M. smegmatis* and 7.4 kb for the  $\Delta$ MsPpm conditional mutant.

### 3.2.6 Conditional depletion of $\Delta$ MsPpm conditional mutant

The  $\Delta$ MsPpm conditional mutant was grown in Tryptic Soy Broth (TSB; BD, Difco) containing 0.05% Tween 80, 25  $\mu$ g/ml kanamycin, 100  $\mu$ g/ml hygromycin B and 50 ng/ml ATc. Subsequently, the  $\Delta$ MsPpm conditional mutant was passaged twice in medium without ATc. To visualise the effects of the conditional depletion of *MSMEG3859* in  $\Delta$ MsPpm on polar lipids and lipoglycans, the strains were grown to

OD 0.8, labelled with 10  $\mu\text{Ci/ml}$  glucose D-[ $^{14}\text{C}(\text{U})$ ] (specific activity 250–360 mCi (9.25–13.3 GBq)/mmol; Perkin Elmer) and incubated at 37 °C for 4 h.

### 3.2.7 Extraction of polar lipids

Polar and apolar lipids were extracted as described in Section 6.10. Incorporation of glucose D-[ $^{14}\text{C}(\text{U})$ ] was quantified by liquid scintillation counting using 5% of the lipid fractions in 5 ml EcoScint A (National Diagnostics). The polar lipid extracts were examined by two dimensional thin-layer chromatography (2D-TLC) on aluminium-backed plates of silica gel 60 F254 (Merck 5554) by spotting equal counts of polar lipid extracts (50,000 cpm), which were then developed using solvent system E for polar lipids: chloroform/methanol/water (60:30:6, v/v/v) in the first direction and chloroform/acetate/methanol/water (40:25:3:6, v/v/v/v) in the second direction. Polar lipids were visualised by 48 h exposure on X-ray films by autoradiography (Kodak Biomax MR film).

### 3.2.8 Extraction and purification of lipoglycans

Lipoglycans were extracted as described previously (Ludwiczak *et al.*, 2001). Briefly, dried cells from a 10 ml volume culture were re-suspended in deionised water. Ethanol extraction was carried out by mixing 50%  $\text{C}_2\text{H}_5\text{OH}$  to the cell suspension and refluxing at 68 °C, for 6 h followed by centrifugation and recovery of the supernatant. This  $\text{C}_2\text{H}_5\text{OH}/\text{H}_2\text{O}$  extraction was repeated five times and the combined supernatants were dried. The dried supernatant was subjected to hot phenol- $\text{H}_2\text{O}$  treatment at 65 °C. The aqueous phase containing the crude lipoglycan fraction was dialysed against

deionised water, dried and the incorporation of glucose D-[ $^{14}\text{C}(\text{U})$ ] was quantified by liquid scintillation counting using 5 % of the lipoglycan fractions in 5 ml EcoScint A (National Diagnostics). Equal counts (50,000 cpm) were loaded on a 15% SDS-PAGE gel and separated by electrophoresis (described in Section 6.14). Lipoglycans were visualised by 48 h exposure on x-ray films by autoradiography (Kodak Biomax MR film).

### 3.2.9 PPM synthase assay

Membranes were prepared as described previously (Besra *et al.*, 1997). Briefly, cells were grown to mid-log phase, harvested, washed with PBS and stored at  $-20\text{ }^{\circ}\text{C}$ . Cells were first washed and resuspended in 30 ml buffer A containing 50 mM MOPS (adjusted to pH 7.9 with KOH), 5 mM  $\beta$ -mercaptoethanol and 10 mM aqueous  $\text{MgCl}_2$  at  $4\text{ }^{\circ}\text{C}$  and subjected to sonication for a total time of 10 min using 60 s pulses and 90 s cooling intervals. The preparations were centrifuged at  $27000\times g$  for 25 min at  $4\text{ }^{\circ}\text{C}$  and the membranes were obtained by further centrifugation of the supernatant at  $100,000\times g$  for 1 h at  $4\text{ }^{\circ}\text{C}$ . The membranes were resuspended in 1 ml of buffer A and the concentration was determined using the BCA Protein Assay Reagent Kit (Thermo Scientific). Reaction mixtures for assessing [ $^{14}\text{C}$ ]Man incorporation consisted of 6.25  $\mu\text{Ci}$  GDP[Man- $^{14}\text{C}(\text{U})$ ] (262 mCi/mmol; Perkin Elmer), 100  $\mu\text{M}$  ATP, 10 mM aqueous  $\text{MgCl}_2$ , 100  $\mu\text{M}$  dithiothreitol, 20 mM  $\text{NaF}_{(\text{aq})}$  and membrane preparations corresponding to 50–400  $\mu\text{g}$  protein in a final volume of 100  $\mu\text{l}$ . Decaprenyl monophosphate was added to the reaction mixtures at a final concentration of 125  $\mu\text{M}$ . The reaction mixtures were then incubated at  $37\text{ }^{\circ}\text{C}$  for 30 min. The enzymic reactions were terminated by the addition  $\text{CHCl}_3/\text{CH}_3\text{OH}/0.8\text{ M}$  aqueous NaOH

(10:10:3 by vol.) (6 ml/100  $\mu$ l) followed by further incubation at 55°C for 20 min. The mixtures were then allowed to cool; 2.625 ml of  $\text{CHCl}_3$  and 1.125 ml of water were added. The mixture was vortexed and centrifuged and the upper aqueous phase discarded. The organic phase was washed three times with 2 ml of  $\text{CHCl}_3$ : $\text{CH}_3\text{OH}$ : $\text{H}_2\text{O}$  (3:47:48 by vol.), dried to yield an organic fraction containing PPMs. These were dried in a scintillation *vial* before scintillation counting using 5 ml of EcoScint A (National Diagnostics) (Gurcha *et al.*, 2002).

### 3.3 Results and Discussion

#### 3.3.1 Confirming the essentiality of *MSMEG3859* in *M. smegmatis*

Previous studies have established the role of *Mt-ppm1* in the biosynthesis of LM and LAM, the presence of which are vital for the survival of *M. tuberculosis* (Gurcha *et al.*, 2002). This evidence indicates that it is an essential gene. We decided to test this hypothesis in *M. smegmatis* using the homologue. A knockout phage  $\text{ph}\Delta\text{MsPpm}$  designed to replace *MSMEG3859-MSMEG3860* in *M. smegmatis* with a hygromycin resistance cassette was constructed. However, due to the failure to yield any transductants, we were unsuccessful in generating a null mutant. In contrast, we were able to produce a *MSMEG3859-MSMEG3860* null mutant by transducing a merodiploid strain containing a second, inducible copy of *MSMEG3859-MSMEG3860* by CESTET (Conditional Expression Specialised Transduction Essentiality Test) (Bhatt *et al.*, 2005); this led to the possibility that either one or both genes are essential in *M. smegmatis*. However, as studies conducted *in vitro* have demonstrated that *MSMEG3859* is sufficient for the enzymatic generation of PPM, it

is more likely that the PPM synthase-encoding *MSMEG3859*, but not the membrane segment-encoding *MSMEG3860*, was an essential gene. To clarify this, CESTET was again employed to test the essentiality of *MSMEG3859* in *M. smegmatis*. First, we constructed a merodiploid strain by introducing a second copy of *MSMEG3859* cloned in pTIC6a, an integrative plasmid driving expression *via* a tetracycline inducible promoter (Ehrt *et al.*, 2005).

The addition of anhydrotetracycline (ATc) to the growth medium could induce expression of this recombinant copy of *MSMEG3859*. After transduction with the knockout phage  $\phi\Delta MsPpm$ , we were able to generate deletion mutants only when transductants were selected on plates containing hygromycin and ATc, leading to the validation that *MSMEG3859* was essential in *M. smegmatis*. We selected one such conditional mutant, which was named  $\Delta MsPpm$  and used this strain for further analysis. Subsequent passages of the  $\Delta MsPpm$  mutant in medium without the inducer ATc led to the loss of cell viability demonstrating that expression of the pTIC6a-driven copy of *MSMEG3859* was necessary for cell growth, confirming the essentiality of *MSMEG3859* (Figure 3.6).



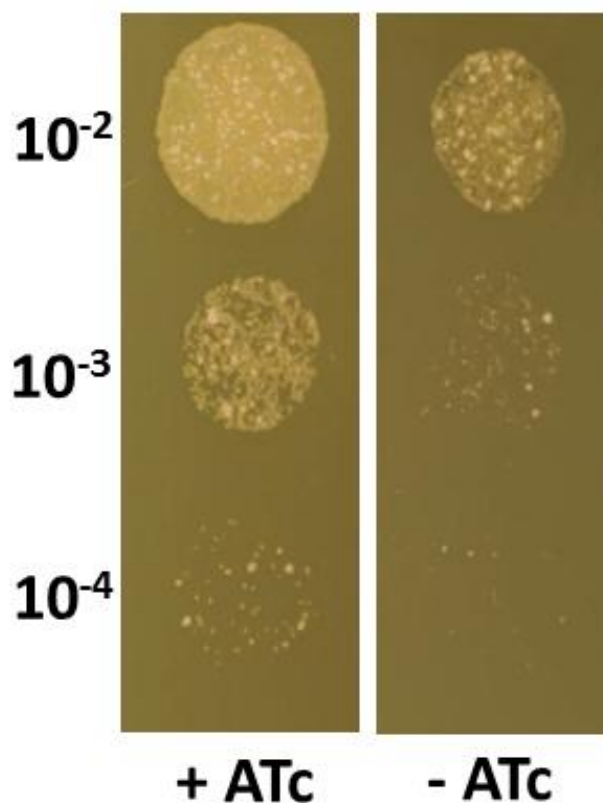


**Figure 3.6. Essentiality of *MSMEG3859* in *M. smegmatis* mc<sup>2</sup>155.** Growth of the  $\Delta$ MsPpm conditional mutant on Tryptic Soy Agar in the presence or absence of the inducer anhydrotetracycline (ATc). 10  $\mu$ l of 10-fold serial dilutions of cultures were spotted on the agar plates and incubated for 3 days at 37 °C.

### 3.3.2 Loss of *MSMEG3859* leads to an alteration in PIM profile and cessation of LM biosynthesis

As previously mentioned in Section 3.1.2,  $Ac_1/Ac_2PIM_4$  is at a key branch point for the biosynthesis of higher PIMs ( $Ac_1/Ac_2PIM_6$ ) and LM/LAM. Using the conditional  $\Delta$ MsPpm mutant, we could determine whether losing the PPM activity of *MSMEG3859*-encoded could lead to a change in the biosynthesis of higher PIMs and LM/LAM. The mutant was grown for 36 hours in media in the presence, or absence, of ATc and labelled with [<sup>14</sup>C]-glucose. The cells were then subjected to lipid

extractions. In the cultures grown in ATc-containing media, all of the PIM intermediates were present (Figure 3.7).

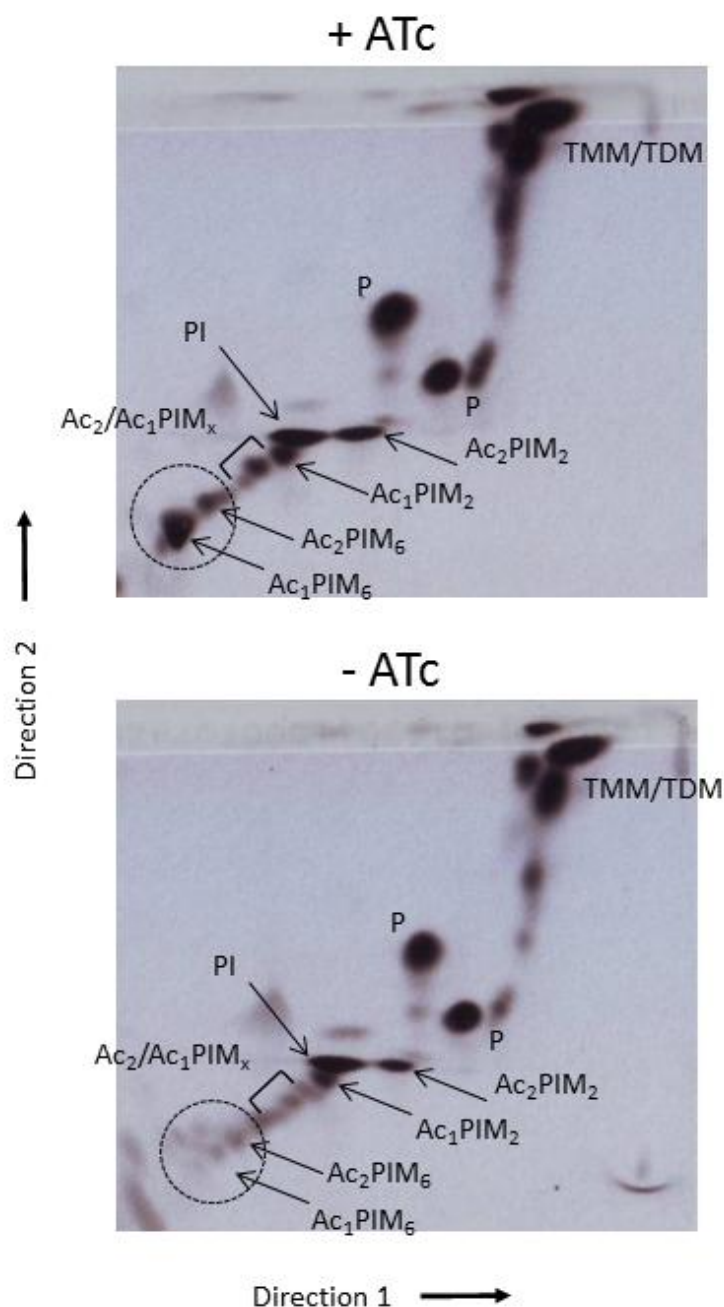


**Figure 3.7. 2D-TLC autoradiograph of [ $^{14}\text{C}$ ]-labelled polar lipids from the  $\Delta\text{MsPpm}$  conditional mutant.** Cultures were grown and labelled in Tryptic Soy Broth in the presence or the absence of anhydrotetracycline (ATc). Equal counts of polar lipid extracts (50,000 cpm) were applied to TLC plates. Solvent system E for polar lipids:  $\text{CHCl}_3/\text{CH}_3\text{OH}/\text{H}_2\text{O}$  (60:30:6, v/v/v) in the first direction and  $\text{CHCl}_3:\text{CH}_3\text{OOH}:\text{CH}_3\text{OH}:\text{H}_2\text{O}$  (40:25:3:6, v/v/v/v) in the second direction. Polar lipids were visualised by 48 h exposure on x-ray films by autoradiography (Kodak Biomax MR film). PIM intermediates are shown by arrows ( $x = 3-5$ ) and the dotted circle indicates the position of the higher PIMs on the TLC plates.

In contrast, cultures of the conditional mutant grown in media without ATc displayed similar amounts of PI accompanied by decreasing levels of  $Ac_1/Ac_2PIM_6$  (Figure 3.7). The loss of  $Ac_1/Ac_2PIM_6$  and accumulation of  $PIM_x$  precursors suggested that *MSMEG3859* is required for the synthesis of higher order PIMs, particularly  $Ac_1/Ac_2PIM_6$ .

Conditional depletion of PPM synthase activity in the  $\Delta MsPpm$  mutant should also affect the biosynthesis of lipoglycans. Cultures that were grown in media without ATc did show diminished levels of  $[^{14}C]LM$  (Figure 3.8). However, we did not detect any major differences in  $[^{14}C]LAM$  levels (Figure 3.8).

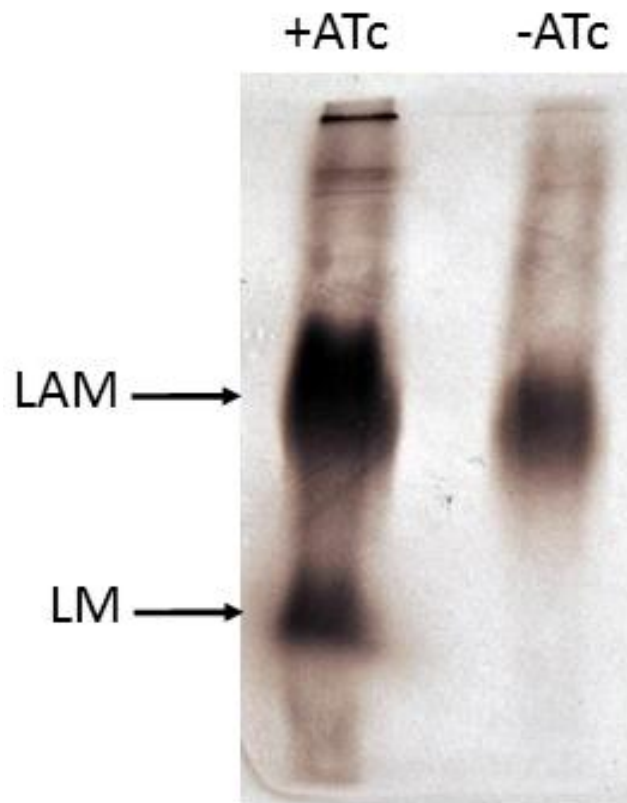


**Figure 3.8. Lipoglycan profile of the  $\Delta MsPpm$  conditional mutant.** Equal counts (50,000 cpm) of  $[^{14}C]$ -labelled lipoglycan fractions were separated on 15% SDS-PAGE gel from cultures of the  $\Delta MsPpm$  conditional mutant with or without anhydrotetracycline (ATc). Lipoglycans were visualised by 48 h exposure on x-ray films by autoradiography (Kodak Biomax MR film).

This observation can be explained by results reported by Besra *et al.*, where dual [<sup>14</sup>C]/[<sup>3</sup>H] dual labelling experiments have shown that residual LM can lead to the production of LAM (Besra *et al.*, 1997). The loss of [<sup>14</sup>C]LM but presence of [<sup>14</sup>C]LAM in the depleted cultures could be explained by residual LM molecules utilising synthesised endogenous PPM generated prior to conditional depletion for the extension of form [<sup>14</sup>C]LAM. Therefore, it is likely that the [<sup>14</sup>C]LAM we observed in the depleted cells was probably generated from residual unlabelled LM, rather than newly synthesised LM. These data suggest that *MSMEG3859*, which encodes the equivalent of *M. tuberculosis* Ppm1/D2, is solely responsible for the PPM synthase activity required for the generation of higher order PIMs and LM/LAM.

### **3.3.3 Effects of loss of *MSMEG3859* on membrane-associated PPM synthase activity**

Membrane preparations from cultures of the  $\Delta$ MsPpm mutant, grown in the presence and in the absence of ATc, were used to assay membrane-associated PPM synthase activity. A PPM synthase assay was used to analyse PPM activity in the membranes using GDP-[<sup>14</sup>C] Man and polyprenol phosphate as substrate. This assay was used to assess the effects of depletion of *MSMEG3859* function on the ability of the membrane preparations to catalyse the formation of PPM (C<sub>50</sub>-P-Man) donors *via* the incorporation of radioactive mannose into polyprenol substrate through pooled organic extracts containing PPMs (Gurcha *et al.*, 2002). While membrane preparations from cultures grown in the presence of ATc were able to catalyse the incorporation of [<sup>14</sup>C] Man into polyprenols, those from cultures grown in the absence of ATc displayed poor PPM synthase activity (Figure 3.9). Thus, the PPM synthase

activity from *MSMEG3859* encoding membrane extracts was significantly increased compared with membrane extracts with loss of *MSMEG3859*. This co-relation between depleted *MSMEG3859* function and low PPM synthase activity confirmed that *MSMEG3859* was the key synthase required to catalyse the production of PPM donors in *M. smegmatis*.

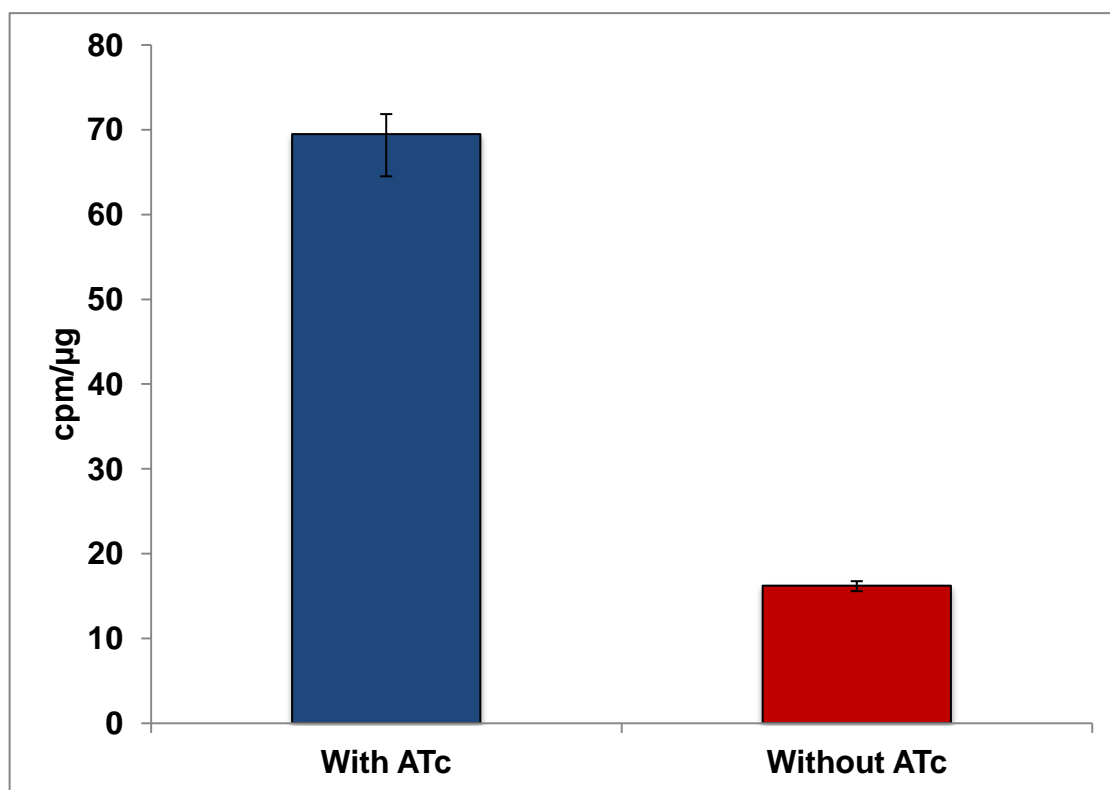


**Figure 3.9. PPM synthase activity in membranes of the  $\Delta$ MsPpm conditional mutant.** Graph shows the transfer of [ $^{14}$ C]-mannose from GDP[Man- $^{14}$ C(U)] (262 mCi/mmol; Perkin Elmer) to polyprenol-phosphate in membrane extracts prepared from cultures grown with or without anhydrotetracycline (ATc).

### 3.3.4 Potential ability of alternative *M. tuberculosis* PPM synthases to rescue viability and restore wild-type phenotype in the $\Delta$ MsPpm mutant

Recent studies have identified two other membrane-associated glycosyltransferases, Rv3779 and Rv3631 (PpgS) in *M. tuberculosis* which are responsible for the transfer

of the GalN substrate for the modification of AG (Skovierová *et al.*, 2010). However, they have also been suggested to have putative roles as PPM synthases in *M. tuberculosis* (Skovierová *et al.*, 2010). As there are no homologues of Rv3779 or Rv3631 (PpgS) present in *M. smegmatis*, the  $\Delta$ MsPpm conditional mutant thus offered us an opportunity to assess the potential roles of Rv3779 and PpgS as alternative PPM synthases. Each gene could be functionally analysed *in vivo* by testing the ability of the  $\Delta$ MsPpm conditional mutant transformed with a plasmid-borne copy of either *Rv3779* or *ppgS* to restore PPM synthase activity and thereby rescue  $Ac_1/Ac_2PIM_6$  biosynthesis when cultured in medium devoid of ATc. As expected,  $Ac_1/Ac_2PIM_6$  biosynthesis was not affected in non-ATc cultures of  $\Delta$ MsPpm containing plasmid clones of either *MSMEG3859* (Figure 3.10). We then tested the ability of the *M. tuberculosis* equivalent, *Mt-ppm1/D2* to rescue the loss of *MSMEG3859* function in the same manner and found  $Ac_1/Ac_2PIM_6$  levels unaffected in the recombinant strains (Figure 3.10) thus demonstrating that *Mt-ppm1/D2* was functional in *M. smegmatis*. However, *Rv3779* was unable to rescue  $Ac_1/Ac_2PIM_6$  biosynthesis in the conditional mutant when grown in the absence of ATc, leading to a loss of  $Ac_1/Ac_2PIM_6$  and a noticeable accumulation of intermediate  $Ac_1/Ac_2PIM_{x,s}$  (Figure 3.10). While *Rv3779* was shown to have PPM synthase activity *in vitro* (Scherman *et al.*, 2009), it surprisingly failed to substitute for loss of *MSMEG3859* in the conditional  $\Delta$ MsPpm mutant. Thus, in contrast to its *in vitro* activity, it is unlikely that *Rv3779* functions *in vivo* as a PPM synthase. However, the predominant role of *Rv3779* in *M. tuberculosis* appears to be the utilisation of polyprenyl-P-D-GalNAc as a donor for the biosynthesis of galactosamine-modified AG (Skovierová *et al.*, 2010).

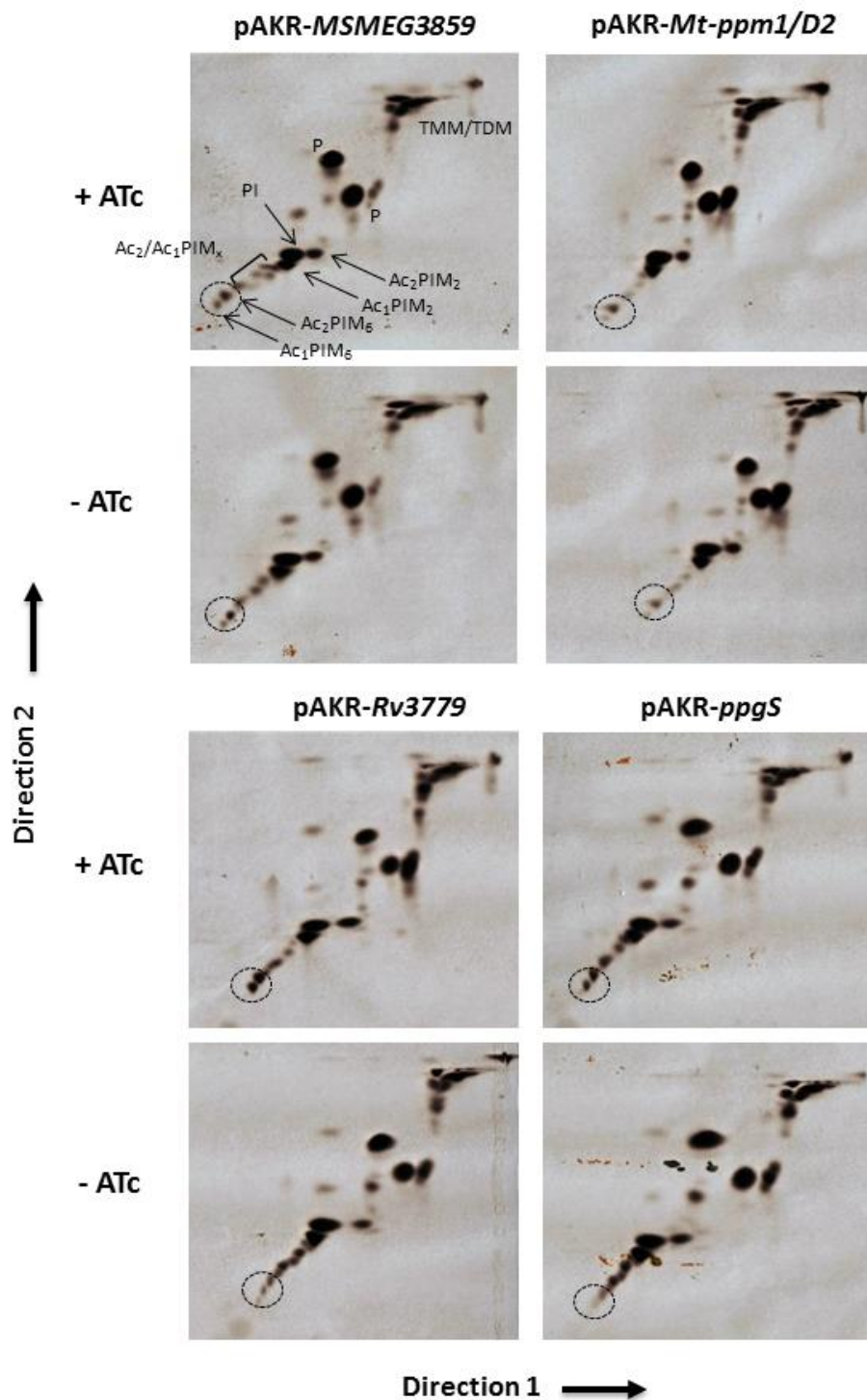


**Figure 3.10. Complementation of the  $\Delta$ MsPpm conditional mutant.** 2D-TLC analysis of [ $^{14}$ C]-labelled polar lipids from the  $\Delta$ MsPpm conditional mutant complemented with (A) pAKR-MSMEG3859 (B) pAKR-Mt-ppm1/D2 (C) pAKR-Rv3779 (D) pAKR-ppgS. System E for polar lipids: CHCl<sub>3</sub>/CH<sub>3</sub>OH/H<sub>2</sub>O (60:30:6, v/v/v) in the first direction and CHCl<sub>3</sub>:CH<sub>3</sub>OOH:CH<sub>3</sub>OH:H<sub>2</sub>O (40:25:3:6, v/v/v/v) in the second direction. Polar lipids were visualised by 48 h exposure on x-ray films by autoradiography (Kodak Biomax MR film). PIM intermediates are shown by arrows (x = 3–5) and the dotted circle indicates the position of the higher PIMs on the TLC plates.

As mentioned above, while PpgS is involved in the generation of polyprenyl-phospho-*N*-acetylgalactosamine (polyprenyl-P-GalNAc) from polyprenyl-P and UDP-GalNAc, it could be envisaged as a secondary, potential PPM synthase. Its syntenic association with the small integral membrane protein Rv3662 is similar to MSMEG3859 and its associated transmembrane protein MSMEG3860, and Mt-Ppm1/D2-Mt-Ppm1/D1, which is fused as one polypeptide. However, *ppgS* was also unable to compensate for the loss of MSMEG3859 in the conditional mutant (Figure 3.10), and thus is unlikely to function as a PPM synthase *in vivo*. Therefore, these results demonstrate that both Rv3779 and PpgS do not have a role as a PPM synthase.

### 3.4 Conclusion

Several studies have displayed the importance of LAM as a key factor in TB pathogenesis. The initial steps in the biosynthesis of PIMs utilise an intracellular nucleotide-derived mannose donor called GDP-Man<sub>p</sub>, whereas a polyprenyl-phosphate-based mannosyl donor is required the synthesis of higher PIMs, LM and LAM in the periplasmic side of the bacterium. While the first polyprenyl-phosphate-based mannose donor to be identified was C<sub>50</sub>-decaprenol-phospho-mannose (C<sub>50</sub>-P-Man<sub>p</sub>, PPM) in *M. tuberculosis*, an additional alkali-stable PPM donor, C<sub>35</sub>-octahydrohepta-prenyl-phosphate-mannose (C<sub>35</sub>-P-Man<sub>p</sub>) was identified in *M. smegmatis* (Takayama and Goldman, 1970; Wolucka and de Hoffmann, 1998). Previous studies have identified a PPM synthase in *M. tuberculosis* encoded by the two-domain gene *Mt-ppm1* and two separate proteins encoded by neighbouring genes in *M. smegmatis* (Gurcha *et al.*, 2002). *Mt-ppm1* was probably formed by the



consequence of a genetic fusion between ancestral genes. Since *ppm1* genes are conserved across mycobacteria, especially *M. leprae* which possess a highly reduced genome (Cole *et al.*, 2001), this leads to the suggestion that PPM synthase is an essential enzyme in mycobacteria.

The ability to generate an *MSMEG3859-MSMEG3860* double mutant in a *MSMEG3859* merodiploid strain indicated that while the PPM synthase-encoding *MSMEG3859* was essential, *MSMEG3860* (which encodes a six transmembrane section-containing membrane-anchored protein) was not essential. This correlated with earlier reports that *MSMEG3859* was sufficient for PPM synthase activity (Gurcha *et al.*, 2002; Baulard *et al.*, 2003). In addition to this, both Rv3779 and PpgS were unable to compensate for the loss of *MSMEG\_3859* in the  $\Delta$ MsPpm conditional mutant, therefore proving that they do not have a role as a PPM synthase.

The results from this Chapter indicate that *ppm1* is the gene encoding the sole PPM synthase in *M. tuberculosis* that is capable of generating the mannose donor for the biosynthesis of higher order PIMs and LM/LAM. Together, the data obtained from the depletion experiments with the conditional mutant highlight the potential of the *MSMEG3859*-encoded PPM synthase as a potential drug target that affects not only viability, but also the biosynthesis of an immunomodulatory mycobacterial lipoglycan.

**4 Deletion of the serine/threonine  
protein kinase H alters phthiocerol  
dimycocerosate synthesis  
in *Mycobacterium tuberculosis***

## 4.1 Introduction

### 4.1.1 Biosynthesis of phthiocerol dimycocerosates (PDIMs)

As explained above in Section 1.6.6, phthiocerol dimycocerosates (PDIMs) are a family of surface-exposed polyketide lipids which are found in the outer membrane segment of *M. tuberculosis*.

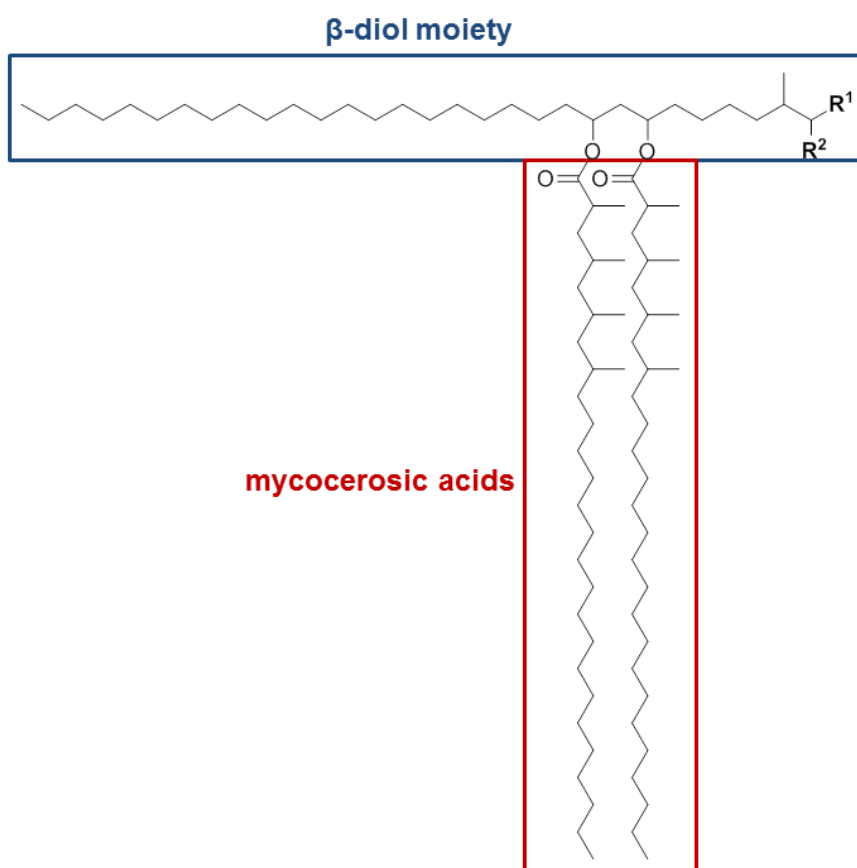


**Figure 4.1. Structure of PDIMs.** The long chain  $\beta$ -diol backbone known as phthiocerols is esterified by polymethyl-branched fatty acids (mycocerosic acids).  $R^1$  is  $\text{CH}_2\text{-CH}_3$  for phthiocerol series A and C or  $\text{CH}_3$  for phthiocerol series B;  $R^2$  is  $\text{OCH}_3$  for the phthiocerol family or is O for the phthiodiolone family (series C).

PDIMs are composed of a mixture of long-chain  $\beta$ -diols ( $\text{C}_{33}\text{--C}_{41}$ ) known as phthiocerols that are esterified by two long-chain polymethyl-branched fatty acids called mycocerosic acids (Figure 4.1) (Minnikin *et al.*, 2002) and have been shown to possess immunological activity in host macrophages during infection (Rousseau *et*

*al.*, 2004; Astarie-Dequeker *et al.*, 2009). PDIM A/B is the phthiocerol dimycocerosate variant with a methoxy group at the terminus of the  $\beta$ -diols, whereas PDIM C is its structural variant that contains a keto group instead.

The biosynthetic pathway of PDIMs has been studied in detail. Biosynthesis is initiated by fatty acyl-AMP ligases called FadD26 and FadD28, which are involved in the activation and transfer of  $C_{12}$ – $C_{18}$  fatty acids for production of the phthiocerol moiety and mycocerosic acids, respectively (Figure 4.2) (Trivedi *et al.*, 2004).

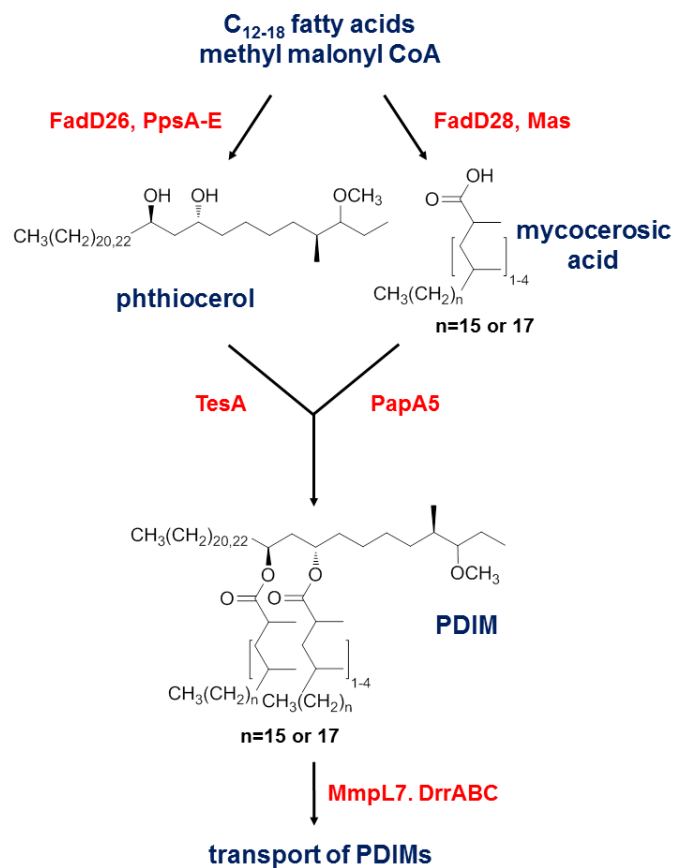


**Figure 4.2. Pathway of phthiocerol dimycocerosates (PDIMs) biosynthesis.** FadD26 and FadD28 activate and transfer fatty acids to PpsA-E and Mas, respectively. PpsA-E synthesise the phthiocerol backbone, which is then released by TesA. In parallel, Mas protein synthesises mycocerosic acids, which are transferred to the phthiocerol backbone by PapA5. MmpL7 and DrrC are responsible for transporting of PDIM to the cell wall. Mas, mycocerosic acid synthase; Pps, phthiocerol synthase.

The activated fatty acids are transported to the type I polyketide synthases (PKSs), PpsA-PpsE, which are responsible for the elongation of straight-chain fatty acids until the synthesis of the final phthiocerol backbone is complete (Azad, 1997; Trivedi *et al.*, 2005). In parallel, activated fatty acids are transferred to an iterative type PKS, the Mas protein, which synthesises mycocerosic acids through sequential additions of methyl malonyl CoA (Azad *et al.*, 1996; Trivedi *et al.*, 2005). PapA5, an acyltransferase protein, catalyses the direct transfer of mycocerosic acids to the  $\beta$ -diol backbone of the phthiocerol to complete the final esterification step (Onwueme *et al.*, 2004; Trivedi *et al.*, 2005). The elongated phthiocerol moiety is released from PpsE through interaction with the type II thioesterase TesA (Alibaud *et al.*, 2011). The newly synthesised PDIMs are then transported to the cell wall by either MmpL7 or DrrABC (Camacho *et al.*, 1999; Cox *et al.*, 1999).

#### **4.1.2 Serine/threonine protein kinase H (PknH)**

Although there is a good understanding of the biosynthesis of PDIMs, there is limited knowledge regarding their regulation. Protein phosphorylation is the central mechanism by which extracellular environmental stimuli are converted into cellular responses. These mechanisms can be enabled by protein kinases that allow the bacterium to adapt its cellular response to survive in hostile environments. Protein kinases are categorised into two families: the sensor histidine kinases, part the two-component regulatory systems, which autophosphorylate a conserved histidine residue (Stock *et al.*, 1989) and the serine/threonine protein kinases (STPK)s, which phosphorylate serine and threonine residues (Hanks *et al.*, 1988). Recently, serine/threonine phosphorylation has been found to play a critical regulatory role in

signal transduction pathways in *M. tuberculosis*. The genome of *M. tuberculosis* possesses 11 different STPKs which have been implicated in the regulation of pathogenesis, cell division and cell-wall biosynthesis (Cole *et al.*, 1998; Av-Gay and Everett, 2000; Chao *et al.*, 2010). Previous studies have identified two STPKs, PknB and PknD, that are associated with PDIM biosynthesis. While PknB was shown to phosphorylate threonine residues in PapA5 (Gupta *et al.*, 2009), PknD may be involved in the phosphorylation of MmpL7 (Pérez *et al.*, 2006). The experimental evidence from these studies proposes that STPKs are involved in the regulation of PDIM production.

The *M. tuberculosis* PknH kinase has previously been shown to phosphorylate enzymes involved in the synthesis of the cell wall. Previous *in vitro* kinase assays provided experimental evidence that PknH directly phosphorylates the endogenous EmbR protein through the recognition of a forkhead-associated domain (FHA), which represented the first example of a protein substrate altered by a STPK in *M. tuberculosis* (Molle *et al.*, 2003). The FHA domain is capable of facilitating protein-protein interactions through recognition of phosphothreonine (Durocher and Jackson, 2002). As EmbR is the transcriptional regulator of the *embCAB* operon, encoding arabinosyltransferases which are involved in the synthesis of the arabinan domain of AG and LAM, this interaction may play a role in the various production of cell-wall components (Molle *et al.*, 2003; Sharma *et al.*, 2006; Zheng *et al.*, 2007). The interaction of PknH with EmbR has also been found to significantly alter EMB resistance by regulating transcription levels of the *embAB* genes which are the cellular target of EMB (Sharma *et al.*, 2006). Furthermore, *in vivo* studies in which

PknH was overexpressed in *M. smegmatis* resulted in a high LAM/LM ratio, which is critical in the virulence of mycobacteria (Sharma *et al.*, 2006). PknH is also involved in the phosphorylation of DacB1, a sporulation-specific penicillin-binding protein, which is involved in cell-wall biosynthesis (Zheng *et al.*, 2007).

Recent studies have investigated the physiological and virulence properties of PknH kinase in *M. tuberculosis* (Papavinasasundaram *et al.*, 2005). In a study by Papavinasasundaram *et al.*, it was demonstrated that the deletion of PknH leads to increased resistance to acidified nitrite stress *in vitro*, suggesting this protein regulates the *in vivo* growth of *M. tuberculosis* in response to nitric oxide (Papavinasasundaram *et al.*, 2005). Moreover, it was shown that the  $\Delta pknH$  mutant leads to improved survival and replication in a BALB/c mouse model of infection, indicating that PknH is needed to facilitate adaptation to the host environment to regulate the *in vivo* growth of *M. tuberculosis* (Papavinasasundaram *et al.*, 2005). Recently, it was also identified that PknH is associated with the *M. tuberculosis* dormancy regulon through phosphorylation of the control enzyme DosR (Chao *et al.*, 2010). Together, these results indicate that PknH plays a central role in regulating the growth of *M. tuberculosis* by controlling the synthesis of cell-wall components and/or transport. In this study, we investigated how PknH affects the biosynthesis of PDIM and the ratio of LAM to LM. To examine this, a *pknH* deletion mutant strain generated in the laboratory of our collaborator was used to carry out a detailed cell wall lipid analysis to observe PDIM production and to characterise LAM and LM levels. Dr. Anaximandro Gómez-Velasco and Prof. Yossef Av-Gay (University of British Columbia) used techniques including radiolabelling, mass spectrometry

(lipidomics) and immunostaining analyses to show PDIM biosynthesis is affected by knocking out the *pknH* gene. The work described in this chapter reflects the lipid analysis and the lipoglycan characterisation done by me as a part of this collaboration.

## 4.2 Materials and methods

### 4.2.1 Bacterial strains and growth conditions

*M. tuberculosis* H37Rv,  $\Delta pknH$  and  $\Delta pknH::pknH$  strains were used in this study (Papavinasasundaram *et al.*, 2005). Glycerol stocks were used to initiate starter cultures in 10 ml 7H9 Middlebrook (BD, Difco) broth supplemented with 10% (v/v) oleic acid/albumin/dextrose/catalase (OADC), and 0.05% (v/v) Tween-80 (Sigma-Aldrich) at 37 °C. Actively growing bacterial cells were used to start 500 ml cultures for rolling conditions (850 cm<sup>3</sup> roller bottles; Greiner Bio-one, catalogue no. 680060, 1.25 rpm) and were incubated at 37 °C. 7H11 agar medium (BD, Difco) was prepared according to the manufacturer's instructions and was supplemented with 10% (v/v) OADC (BD, Difco). Antibiotics were supplemented 25 µg/ml kanamycin and 50 µg/ml hygromycin as required:

### 4.2.2 Extraction of polar lipids and apolar lipids

For cell-wall lipid analysis, mycobacterial strains were grown at early exponential phase (OD<sub>600</sub> ~1). Polar and apolar lipids were extracted using the method described in Section 6.10. Each lipid extract (100 µg) was loaded onto aluminium-backed plates of silica gel 60 F254 (Merck 5554) and the lipids were separated by 2D-TLC using



solvent systems A–E (Dobson, 1985). To visualise PDIMs, lipids were separated using the system A solvent system: thrice with petroleum ether (60-80 °C): EtOAc (98:2, v/v) in the first direction and once with petroleum ether (60-80 °C)/ acetone (98:2, v/v) in the second direction. The TLC plates were developed by staining with 5 % (w/v) ethanolic phosphomolybdic acid for detecting all lipids or  $\alpha$ -naphthol-sulfuric acid for detecting carbohydrate containing lipids, followed by charring at 100 °C.

#### 4.2.3 Extraction, purification and characterisation of lipoglycans

Lipoglycans (LAM and LM) were extracted as described previously (Ludwiczak *et al.*, 2001). Briefly, dried cells from a 10 ml volume culture were re-suspended in deionised water. Ethanol extraction was carried out by mixing 50% EtOH to the cell suspension and refluxing at 68 °C for 6 h, followed by centrifugation and recovery of the supernatant. This EtOH/H<sub>2</sub>O extraction was repeated five times and the combined supernatants were dried. The dried supernatant was subjected to hot phenol-H<sub>2</sub>O treatment at 65 °C (Ludwiczak *et al.*, 2001). The aqueous phase containing the crude lipoglycan fraction was dialysed against deionised water and dried. To determine the LAM/LM ratio, equal amounts of the extracted lipoglycans (10  $\mu$ g/ml) were loaded into 15% SDS-PAGE gel, separated by electrophoresis (described in Section 6.14) and visualised using Pro-Q emerald glycoprotein stain (Invitrogen) as explained in the manufacturer's handbook. The LAM/LM ratio was calculated by densitometric analysis. Glycoside composition was determined as described previously (Tatituri, 2007). Lipoglycan samples were per-O-methylated and then hydrolysed using 250  $\mu$ l of 2 M trifluoroacetic acid at 120 °C for 2 h, reduced using 100  $\mu$ l of a 10 mg/ml solution of NaB<sub>2</sub>D<sub>4</sub> (1 M aqueous NH<sub>4</sub>OH /EtOH, 1:1, v/v),

and per-*O*-acetylated by treating with 100  $\mu\text{l}$  of acetic anhydride for 1 h at 110  $^{\circ}\text{C}$ . After cooling, 100  $\mu\text{l}$  of toluene was added to the reaction mixture and the volatiles removed under compressed  $\text{N}_2$ . The resulting alditol acetates were partitioned between 2 ml  $\text{H}_2\text{O}$  and 2 ml  $\text{CHCl}_3$  and the organic phase dried under compressed  $\text{N}_2$ . The alditol acetates were examined by gas chromatography (GC) using a Thermoquest Trace GC 2000 equipped with flame ionisation detector. Parameters, conditions and analysis were performed as described previously (Tatituri *et al.*, 2007).

For radiolabelling experiments [ $1\text{-}^{14}\text{C}$ ]-propionate  $3.7 \times 10^{10}$  Bq  $\text{ml}^{-1}$  [specific activity 54 mCi  $\text{mmol}^{-1}$  ( $1.998$  GBq  $\text{mmol}^{-1}$ ); American Radiolabeled Chemicals] was added to 10 ml mycobacterial cultures at 37  $^{\circ}\text{C}$  at different time points: 12 and 24 h, 5 and 10 days. PDIMs were extracted and activity was measured in a scintillation counter (Beckman). PDIMs were purified as above using preparative TLC. Equal radioactive counts were loaded onto 2D-TLC and autoradiograms were visualised using a Phosphorimager SI (Molecular Dynamics). For lipid quantification, spots were scraped from TLC plates and subjected to scintillation counting. For statistical analysis three independent biological replicates were used.

#### **4.2.4 Fourier transform ion cyclotron resonance (FT-ICR) MS analysis**

Total lipids were extracted using the Bligh–Dyer method (Bligh and Dyer, 1959) from mycobacterial strains that were grown in the conditions described in Section 4.2.1. Tween-80, used as a supplement in the culture, was removed to avoid interference with the results by resuspending cells extracts in a hexane/water mixture (50:50, v/v),

mixed thoroughly and centrifuged at 3500 × g for 5 min (Jain *et al.*, 2007). The organic layer was extracted with water five times. For lipidomic analysis, total lipids were resuspended in a chloroform/methanol mixture (2:1, v/v) and introduced into an Apex-Oe 12-Tesla Hybrid quadrupole-FT-ICR machine (Bruker Daltonics), which was equipped with an Apollo electrospray ionization (ESI) ion source. Samples were infused into the MS instrument at a flow rate of 2 µl/min and were ionised with ESI. Mass spectra were acquired within a mass to charge (m/z) ratio range of 250–300 in either positive or negative mode, with broadband detection and using a data acquisition size of 1024 kilobytes *per* second. Each spectrum was accumulated from 100 scans. Total abundance of lipid species was calculated by summing the peak intensities as measured by FT-ICR, as reported previously by Jain *et al.* (Jain *et al.*, 2007).

#### **4.2.5 Production of single-chain, fragment-variable (scFv) antibodies**

Purified PDIMs were kindly provided by Dr Jean-Marc Reytrat (INSERM-UMR, France). ScFv antibodies against purified PDIMs were selected as described previously (Bach *et al.*, 2001). Briefly, 1.7 mg purified PDIMs was dissolved in 100 µl chloroform, followed by the addition of 100 µl 0.1 M 2-(*N*-morpholino) ethanesulfonic acid, (pH 4.5). The sample was sonicated, mixed with 30 µl 10 nM stock solution of hydrazine and incubated at 65 °C for 10 min. After cooling down the reaction to room temperature, the mixture was conjugated to 4 mg BSA using 1-ethyl-3-[3-dimethylaminopropyl] carbodiimide hydrochloride (Pierce), according to the manufacturer's instructions. The Tomlinson I scFv antibodies library was kindly supplied by Geneservice, Cambridge, UK. The scFv antibodies were screened

according to the instructions supplied with the library. PDIMs coupled to BSA were used as antigens for screening. Selected antibodies were subcloned into pMAL-C5X (New England Biolabs) and generated as recombinant proteins fused to a maltose-binding protein (MBP) as described previously (Bach *et al.*, 2001).

#### **4.2.6 Immunostaining and fluorescence microscopy**

Bacteria were labelled with rhodamine (10 mg/ml) for 1 h at 37 °C with gentle rocking. Labelled bacteria were washed three times with PBS and three times with double-distilled water and were immobilised on coverslips by flaming. Coverslips containing bacterial cells were incubated with scFv antibodies at room temperature for 30 min. Unbound antibodies were washed away with PBS for 10 min and this step was repeated three times. Coverslips were further incubated with an anti-MBP antibody (1:1000 dilution) mixed with goat FITC-conjugated anti-mouse IgG secondary antibody (1:1000 dilution) at room temperature for 20 min. Coverslips were washed three times again with PBS for 10 min and mounted on glass slides containing FluorSave (Calbiochem). Fluorescence microscopy was used to analyse samples as described previously by Sendide *et al.* (Sendide *et al.*, 2004).

#### **4.2.7 Isobaric tags for relative and absolute quantitation (iTRAQ) analysis**

The iTRAQ (Isobaric Tags for Related and Absolute Quantitation) analysis was performed as previously described (Chao *et al.*, 2010). Strains were grown in rolling cultures, harvested, washed and treated with 3 mM NaNO<sub>2</sub>. Total proteins were extracted, digested with trypsin at 37 °C overnight and then labelled with iTRAQ

reagents. The labelled peptides were then separated using a strong cation exchange column called Polysulfoethyl A [100×4.6 mm, 5 μM, 300 Å (30 nm); Poly LC, Columbia, MD] in the first dimension. Initially, the column was allowed to equilibrate in buffer A [10 mM KH<sub>2</sub>PO<sub>4</sub>, pH 2.7 and 25% acetonitrile (ACN)] for 20 min and then a gradient was applied for 30 min in 0–35% buffer B (10 mM KH<sub>2</sub>PO<sub>4</sub>, pH 2.7, 25% ACN, 0.5 M KCl). The flow rate was fixed at 0.5 ml/min. LC-MS/MS analysis was performed to analyse tagged peptides were by using an integrated Famos autosampler, Switchos II switching pump and Ultimate micropump system (LC Packings, Amsterdam) with a hybrid Quadrupole-time of flight (TOF) LC-MS/MS mass spectrometer (QStar Pulsar i), equipped with a nanoelectrospray ionization source (Proxeon, Odense, Denmark) and fitted with 10 μm fused-silica emitter tip (New Objective, Woburn, MA). The second dimensional chromatographic separation was conducted using a 75 μm×15 cm C18 PepMap Nano LC column [3 μm, 100 Å (10 nm); LC Packings, Amsterdam] and a 300 μm×5 mm C18 PepMap 2 Guard column [5 μm, 100 Å (10 nm); LC Packings, Amsterdam] prior to switching inline with the column and the MS. The mobile phase (solvent A) comprised of water/ACN (98:2, v:v) with 0.05% formic acid for sample injection and equilibration on the guard column at a flow rate of 100 μl/min. The tapping column was switched inline to producing a linear gradient by mixing it with solvent B, which was made up of ACN/water (98:2, v/v) with 0.05% formic acid, and the flow rate was decreased to 200 nl/min for high resolution chromatography and introduction into the mass spectrometer. Analyst QS 1.0 software Service Pack 8 (ABI MDS SCIEX, Concord, Canada) was used to automatically attain MS data. An information-dependent acquisition method, consisting of a 1 s TOF MS survey scan of mass range 400–

1200 atomic mass units (amu) and two 2.5 s product ion scans of mass range 100–1500 amu. The two most-intense peaks over 20 counts, with charge state 2–5, were selected for fragmentation, and a 6 amu window was used to prevent the peaks from the sample isotopic cluster from fragmenting again. MS/MS was put on an exclude list for 180 s once an ion was selected. Curtain gas was at 23 °C, nitrogen was used as the collision gas and ionisation tip voltage was 2700 V.

#### **4.2.8 MS data analysis**

Data were obtained and analysed from two independent experiments. ProteinPilot 2.0.1 (Applied Biosystems/MDS Sciex) was used for the identification and quantification of the proteins. The Paragon algorithm integrated in the ProteinPilot software was used for peptide identification and was further processed by Pro Group algorithm for peptide identification and isoform-specific quantification, and the iTRAQ peak data were standardised for loading error by auto-biased corrections calculated using the ProteinPilot software. ProteinPilot software calculates an unused score of 2 for a peptide with a 99% identity confidence and an unused score of 1.3 for a peptide with 95% confidence level. An unused score of >2 indicates that a minimum of two peptides, one peptide with >95% confidence plus at least one other peptide with less than 95% confidence, were used exclusively for the identification of that protein. With a protein group of highly homologous proteins (identical peptides), peptides are arbitrarily assigned to one protein for which an unused score and iTRAQ ratio is determined. The percentage of protein covered by identified sequences at a 95% confidence level [% Cov(95)] is calculated by dividing the number of amino acids of peptides identified with 95% confidence by the total number of amino acids in the

protein. Relative quantification was performed on MS/MS scans and denotes the ratio of the areas under the peaks at 115 Da and 114 Da (untreated  $\Delta pknH$ /WT), and 117 Da and 116 Da (nitrite-treated  $\Delta pknH$ /WT).

#### 4.2.9 Statistical analysis

Statistical significance was determined with the unpaired two-tailed Student's test with GraphPad Prism Version 5.  $P \leq 0.05$  was considered statistically significant.

### 4.3 Results and Discussion

#### 4.3.1 The $\Delta pknH$ mutant produces low levels of PDIMs

Previous studies have indicated that PknH may be involved in the synthesis of cell-wall components. In our initial analysis, we characterised morphological differences in colony formations of all strains (Figure 4.3).

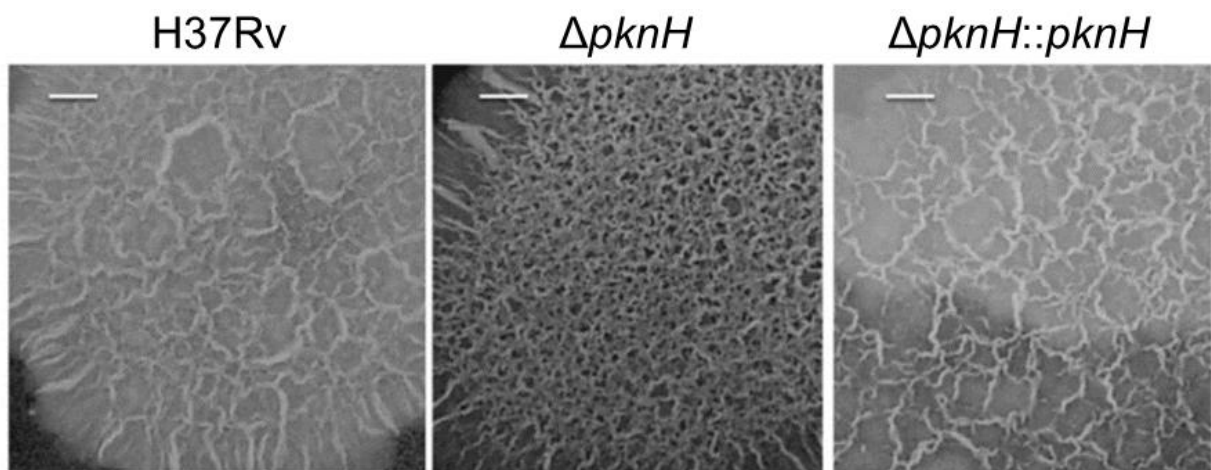


**Figure 4.3. Colony morphology.** Colonies of H37Rv wild-type,  $\Delta pknH$  and  $\Delta pknH::pknH$  strains were grown on 7H10 agar plates supplemented with OADC. 10  $\mu$ l aliquots from cultures at  $OD_{600}$  0.010 were inoculated to obtain colonies. Plates were sealed and incubated at 37 °C for 3 weeks. Scale bars = 1 mm. (Gómez-Velasco *et al.*, 2013).

We observed similar cording appearance for both the parental and complemented strains; however, the  $\Delta pknH$  displayed a more ruffled morphology. As the cording appearance has been associated with virulence in *M. tuberculosis* the loss of PknH may have implications for the overall cell wall physical structure and for *M. tuberculosis* physiology.

Next, we examined whether deletion of the *pknH* gene caused an alteration of specific cell-wall components by using a range of 2D-TLC solvent systems designed to profile a wide series of mycobacterial lipids (Dobson *et al.*, 1985).

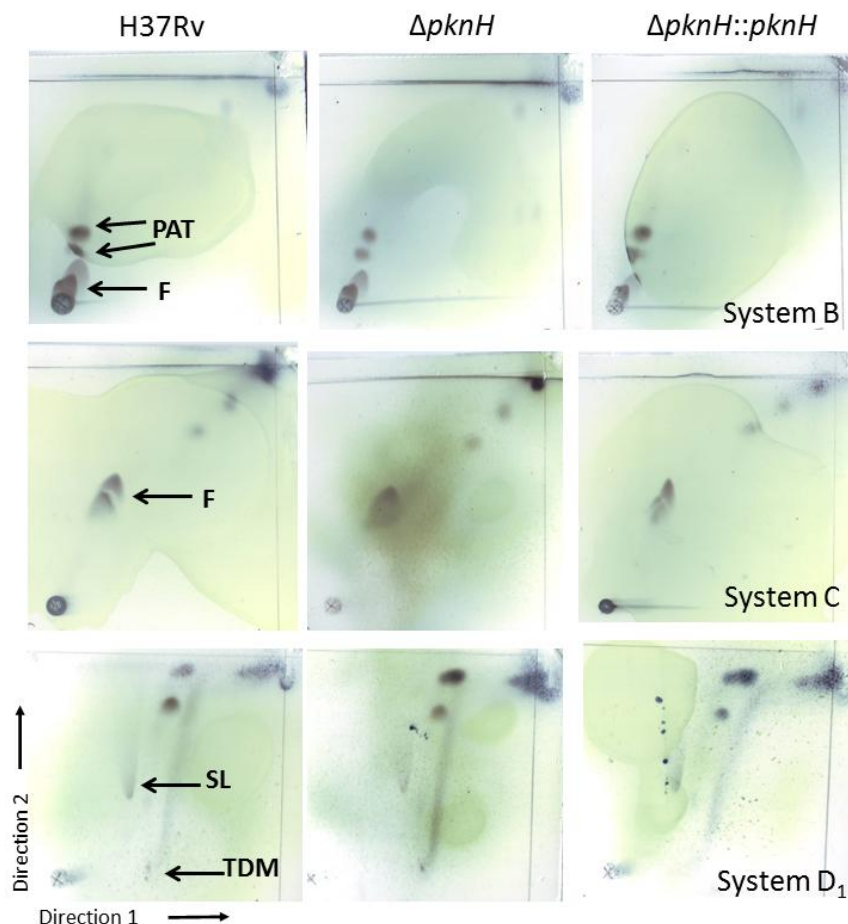


**Figure 4.4. Apolar lipid profile of the  $\Delta pknH$  mutant strain.** Solvent systems SB-SD1 were designed to visualise apolar lipids. F, free fatty acid; PAT, pentaacyl trehalose; SL, sulfolipid; TDM, trehalose dimycolates. TLC plates were developed by staining with 5 % (w/v) ethanolic phosphomolybdic acid for detecting all lipids, followed by charring at 100 °C. (Gómez-Velasco *et al.*, 2013).



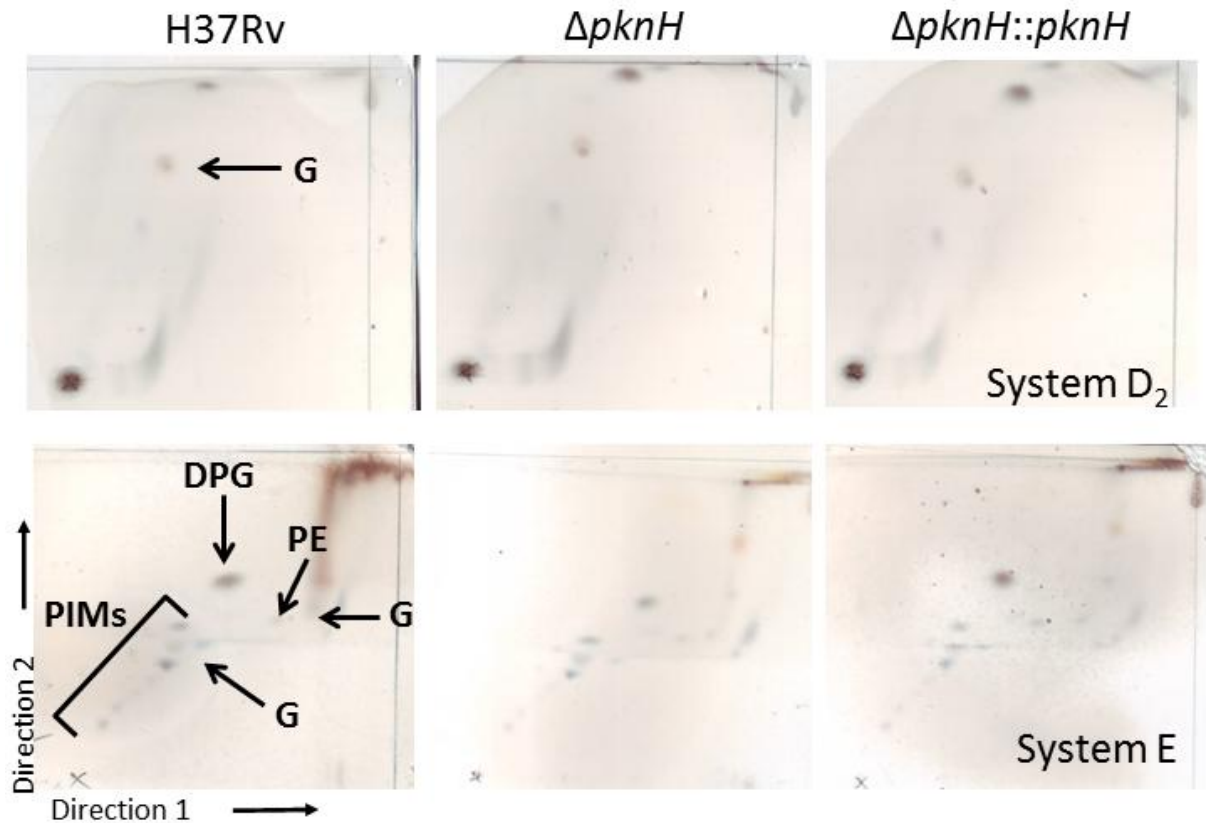


**Figure 4.5. Polar lipid profile of the  $\Delta pknH$  mutant strain.** Solvent systems SD2-SE were designed to visualise polar lipids. TLC plates were developed by staining with  $\alpha$ -naphthol-sulfuric acid for detecting carbohydrate containing lipids, followed by charring at 100 °C. DPG, diphosphotidyl-glycerol; G, glycolipid; PE, phosphatidylethanolamine; PIMs, phosphatidyl-*myo*-inositol mannosides. (Gómez-Velasco *et al.*, 2013).

While there were no apparent differences in the cell-wall lipids between the wild type and the  $\Delta pknH$  strain analysed using systems B-E (Figure 4.4 & 4.5) using system A, it was clear that the  $\Delta pknH$  mutant failed to produce observable levels of PDIMs (Figure 4.6). In the complemented strain,  $\Delta pknH::pknH$ , PDIM levels were restored which shows that the  $\Delta pknH$  deletion mutant was able to re-establish the wild-type phenotype, thus ruling out the possibility of polar effects associated with knockouts of PDIM biosynthetic genes (Domenech and Reed, 2009).

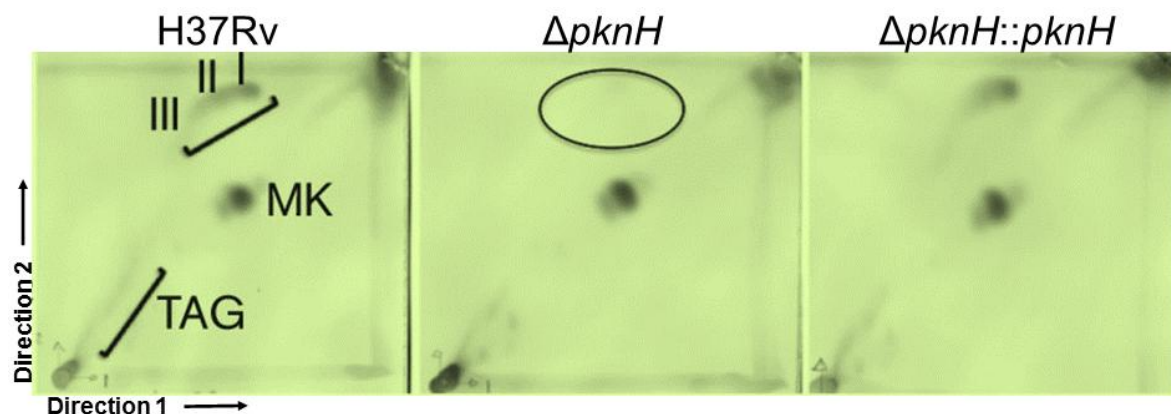


**Figure 4.6 Apolar lipid profile 2D-TLC of the  $\Delta pknH$  mutant strain.** Lipids separated using system A solvent system: thrice with petroleum ether (60-80 °C): EtOAc (98:2, v/v) in the first direction and once with petroleum ether (60-80 °C)/ acetone (98:2, v/v) in the second direction. TLC plates were developed by staining with 5 % (w/v) ethanolic phosphomolybdic acid for detecting all lipids or followed by charring at 100 °C. PDIMs were not produced in  $\Delta pknH$ , as shown by the absence of a spot in the region marked with an ellipse. PDIMs (I, phthiocerol series A; II, phthiocerol series B; III, series C in phthiodiolone family); MK, menaquinones; TAG, triacylglycerols. (Gómez-Velasco *et al.*, 2013).

For further confirmation that the deletion of PknH resulted in absence of PDIMs, apolar lipids from each strain were analysed by labelling the cell cultures with [ $1\text{-C}^{14}$ ]-propionate which were monitored at different time points (12 and 24 h, 5 and 10 days) (Figure 4.7). As the growth of all the strains were similar (Papavinasasundaram *et al.*, 2005), equal radioactivity was loaded on to 2D-TLCs to normalise the difference in PDIMs production. Thus, the spots corresponding to PDIMs (series A/B and C, I/II and III, in figures, respectively) from wild-type,  $\Delta pknH$  and complemented strains were quantified by scintillation counting. Using this sensitive technique, it was shown that PDIMs were not entirely obliterated, but rather the observed general trend was the reduction in the level of PDIMs produced by the  $\Delta pknH$  strain compared to the parental and complemented strains their levels (Figure 4.7).

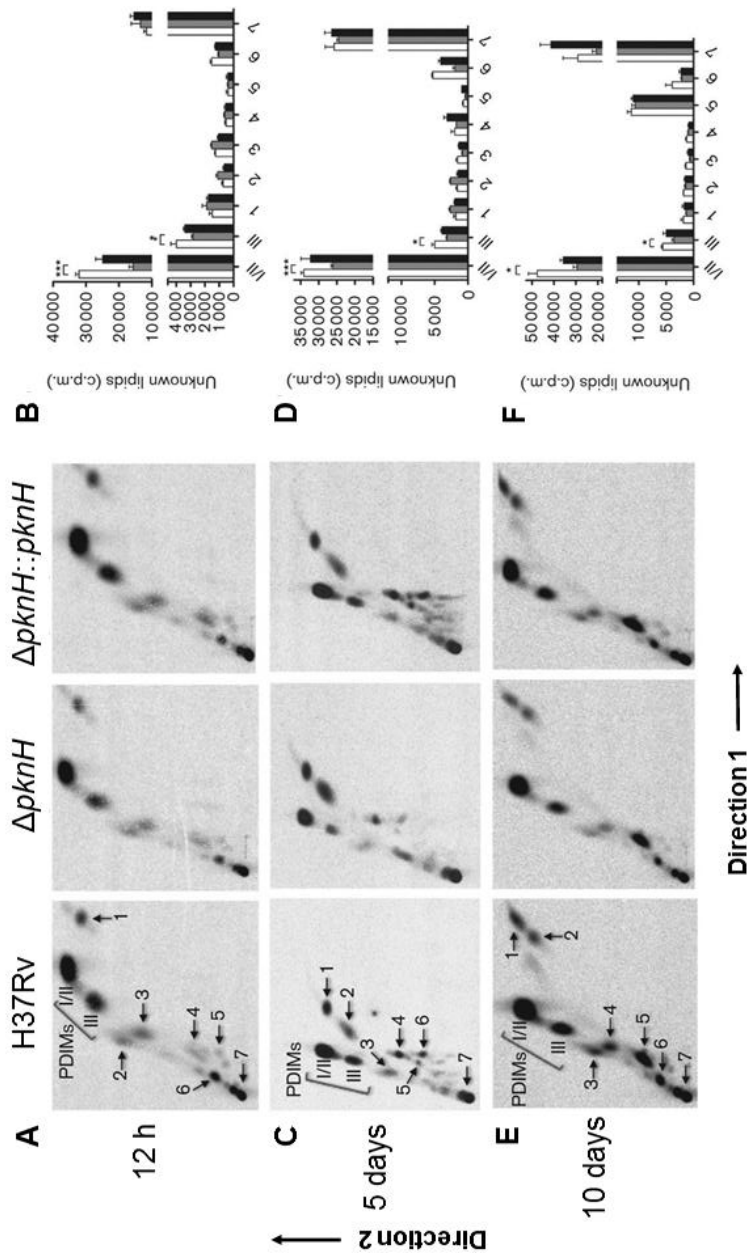


**Figure 4.7. PDIMs production using propionate as carbon source.** Mycobacterial strains grown in 7H9 medium supplemented with OADC were labelled with [ $^{14}\text{C}$ ]-propionate and were further incubated at 37 °C to different time points. Apolar lipids were visualised by loading equal amounts of each sample (100,000 cpm) on a TLC plate and plates were resolved as described in Methods. (A and B) show apolar lipid profiles for H37Rv,  $\Delta pknH$  and  $\Delta pknH::pknH$  12 h, (C and D) 5 days and (E and F) 10 days. Lipids were visualised by exposure to Phosphorimager and spots were identified as PDIMs I, II and III, as described above. For lipid quantification spots from TLC plates, as shown in each 2D-MS were scraped and subjected to liquid scintillation counting. (B, D, F) Quantification of unknown lipids 1–7. The values are the means  $\pm$  SEM from three independent biological experiments. \* $P \leq 0.05$ , \*\*\* $P \leq 0.001$ , significant differences compared with wild-type samples by Student's t-test. White bars, H37Rv; grey bars,  $\Delta pknH$ ; black bars,  $\Delta pknH::pknH$ . (Gómez-Velasco *et al.*, 2013).

While the profile of apolar lipids from propionate-labelled cells remained similar at 12 and 24 h (Figure 4.7A & B), their levels were altered at 5 (Figure 4.7C & D) and 10 days (Figure 4.7E & F). However, levels and lipid profiles of unknown lipids changed at 5 days (C, D) and 10 days (E, F). Thus, radiolabelled-culture analysis, with [ $^{14}\text{C}$ ]-propionate, shows there is a reduction in PDIM synthesis in the  $\Delta pknH$  mutant.

### 4.3.2 Structural analysis of total lipids from the $\Delta pknH$ strain

Total lipids were extracted from mycobacterial strains by the Bligh–Dyer method (Bligh and Dyer, 1959) and were then subjected to FT-ICR MS analysis, which has been previously used to analyse complex lipids from *M. tuberculosis* (Jain *et al.*, 2007). The intensity of a series of molecular ions corresponding to PDIM masses ( $\text{C}_{86}$ – $\text{C}_{100}$ ) in the range of  $m/z$  range 1300–1600 were observed in the FT-ICR mass spectra (Figure 4.8). These PDIMs species were more abundant in the parental wild-type strain compared to the  $\Delta pknH$  mutant (Figure 4.8). There was significant reduction of the relative abundances of both PDIM A–B and PDIM C lipid groups in the mutant strain (Fig. 4.9 & 4.10). While ion species in the region between 1390 and 1449  $m/z$ , corresponding mainly to dimycocerosates A and B, were absent in the  $\Delta pknH$  mutant, these peaks were more abundant in the wild-type strain, thereby suggesting there is a higher production of these cell components in the wild-type (Figure 4.8). There was partial re-establishment of the production of these same ion molecular species in the complemented strain (Figure 4.8). Together, results from this sensitive MS technique and radiolabelled-lipid experiments confirm that PDIMs are produced at lower levels in the  $\Delta pknH$  strain compared to its parental strain.

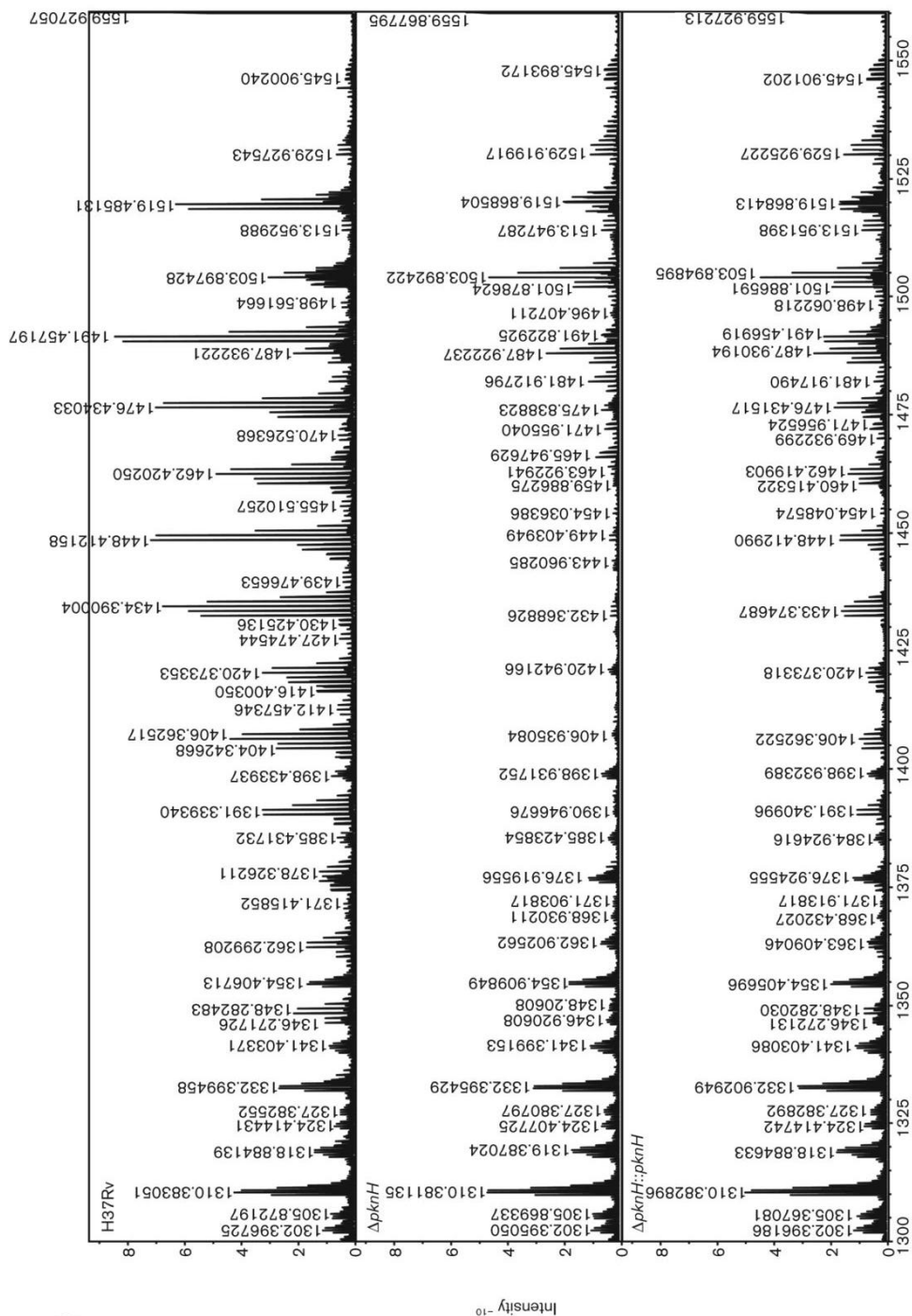


**Figure 4.8. PDIMs region of FT-ICR mass spectra.** Total lipids were extracted by the method described by Bligh-Dyer method. A series of molecular ions corresponding to PDIM masses (m/z 1300–1600) were observed. Based on the relative intensity, PDIMs were more abundant in the wild-type and complemented strains compared with the  $\Delta$ pknH strain. (Gómez-Velasco *et al.*, 2013)

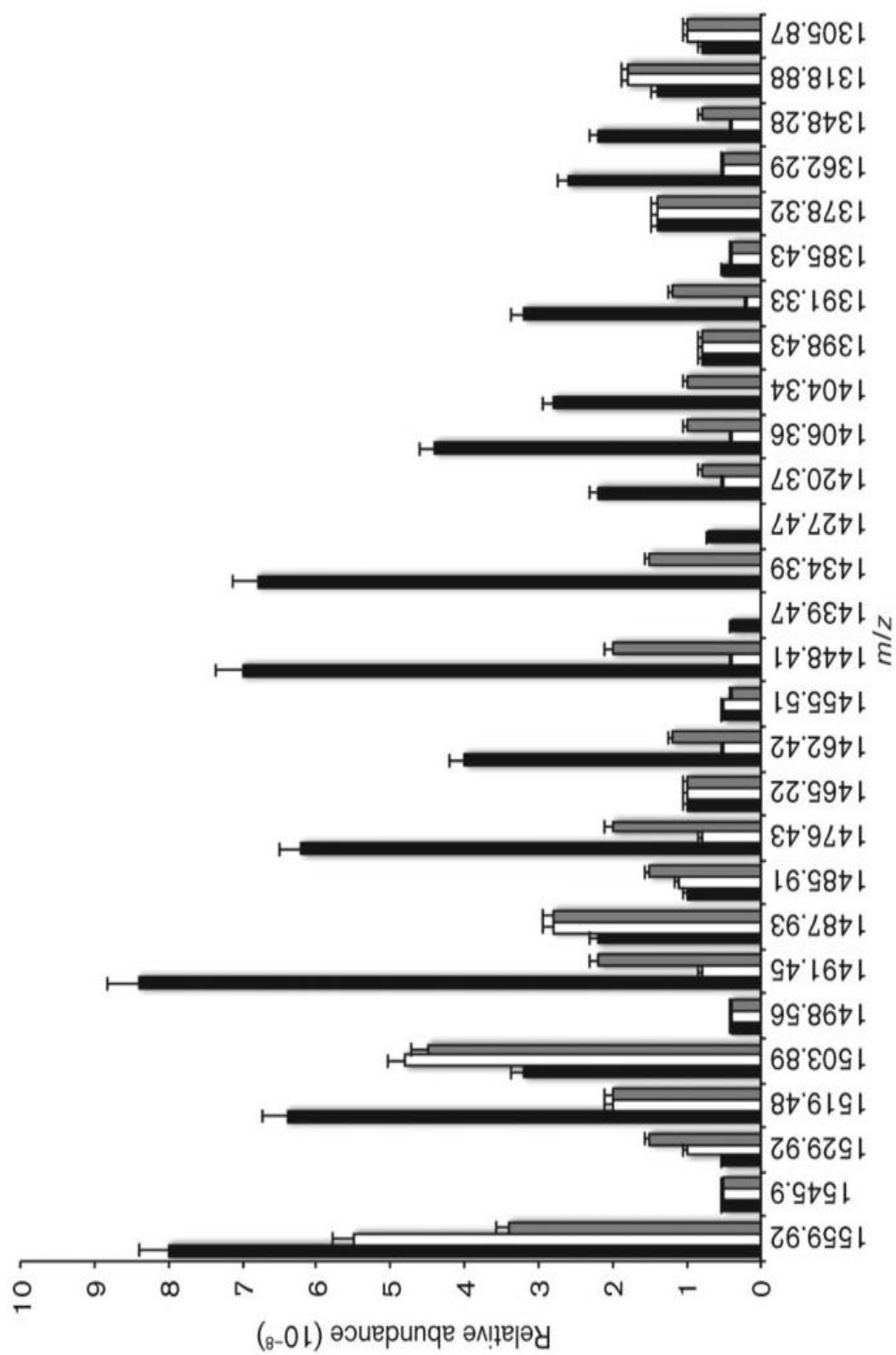


**Figure 4.9. Relative abundance of ion species corresponding to dimycoserates A/B.** Abundance is shown as measured by FT-ICR. Black bars, H37Rv; white bars, ΔpknH; grey bars, ΔpknH:ΔpknH. Error bars represent SEM. (Gómez-Velasco *et al.*, 2013).

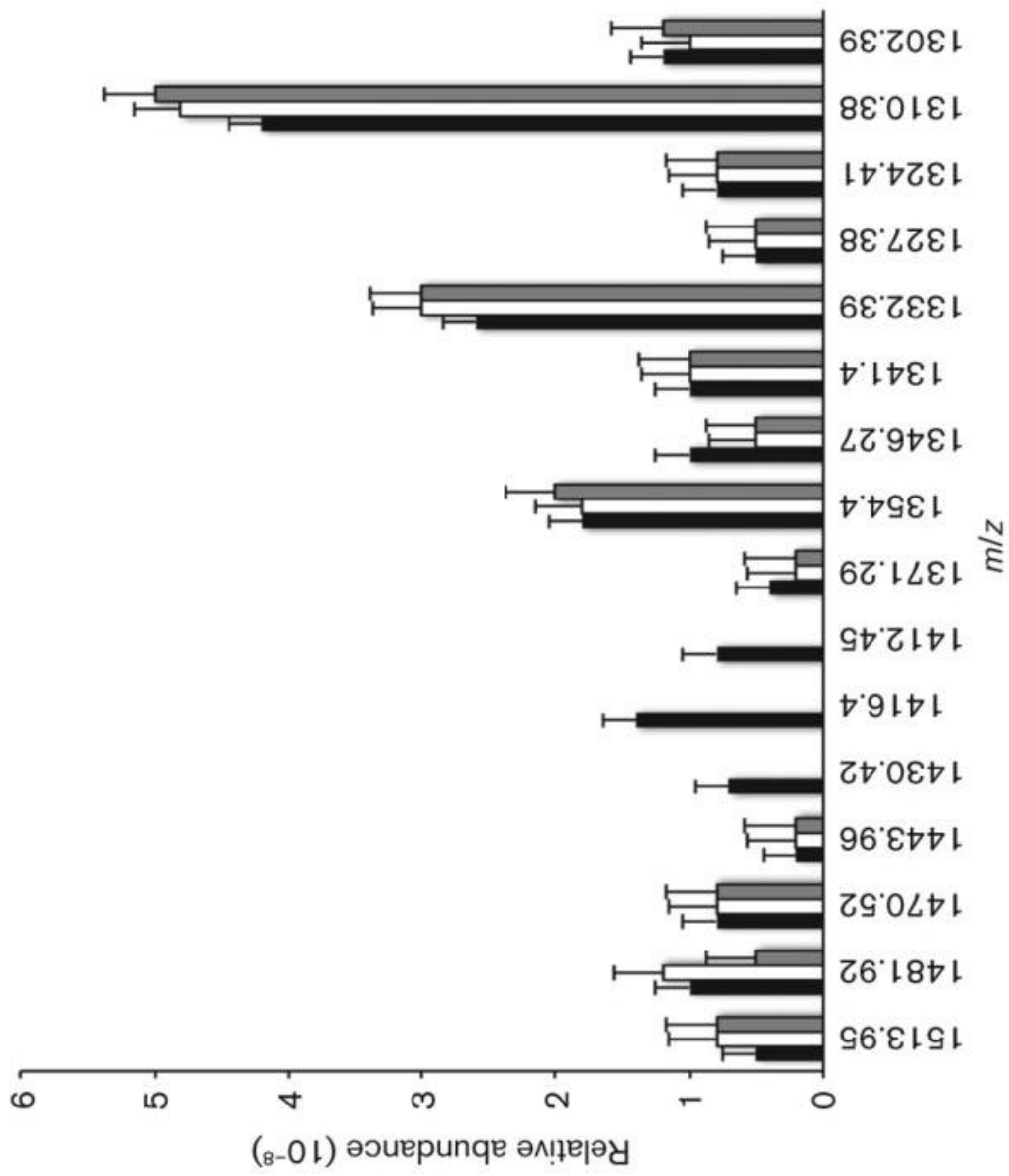


**Figure 4.10. Relative abundance of ion species corresponding to dimycocerosates C.** Abundance is shown as measured by FT-ICR. Black bars, H37Rv; white bars,  $\Delta pknH$ ; grey bars,  $\Delta pknH::pknH$ . Error bars represent SEM. (Gómez-Velasco *et al.*, 2013).

### 4.3.3 Detection of PDIMs using immunofluorescence microscopy

Both the mass spectrometry and TLC based techniques are unable to distinguish between lipids located in the cytosol and cell wall. To confirm whether the observed PDIM levels reflect the relative abundance of these lipids on the cell wall, synthetic antibodies (scFv) against PDIMS were produced and used them to monitor the synthesis of PDIMs using fluorescence microscopy in the mycobacterial strains. As it is known that *M. smegmatis* is unable to produce PDIMs, this bacterium was incubated with the antibodies and was used as a negative control in this experiment. In the analysis of wild-type *M. tuberculosis*, we observed high-intensity labelling and 100% co-localisation for scFv antibodies against PDIMs (Figure 4.11A). However, in the  $\Delta pknH$  strain, a weaker fluorescence signal was detected, which corresponds to 18% of the relative fluorescence compared to the wild-type strain (Figure 4.11B). Interestingly, a stronger fluorescence signal was observed in the complemented strain in comparison to the parental strain, suggesting that the uncontrolled expression of *pknH* may lead to the overproduction of PDIMs.



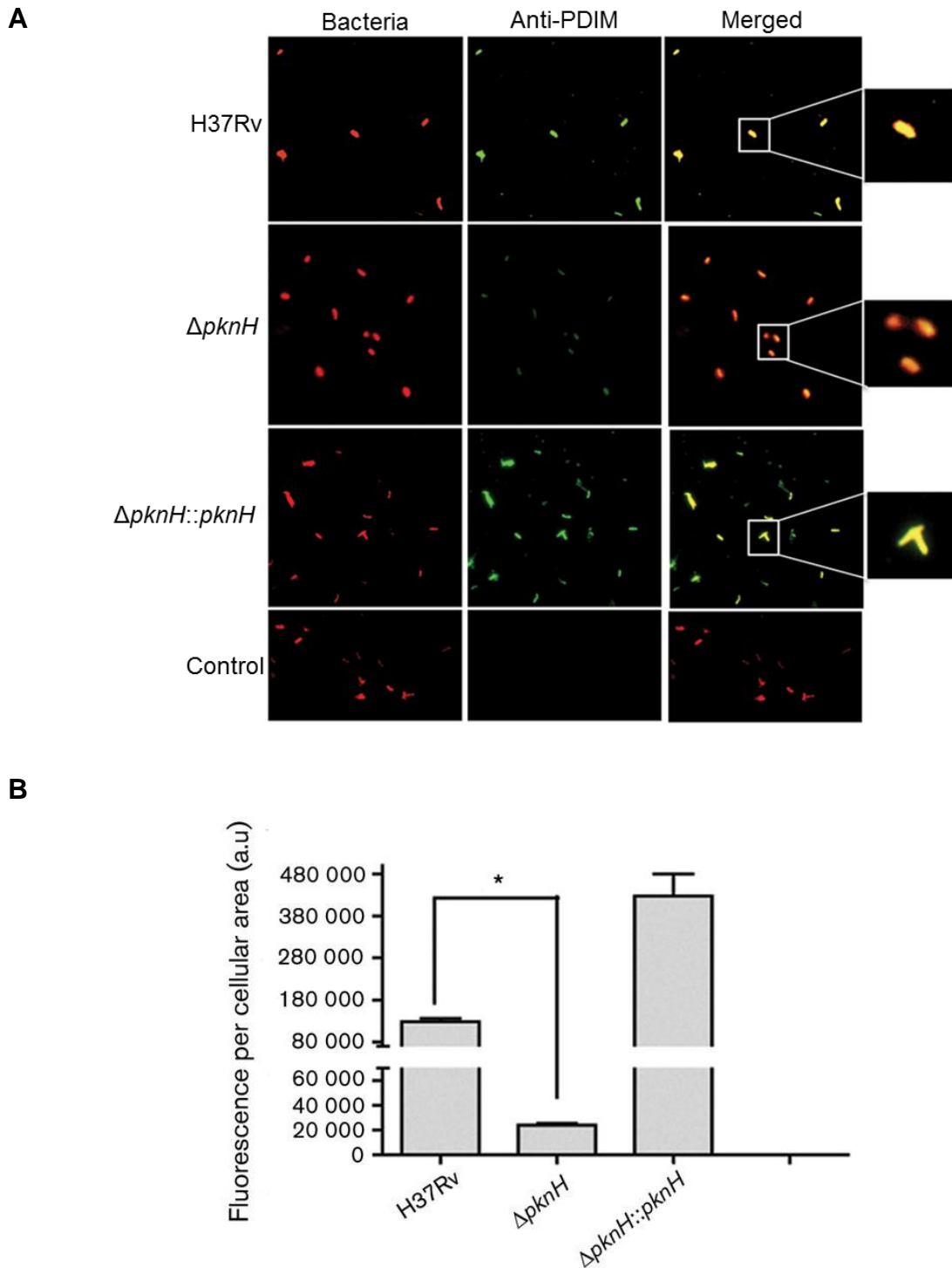


**Figure 4.11. Immunofluorescence microscopy analysis.** (A) Immunofluorescence microscopy analysis. Cells were labelled with rhodamine and scFv antibodies against PDIMs were used as primary antibodies. Anti-MBP antibody coupled to goat anti-mouse IgG-FITC was used as the secondary antibody. The merged images are shown in the panels on the right. *M. smegmatis* was used as a negative control. (B) Immunofluorescence detection. Data represent the means $\pm$ SD of green fluorescence intensity (labelled PDIMs) in arbitrary units (a.u.), which corresponds to labelled PDIMs, *per* cellular area;  $n=50$  single bacterial cells. \* $P\leq 0.05$ . (Gómez-Velasco *et al.*, 2013).

#### **4.3.4 Proteins involved in PDIM production are differentially regulated in the $\Delta pknH$ strain**

Recently, the proteome of the  $\Delta pknH$  strain has been analysed and compared with that of the wild-type H37Rv strain. In that study, cultures grown under rolling conditions with or without the inducer nitric oxide in the form of 3 mM acidified nitric oxide were labelled with iTRAQ reagents. Using this proteomic approach, it was shown that the activation of the DosR regulon was subdued in the  $\Delta pknH$  mutant in response to nitric oxide, indicating that PknH plays an important role in the control of the mycobacterial dormancy regulon (Chao *et al.*, 2010). For the current study, the iTRAQ analysis data was examined and compared between the wild-type and the  $\Delta pknH$  mutant strains, with particular focus on proteins involved in the biosynthesis of PDIMs. We detected that, without induction with nitric oxide, the levels of six out of the seven proteins participating in the production of PDIMs were similar when the mutant was compared with the wild-type strain. Interestingly, we observed higher levels of PpsE levels in the  $\Delta pknH$  strain compared with those in the parental strain and these levels remained high even with induction of nitric oxide (Table 4.1). However, in the presence of the nitric oxide treatment, the expression of PpsD protein was significantly induced. Thus, the iTRAQ analysis shows that the expression of selected proteins of the PDIM biosynthetic pathway is affected by PknH and is triggered by nitric oxide.

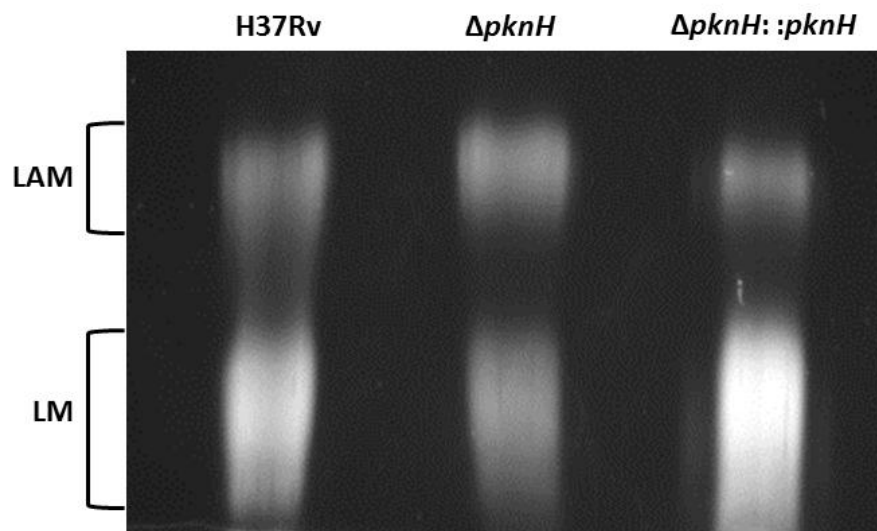
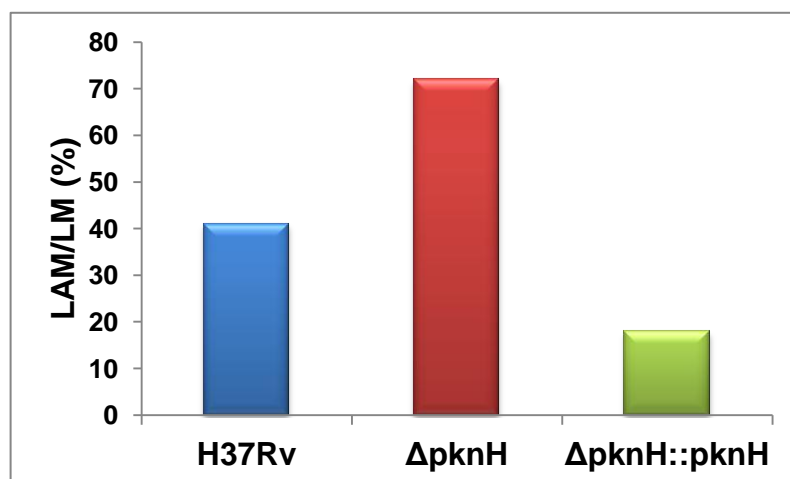
**Table 4.1. iTRAQ analysis of proteins encoded by the PDIM biosynthetic pathway in  $\Delta pknH/pknH$  in presence or absence with 3 mM acidified nitric oxide. (Gómez-Velasco *et al.*, 2013).**

Protein	ORF	Untreated ratio	Treated ratio (no. of peptides)
<b>PpsA</b>	Rv2931	1.05	0.93 (1)
<b>PpsD</b>	Rv2934	0.97	1.48 (1)
<b>PpsE</b>	Rv2935	2.36	1.93 (6)
<b>PapA5</b>	Rv2939	1.16	1.16 (1)
<b>Mas</b>	Rv2940c	1.20	0.89 (8)
<b>FadD28</b>	Rv2941	1.05	0.94 (7)
<b>Ketoreductase</b>	Rv2951c	1.06	1.11 (2)

#### 4.3.5 Lipoglycan profiles of wild type, $\Delta pknH$ and $\Delta pknH::pknH$ strains

Results from previous *in vitro* and *in vivo* studies have provided evidence of the phosphorylation and interaction between PknH and EmbR (Molle *et al.*, 2003; Sharma *et al.*, 2006; Zheng *et al.*, 2007). In *M. smegmatis*, overexpression of PknH has a positive regulatory effect on transcription of the *embCAB* operon *via* phosphorylation of EmbR, catalysing the arabinosylation of LM to LAM and leading to a higher LAM/LM ratio (Sharma *et al.*, 2006). In view of this, we decided to extend our study to *M. tuberculosis* to characterise and quantify the lipoglycans in the  $\Delta pknH$  strain and compare these with those of the parental and complemented strains. Extracted LAM and LM were purified and analysed on 15% SDS-PAGE, as shown in Figure 4.9A From the 15% SDS-PAGE gel, it was shown that there were higher levels of LAM in the  $\Delta pknH$  strain compared to the wild-type and complemented

strains; however, LM levels were less in the  $\Delta pknH$  strain compared to wild-type and complemented strains. Therefore, the ratio of LAM to LM was significantly different between the wild-type and  $\Delta pknH$  strains. For comparative analysis between each strain, the LAM/LM ratio was calculated using densitometric analysis (Figure 4.12B). The LAM/LM ratio was twofold higher in the mutant strain, whereas the complemented strain showed a similar LAM/LM ratio to the parental strain (Figure 4.12B).

**A****B**

**Figure 4.12. Lipoglycan profiles of wild type,  $\Delta pknH$  and  $\Delta pknH::pknH$  strains.** (A) Lipoglycans were extracted and analysed using 15% SDS-PAGE and visualised using a Pro-Q emerald glycoprotein stain (Invitrogen) specific for carbohydrates. (B) Ratio of LAM/LM was calculated using densitometric analysis.

#### 4.4 Conclusion

*M. tuberculosis* is known to have a remarkable ability to persist within the infected host cell, where it can survive in a non-replicating state for several years. Despite the presence of an intact immune system, the tubercle bacillus can employ several survival strategies that can overcome cell-mediated mechanisms of immunity, thus allowing it to become a successful pathogen.

These strategies are linked to the presence of a unique cell envelope, which contains many components shown to exhibit immunological activity, such as LAM (Mishra, Driessen, *et al.*, 2011) and PDIMs (Rousseau *et al.*, 2004; Astarie-Dequeker *et al.*, 2009; Kirksey *et al.*, 2011). Although there is vast knowledge regarding the biosynthesis of cell-wall components, little is known about their regulation. An increased understanding of the processes involved can enhance our knowledge of the pathogenesis of TB. It is vital for the mycobacterial pathogen to modulate the production of cell-wall components during infection in response to environmental stimuli during infection. Recently, *in vitro* kinase studies have suggested that STPKs, present on the mycobacterial membrane, are key regulatory enzymes involved in the communication of such stimuli (Chao *et al.*, 2010). However, little is known the *in vivo* interactions between STPKs and the biosynthetic enzymes of the cell wall.

It has been demonstrated that infection of BALB/c mice with a *pknH* deletion strain leads to a hypervirulent phenotype, which suggested that PknH is involved in controlling the *in vivo* survival of *M. tuberculosis* (Papavinasasundaram *et al.*, 2005). In the study, we carried out 2D-TLC analysis of cell wall lipid analyses to observe

whether knocking out the *pknH* gene affected cell wall lipid biosynthesis. The most significant result was that PDIMs were not produced in the  $\Delta pknH$  strain, which suggested PknH was a positive regulator in the production of PDIMs. Through further experiments using more sensitive techniques including radiolabelled 2D-TLC, mass spectrometry and immunostaining, it was found that synthesis of PDIMs were not completely abolished, but their overall levels in the deletion mutant were lower compared to the wild-type and complemented strains. Recent studies have demonstrated the association of STPKs with the biosynthesis of PDIMs precursors. For example, PknB is involved in the phosphorylation of threonine residue(s) on PapA5 (Gupta *et al.*, 2009), whereas MmpL7, a protein responsible for the transport of PDIMs, was identified as an endogenous substrate of PknD (Pérez *et al.*, 2006). Together, these data suggest that different STPKs work together to regulate the biosynthesis of PDIMs.

Although PDIMs were found to be produced at low levels in the mutant strain, it could not be disregarded that deletion of the *pknH* gene can potentially affect the biosynthesis of other cell wall components or other signalling pathways. It is well known that PknH induces the transcription of the *embCAB* operon via phosphorylation of EmbR (Molle *et al.*, 2003; Zheng *et al.*, 2007). Moreover, the over-expression of *pknH* in *M. smegmatis* leads to a high LAM/LM ratio (Sharma *et al.*, 2006). Both LAM and LM behave as ligands for cell receptors on the host cell and play a critical role in the pathogenesis of *M. tuberculosis*, since they are located on its cell surface. Increasing evidence has led to the hypothesis that *M. tuberculosis* adapts to its human host by cloaking its cell envelope with mannosylated structures

which mimic the glycoforms of mammalian mannoproteins (Torrelles and Schlesinger, 2010). During phagocytosis, these mannosylated molecules are able to interact with the mannose receptor on macrophages, which contributes to the intracellular survival of bacilli by regulating phagosome-lysosome fusion events (Torrelles and Schlesinger, 2010). Therefore, the amount and nature of the mannose exposed on the cell surface might influence the phagocytosis event and host response to *M. tuberculosis* (Torrelles and Schlesinger, 2010). While strains with abundant mannose on their surface have become more host adapted, bacilli strains with reduced mannose are considered hypervirulent (Torrelles and Larry S Schlesinger, 2010). The more host-adapted strains may be highly successful in forming an infection and could be more likely to establish a latent infection (Torrelles and Schlesinger, 2010). In light of this hypothesis, an unbalanced LAM/LM ratio might go some way to explaining why the  $\Delta pknH$  strain became hypervirulent. In this study, our lipoglycan analysis revealed that the LAM/LM ratio was twofold higher in the  $\Delta pknH$  strain compared with that in the parental strain. This result could potentially be due to the transcriptional effect of the *embCAB* operon via EmbR phosphorylation. Furthermore, deletion of *pknH* in *M. tuberculosis* resulted in reduced transcription of *embB* and *embC* in cultures treated with sublethal doses of EMB (Papavinasasundaram *et al.*, 2005).

The iTRAQ analysis has enabled us to get a better understanding of the signalling cascade that is mediated by PknH. Experimental data has revealed that seven proteins participating in the biosynthesis of PDIMs are differentially regulated. In particular, it was interesting to note that amongst all the proteins that were detected

in the iTRAQ experiment, the expression of PpsE protein was maintained in cultures in the presence and absence of nitric oxide. PpsE, a PKS, is the last enzyme required in synthesis of the  $\beta$ -diol backbone of PDIMs (Trivedi *et al.*, 2005). In view of the upregulation of this enzyme, it is suggested that PpsE plays a critical role in PDIMs biosynthesis. In fact, studies have previously demonstrated the interaction of PpsE with TesA and MmpL7 (Rao and Ranganathan, 2004; Jain and Cox, 2005). Jain *et al.* has demonstrated that a domain of MmpL7 biochemically interacts with PpsE, which suggests that MmpL7 acts not only as a transporter but also as a scaffold to couple PDIM synthesis (Jain and Jeffery S Cox, 2005). PpsE can also form an interaction with the type II thioesterase TesA, an enzyme that might not only be involved in releasing the elongated phthiocerol backbone from PpsE, but also participate in housekeeping functions that remove inappropriate acyl units and/or aberrant acyl intermediates (Rao and Ranganathan, 2004). Together, these results indicate that PpsE may play a role as an activator or inhibitor during final PDIM synthesis. On the other hand, the upregulation of PpsE in  $\Delta pknH$  strains treated with nitric oxide could be a result of the protein sensing the incorrect production of PDIMs, due to the lack of signalling by PknH. The replication, transcription and translation of a gene cluster ~50 kbp leads to the biosynthesis of PDIM, which represents a high energy process. Thus, it is tempting to suggest that phosphorylation, regulation by STPKs and protein–protein complexes may efficiently coordinate PDIM synthesis.

The results from this study have shown that PknH contributes to the production and synthesis of *M. tuberculosis* cell-wall components. However, further experiments are necessary to understand fully how PDIM production is regulated by PknH alongside



other STPKs. PknH has also been established as playing an important role in TB pathogenesis through interaction with EmbR, a transcriptional regulator of arabinan metabolism in *M. tuberculosis*. Future efforts are needed to discover the exact role of the PknH-EmbR signalling system in mycobacterial pathogenesis, which eventually could become a therapeutic target.

# **5 General Conclusions**

The rapid increase in the number of cases of MDR- and XDR-TB has led to an urgent need for the identification of novel drug targets in *M. tuberculosis* and the development of active inhibitors against them. The unique lipid-rich cell wall of mycobacteria, which provides physical protection to the bacilli and can also play an important role in virulence, is an attractive target for the discovery of anti-TB drugs. Thus, improving our understanding of the structure and biosynthetic pathways of the mycobacterial cell wall can mediate the development of novel anti-mycobacterial drug targets.

This Chapter summarises the findings of three different research themes covered in this thesis in relation to the investigation of novel targets against mycobacteria: identifying the cellular target of a compound with inhibitory activity against mycobacteria, studying the essentiality of a PPM synthase in biosynthesis of lipoglycans and characterising the effects of the disruption of a protein kinase in the synthesis of cell-wall components.

Amongst several compounds from the ChemBridge library, AKR334 was selected for further studies to determine its cellular target as it displayed encouraging MIC values against *M. tuberculosis* (Ananthan *et al.*, 2009; Maddry *et al.*, 2009) and *M. smegmatis*. In recent times, the use of whole-cell screening has been a successful strategy in the identification of new anti-TB drugs including TMC207 (Andries *et al.*, 2005) and novel drug targets including DprE1 (Makarov *et al.*, 2009; Christophe *et al.*, 2009) and MmpL3 protein (La Rosa *et al.*, 2012; Tahlan *et al.*, 2012; Grzegorzewicz *et al.*, 2012; Remuiñán *et al.*, 2013). Thus, we used the same method

to identify the target of AKR334. From the comparative analysis of the whole-genomic sequence of the AKR334-resistant mutant and its parental strain, it was found that the mutant had SNPs in the *mmpL3* gene and the promoter sequence of the glycerol operon. Previous studies have shown that depletion of the *mmpL3* gene leads to the accumulation of TMM molecules, thereby confirming that MmpL3 functions as an essential membrane exporter of TMM (Varela *et al.*, 2012). Treatment of *M. bovis* BCG with THPP and spiro analogues identified these compounds as inhibitors of the MmpL3 protein (Remuiñán *et al.*, 2013). When *M. smegmatis* cultures were treated with AKR334, TMM levels remained the same in untreated and treated cells. This suggests that MmpL3 is not the cellular target of AKR334.

The glycerol operon consists of a cluster of genes that are involved in the transport and metabolism of glycerol. In the AKR334-resistant mutant genomic sequence, single base change mutation (A to G) was detected in the promoter sequence of the glycerol operon. Overexpression of the genes in the glycerol operon did not cause resistance to AKR334 and we were unable to generate recombinant constructs containing the glycerol operon promoter sequence from the resistant mutant strains to validate the cellular target of AKR334. However, we were able to show that AKR334 had a greater inhibitory effect against *M. smegmatis* grown in glycerol-containing media compared to *M. smegmatis* grown in acetate-containing media. Previous studies have identified PI and A039 compounds as inhibitors of the *glpK* gene in *M. tuberculosis* by demonstrating their ability to induce self-poisoning of *M. tuberculosis* by promoting accumulation of glycerol phosphate and ATP depletion (Pethe *et al.*, 2010; Stanley *et al.*, 2012). To discover whether AKR334 has a similar

mechanism of action to these inhibitors, further work by liquid chromatography/mass spectrometry (LC/MS) techniques can be used to examine the relative abundances of glycerol phosphate and ATP in various concentrations of the compound. Additionally, reverse transcription PCR experiments can be used to identify whether the expression of glycerol operon genes is altered in the AKR334-resistant mutant strain; this will further validate that the mode of action of AKR334 is related to glycerol metabolism.

A PPM synthase encoded by Mt-Ppm1 (Rv2051c) has previously been shown to generate polyprenyl-phosphate-based mannosyl donors, such as C<sub>50</sub>/C<sub>50</sub>-P-Man<sub>p</sub>, that are required for the biosynthesis of higher PIMs, LM and LAM (Gurcha *et al.*, 2002). While this PPM synthase in *M. tuberculosis* is encoded by the two-domain gene *Mt-ppm1*, two neighbouring genes, in *M. smegmatis* it is encoded by *MSMEG\_3859* (Domain 2) and *MSMEG\_3860* (Domain 1) (Gurcha *et al.*, 2002). *In vitro* studies have previously demonstrated that Mt-ppm1/D2 and *MSMEG\_3859* are sufficient for PPM synthase activity (Gurcha *et al.*, 2002; Baulard *et al.*, 2003). However, our findings have not only demonstrated the *in vivo* role of *MSMEG\_3859* (Domain 2, *Ms-ppm1*) in *M. smegmatis*, but they have also confirmed its essentiality in *M. smegmatis* by using CESTET, a genetic tool for testing gene essentiality. Additionally, using the ΔMsPpm conditional mutant, we were able to show that Rv3779 and PpgS, glycosyltransferases involved in AG biosynthesis, were unable to restore PPM synthase activity in absence of *MSMEG\_3859* activity; thus, discounting previous studies predicting their functionality as a potential secondary PPM synthase (Scherman *et al.*, 2009; Skovierová *et al.*, 2010). Together, these results indicate that

*ppm1* is the gene encoding the sole PPM synthase in *M. tuberculosis* that can produce mannose donors for the synthesis of higher PIMs, LM and LAM and is a potential drug target for future anti-TB agents.

*M. tuberculosis* possesses a distinct cell wall that is which plays a critical role in the interaction of the pathogen with its human host. Emerging evidence suggests that the synthesis of complex cell-wall complex is facilitated by serine/threonine protein kinases (STPKs). Using *in vivo* radiolabelling, MS and immunostaining analyses, we were able to show that deletion of one of the STPKs, PknH, leads to the attenuation of the synthesis of PDIMs, a major *M. tuberculosis* virulence lipid (Cox *et al.*, 1999; Camacho *et al.*, 2001; Rousseau *et al.*, 2004; Astarie-Dequeker *et al.*, 2009). We also found that several proteins involved in the PDIM biosynthetic pathway are differentially expressed in the deleted *pknH* strain. Furthermore, when we analysed the composition of the major lipoglycans, LAM and LM, and found a twofold higher LAM/LM ratio in the mutant strain. Thus, we provide experimental evidence that PknH contributes to the production and synthesis of *M. tuberculosis* cell-wall components. As PknH has previously been established as playing an important role in TB pathogenesis *via* interaction with EmbR, a transcriptional regulator of arabinan metabolism in *M. tuberculosis*, it is important that future work is conducted to examine the exact role of the PknH-EmbR signalling system in mycobacterial pathogenesis to increase our understanding of host-pathogen interactions. Together our results in this study demonstrated that PknH mediates the biosynthesis of cell-wall components that possess immunomodulatory activity; thus, PknH could potentially be a novel target for anti-TB drugs.

## **6 General Material and Methods**

### 6.1 Polymerase Chain Reaction (PCR)

Forward and Reverse primers were designed in order to amplify the genes of interest. All oligonucleotides were supplied by Eurofins MWG Operon (Ebersberg, Germany). All reaction mixtures for the PCR using Phusion® High-Fidelity DNA Polymerase (New England Labs) contained the components in Table 6.1.

**Table 6.1 PCR reaction components.**

Component	Concentration	20 µl reaction
Milli Q water	-	11.8 µl
5X Phusion HF or GC Buffer	1x	4 µl
10 mM dNTPs	200 µM	0.4 µl
10 µM Forward Primer	10 pmol/µl	1 µl
10 µM Reverse Primer	10 pmol/µl	1 µl
Template DNA	<250 ng	0.4 µl
DMSO	100%	1 µl
MgCl <sub>2</sub>	500 mM	0.2 µl
Phusion DNA Polymerase	2 U/µl	0.2 µl

PCR was performed in the Eppendorf mastercycler using the programme in Table 6.2.



**Table 6.2 Gradient PCR programme.**

Step	Temperature	Duration
<b>Initial Denaturation</b>	<b>98°C</b>	30 s
	<b>98°C</b>	10 s
<b>x35 cycles</b>	<b>65-80°C</b>	30 s
	<b>72°C</b>	30 s/kb
<b>Final Extension</b>	<b>72°C</b>	10 min
<b>Hold</b>	<b>4°C</b>	∞

Agarose gel electrophoresis was used to separate PCR products. Molecular biology grade agarose (Bioline) was dissolved in Tris-acetate-EDTA (TAE) buffer to produce 0.8% or 1% agarose gels. PCR product was mixed with 6× loading dye and separated on the agarose gel by electrophoresis (110 – 140 V, 400mA) in TAE buffer alongside 1 kb DNA ladder (New England Labs). DNA was visualised by staining the gel with ethidium bromide for 15 mins and examined under UV light (Bio-Rad Gel Doc systems). DNA bands were excised with a clean scalpel and extracted from the gel using the QIAquick Gel Extraction Kit (Qiagen) according to the manufacturer's instructions.

## 6.2 DNA digestion

Double restriction enzyme digestion reactions contained 2 µl of restriction digest buffer, 10 µl of purified DNA (plasmid /genomic DNA /PCR product) 1 µl of each restriction enzyme and 2 µl of 10× Bovine Serum Albumin (BSA) (wherever required). The reaction mixture was made to a final volume of 50 µl with distilled water. The reaction was incubated at 37 °C for 2 hours. DNA fragments were separated by

electrophoresis in a 1% w/v agarose gel and DNA fragments of the expected size were cut out of the gel and extracted as previously described in Section 6.1.

### 6.3 DNA ligation

Digested DNA fragments with compatible ends can be ligated using T4 DNA ligase (New England Labs). The ligation mixture contained 1  $\mu$ l of T4 DNA ligase enzyme, 2  $\mu$ l of 10 $\times$  T4 ligase buffer and required concentrations of DNA fragments. DNA ligation reactions were made to a final volume of 10  $\mu$ l using distilled water and incubated at room temperature for 4 hours before leaving overnight at 4 °C. Samples were either stored at -20°C until further use or used instantly for transformation to *E. coli* Top10 (DH5 $\alpha$ MCR) cells as described below in Section 6.5.

### 6.4 Preparation of chemical competent *E. coli* cells

A single colony of *E. coli* Top10 (DH5 $\alpha$ MCR) was inoculated into 2.5 ml LB medium and incubated at 37°C overnight. The overnight culture was then used to inoculate 250 ml LB medium with 20 mM MgSO<sub>4</sub>. Cells were grown to an OD<sub>600</sub> 0.4-0.6 and then harvested by centrifugation at 4500 $\times$ g for 10 min at 4 °C. Cell pellets were gently resuspended in 1/4th volume of ice-cold TFB1 (30 mM potassium acetate, 10 mM CaCl<sub>2</sub>, 50 mM MnCl<sub>2</sub>, 100 mM RbCl<sub>2</sub>, 15% glycerol, filter-sterilised and stored at 4°C) and resuspended cells were incubated on ice for 5 min. Cells were harvested by centrifugation as described previously and were then gently resuspended in 1/25 of the volume of ice-cold TFB2 (10 mM MOPS or PIPES, pH 6.5, 75 mM CaCl<sub>2</sub>, 10 mM

RbCl<sub>2</sub>, 15% glycerol, filter-sterilised and stored at 4°C). Cells were incubated on ice for 15-60 min and then stored as 100 µl aliquots at -70°C.

### **6.5 Transformation of *E. coli* competent cells**

*E. coli* competent cells were thawed on ice and mixed with 5 µl of ligation mix. Cells and the ligation reaction were mixed gently and then incubated on ice for 30 min. Cells were then transformed by heat shock at 42°C for 90 seconds followed by which the cells were placed on ice to cool. 500 µl of LB broth was added into the tube and incubated at 37°C for 1 hour with shaking. The transformed cells were then plated onto appropriate selection plates.

### **6.6 Plasmid extraction**

*E. coli* colonies grown on selection plates were used to inoculate 5 ml of LB broth supplemented with appropriate antibiotic and incubated shaking at 37°C overnight. Cultures were harvested by centrifugation and plasmids were extracted using the QIAprep Spin Miniprep Kit (QIAGEN) according to the manufacturer's instructions. All constructs were verified by DNA sequencing performed by Eurofins MWG Operon (Ebersberg, Germany).

### **6.7 Preparation of *M. smegmatis* electrocompetent cells**

*M. smegmatis* cells were grown to OD<sub>600</sub> 0.8 and washed with 1 volume (original volume of culture) of 10% glycerol (filter-sterilised, pre-cooled to 4°C) twice and

harvested by centrifugation at 4°C at 4500g. Cells were resuspended in 1/10 volume of 10% glycerol and aliquoted (200 µl) for immediate use or can be stored at -70°C.

### **6.8 Electroporation of *M. smegmatis***

A 200 µl aliquot of *M. smegmatis* electrocompetent cells was thawed on ice and 3-5 µl of plasmid dissolved in water was added to the cells. The mix was left on ice for 15 minutes and then placed into a chilled 1 mm electroporation cuvette. Electroporation was done using an Eppendorf Electroporator (model no - 2510) at 1800V. 800 µl of TSB broth was added and cells were allowed to recover at 37°C for at least one generation time before plating on TSB agar with appropriate antibiotics.

### **6.9 *M. smegmatis* genomic DNA extraction**

Cells were resuspended in 450 µl of glucose Tris-EDTA (GTE) solution (25 mM Tris-HCl pH 8.0, 10 mM EDTA, 50 mM glucose) and 50 µl of freshly prepared lysozyme solution (10 mg/ml) was added. After overnight incubation at 37 °C, 500 µl of 10% sodium dodecyl sulfate (SDS) (Sigma-Aldrich) and 250 µl of Proteinase K (10 mg/ml) (Sigma-Aldrich) were added. After incubating the cells at 55 °C for 3 to 4 hours, 1 ml of 5 M NaCl was added and the cells were incubated at 65 °C for 15 min. Chloroform: isoamyl alcohol (24:1) (Fisher Scientific) extraction was performed twice to exclude protein. The DNA was precipitated with 2.8 ml of isopropanol (0.7 volume of total mixture). The samples were mixed gently by inverting the tubes, centrifuged at 3000 rpm for 5 min and the supernatant was discarded. The DNA pellet was washed with 10 ml of 70% ethanol and centrifuged at 3000 rpm for 5 min. After repeating the

ethanol wash, the supernatant was discarded and the DNA pellet was air-dried for 5 min. The DNA pellets were dissolved in Tris-EDTA buffer containing 10 mM and 1 mM EDTA and stored at  $-20\text{ }^{\circ}\text{C}$ .

### **6.10 Apolar and polar lipid extraction**

Polar and apolar lipids were then extracted as described previously (Dobson *et al.*, 1985). *M. smegmatis* cells were treated in 2 ml of  $\text{CH}_3\text{OH}$ : 0.3 % aqueous NaCl (100:10, v/v) and 2 ml petroleum ether (60-80  $^{\circ}\text{C}$ ) for 30 min. The suspension was centrifuged and the upper layer containing the apolar lipids was separated. An additional 2 ml of petroleum ether (60-80  $^{\circ}\text{C}$ ) was added to the lower layer, mixed and centrifuged as described above. The two upper petroleum ether fractions were combined and dried under compressed  $\text{N}_2$ . For polar lipids, 2.3 ml of  $\text{CHCl}_3$ :  $\text{CH}_3\text{OH}$ : 0.3% aqueous NaCl (90:100:30, v/v/v) was added to the lower aqueous phase which was mixed for 1 h. This mixture was centrifuged and the supernatant was separated. The remaining residue was re-extracted twice with 750  $\mu\text{l}$  of  $\text{CHCl}_3$ :  $\text{CH}_3\text{OH}$ : 0.3% aqueous NaCl (50:100:40, v/v/v). Equal amounts of  $\text{CHCl}_3$  and 0.3% NaCl (1.3 ml of each) were added to the pooled supernatant which was stirred for 1 h. The mixture was centrifuged and the lower layer containing the polar lipids was recovered, dried under compressed  $\text{N}_2$ , and resuspended in  $\text{CHCl}_3$ : $\text{CH}_3\text{OH}$  (2:1, v/v).

### **6.11 Thin layer chromatography (TLC) analysis for lipids**

Equivalent amounts of radioactivity were spotted on TLC plates (5554 silica gel 60F524; Merck) for further 2D-TLC analysis using following solvent systems. In case

of cold samples, 100 µg of apolar or polar lipids were spotted on TLC plates for 2D separation and analysis. Cold samples were stained with 5 % (w/v) ethanolic phosphomolybdic acid for detecting all lipids or  $\alpha$ -naphthol-sulfuric acid for detecting carbohydrate containing lipids, followed by charring at 100 °C. Radioactive-labelled lipids were visualised by 48 h exposure on X-ray films by autoradiography (Kodak Biomax MR film).

### 6.12 Solvent systems for 2D-TLC analysis

Apolar lipids are separated by systems A, B, C and D. Polar lipids are separated using systems D and E. The solvent systems are described in Table 6.3.

**Table 6.3** Developing system of 2D- TLC analysis for lipid

System	Direction 1	Direction 2
<b>A</b>	Petroleum Ether (b.p. 60-80 °C)/ Ethyl Acetate 98 : 2 (v/v)	Petroleum Ether (b.p. 60-80 °C)/Acetone 92 : 8 (v/v)
<b>B</b>	Petroleum Ether (b.p. 60-80 °C)/Acetone 92 : 8 (v/v)	Toluene/Acetone 95 : 5 (v/v)
<b>C</b>	Chloroform/Methanol 96 : 4 (v/v)	Toluene/Acetone 80 : 20(v/v)
<b>D</b>	Chloroform/ Methanol /Water 100 : 14 : 0.8 (v/v/v)	Chloroform/Acetone/ Methanol /Water 50 : 60 : 2.5 : 3 (v/vv/v)
<b>E</b>	Chloroform/ Methanol /Water 60 : 30 : 6 (v/v/v)	Chloroform/Acetic Acid/ Methanol /Water 40 : 25 : 3 : 6 (v/vv/v)

### **6.13 Dialysis of lipoglycans**

Dialysis of lipoglycans was performed using a low molecular weight cut off dialysis tubing, Spectra/Por membrane 6, MWCO 3,500 kDA purchased from Spectrum Labs, according to manufacturer's instructions.

### **6.14 SDS-PAGE**

SDS-polyacrylamide gel electrophoresis technique was used for the separation of lipoglycans. Resolving gels of either 15% (w/v) acrylamide and a stacking gel of 12% were prepared and cast in the electrophoresis apparatus according to the manufacturer's instructions and run at 200 mV and 25 mA/gel until completion. Lipoglycans were visualised using Pro-Q Emerald Glycoprotein stain (Invitrogen) according to the manufacturer's protocol. Radiolabelled lipoglycans were visualised by 48 h exposure on x-ray films by autoradiography (Kodak Biomax MR film).

# 7 References



- Abrahams, K.A., Cox, J.A.G., Spivey, V.L., Loman, N.J., Pallen, M.J., Constantinidou, C., *et al.* (2012) Identification of novel imidazo[1,2-*a*]pyridine inhibitors targeting *Mycobacterium tuberculosis* QcrB. *PLoS One* **7**: e52951.
- Alderwick, L.J., Seidel, M., Sahm, H., Besra, G.S., and Eggeling, L. (2006) Identification of a novel arabinofuranosyltransferase (AftA) involved in cell wall arabinan biosynthesis in *Mycobacterium tuberculosis*. *J Biol Chem* **281**: 15653-61.
- Alibaud, L., Rombouts, Y., Trivelli, X., Burguière, A., Cirillo, S.L.G., Cirillo, J.D., *et al.* (2011) A *Mycobacterium marinum* TesA mutant defective for major cell wall-associated lipids is highly attenuated in *Dictyostelium discoideum* and zebrafish embryos. *Mol Microbiol* **80**: 919-34.
- Ananthan, S., Faaleolea, E.R., Goldman, R.C., Hobrath, J.V., Kwong, C.D., Laughon, B.E., *et al.* (2009) High-throughput screening for inhibitors of *Mycobacterium tuberculosis* H37Rv. *Tuberculosis (Edinburgh, Scotland)* **89**: 334-53.
- Andries, K., Verhasselt, P., Guillemont, J., Göhlmann, H.W.H., Neefs, J.-M., Winkler, H., *et al.* (2005) A diarylquinoline drug active on the ATP synthase of *Mycobacterium tuberculosis*. *Science* **307**: 223-7.
- Appelmelk, B.J., den Dunnen, J., Driessen, N.N., Ummels, R., Pak, M., Nigou, J., *et al.* (2008) The mannose cap of mycobacterial lipoarabinomannan does not dominate the *Mycobacterium*-host interaction. *Cell Microbiol* **10**: 930-44.
- Armstrong, J.A., and Hart, P.D. (1971) Response of cultured macrophages to *Mycobacterium tuberculosis*, with observations on fusion of lysosomes with phagosomes. *J Exp Med* **134**: 713-40.
- Astarie-Dequeker, C., Le Guyader, L., Malaga, W., Seaphanh, F.-K., Chalut, C., Lopez, A., and Guilhot, C. (2009) Phthiocerol dimycocerosates of *Mycobacterium tuberculosis* participate in macrophage invasion by inducing changes in the organization of plasma membrane lipids. *PLoS Pathog* **5**: e1000289.
- Av-Gay, Y., and Everett, M. (2000) The eukaryotic-like Ser/Thr protein kinases of *Mycobacterium tuberculosis*. *Trends Microbiol* **8**: 238-44.
- Azad, A.K. (1997) Gene Knockout Reveals a Novel Gene Cluster for the Synthesis of a Class of Cell Wall Lipids Unique to Pathogenic Mycobacteria. *J Biol Chem* **272**: 16741-16745.
- Azad, A.K., Sirakova, T.D., Rogers, L.M., and Kolattukudy, P.E. (1996) Targeted replacement of the mycocerosic acid synthase gene in *Mycobacterium bovis* BCG produces a mutant that lacks mycosides. *Proc Natl Acad Sci U S A* **93**: 4787-92.
- Azuma, I., Thomas, D.W., Adam, A., Ghuyssen, J.M., Bonaly, R., Petit, J.F., and Lederer, E (1970) Occurrence of *N*-glycolylmuramic acid in bacterial cell walls. A preliminary survey. *Biochim Biophys Acta* **208**: 444-51.

- Bach, H., Mazor, Y., Shaky, S., Shoham-Lev, A., Berdichevsky, Y., Gutnick, D.L., and Benhar, I. (2001) *Escherichia coli* maltose-binding protein as a molecular chaperone for recombinant intracellular cytoplasmic single-chain antibodies. *J Mol Biol* **312**: 79-93.
- Ballou, C.E., and Lee, Y.C. (1964) The structure of a myoinositol mannoside from *Mycobacterium tuberculosis* glycolipid. *Biochemistry* **3**: 682-5.
- Banerjee, A., Dubnau, E., Quemard, A., Balasubramanian, V., Um, K.S., Wilson, T., et al. (1994) *inhA*, a gene encoding a target for isoniazid and ethionamide in *Mycobacterium tuberculosis*. *Science* **263**: 227-30.
- Bardarov, S., Bardarov Jr, S., Pavelka Jr, M.S., Sambandamurthy, V., Larsen, M., Tufariello, J., et al. (2002) Specialized transduction: an efficient method for generating marked and unmarked targeted gene disruptions in *Mycobacterium tuberculosis*, *Mycobacterium bovis* BCG and *Mycobacterium smegmatis*. *Microbiology* **148**: 3007-17.
- Barral, D.C., and Brenner, M.B. (2007) CD1 antigen presentation: how it works. *Nat Rev Immunol* **7**: 929-41.
- Barry, C.E., Lee, R.E., Mdluli, K., Sampson, A.E., Schroeder, B.G., Slayden, R.A., and Yuan, Y. (1998) Mycolic acids: structure, biosynthesis and physiological functions. *Prog Lipid Res* **37**: 143-79.
- Baulard, A.R., Gurcha, S.S., Engohang-Ndong, J., Gouffi, K., Locht, C., and Besra, G.S. (2003) *In vivo* interaction between the polyprenol phosphate mannose synthase Ppm1 and the integral membrane protein Ppm2 from *Mycobacterium smegmatis* revealed by a bacterial two-hybrid system. *J Biol Chem* **278**: 2242-8.
- Belanger, A.E., Besra, G.S., Ford, M.E., Mikusová, K., Belisle, J.T., Brennan, P.J., and Inamine, J.M. (1996) The *embAB* genes of *Mycobacterium avium* encode an arabinosyl transferase involved in cell wall arabinan biosynthesis that is the target for the antimycobacterial drug ethambutol. *Proc Natl Acad Sci U S A* **93**: 11919-24.
- Belisle, J.T. (1997) Role of the Major Antigen of *Mycobacterium tuberculosis* in Cell Wall Biogenesis. *Science* **276**: 1420-1422.
- Berg, S., Kaur, D., Jackson, M., and Brennan, P.J. (2007) The glycosyltransferases of *Mycobacterium tuberculosis* - roles in the synthesis of arabinogalactan, lipoarabinomannan, and other glycoconjugates. *Glycobiology* **17**: 35-56R.
- Bernheim, F. (1940) The effect of salicylate on the oxygen uptake of the tubercle bacillus. *Science* **92**: 204.
- Besra, G.S., and Brennan, P.J. (1997) The mycobacterial cell wall: biosynthesis of arabinogalactan and lipoarabinomannan. *Biochem Soc Trans* **25**: 845-50.

- Besra, G.S., Morehouse, C.B., Rittner, C.M., Waechter, C.J., and Brennan, P.J. (1997) Biosynthesis of mycobacterial lipoarabinomannan. *J Biol Chem* **272**: 18460-6.
- Bhamidi, S., Scherman, M.S., Rithner, C.D., Prenni, J.E., Chatterjee, D., Khoo, K.-H., and McNeil, M.R. (2008) The identification and location of succinyl residues and the characterization of the interior arabinan region allow for a model of the complete primary structure of *Mycobacterium tuberculosis* mycolyl arabinogalactan. *J Biol Chem* **283**: 12992-3000.
- Bhatt, A., Kremer, L., Dai, A.Z., Sacchettini, J.C., and Jacobs, W.R. (2005) Conditional depletion of KasA, a key enzyme of mycolic acid biosynthesis, leads to mycobacterial cell lysis. *J Bacteriol* **187**: 7596-606.
- Bhatt, A. and Jacobs, W.R. (2009) Gene essentiality testing in *Mycobacterium smegmatis* using specialized transduction. *Methods Mol Biol* **465**: 325-36.
- Birch, H.L., Alderwick, L.J., Appelmelk, Ben J, Maaskant, J., Bhatt, A., Singh, A., et al. (2010) A truncated lipoglycan from mycobacteria with altered immunological properties. *Proc Natl Acad Sci U S A* **107**: 2634-9.
- Birch, H.L., Alderwick, L.J., Bhatt, A., Rittmann, D., Krumbach, K., Singh, A., et al. (2008) Biosynthesis of mycobacterial arabinogalactan: identification of a novel alpha(1-->3) arabinofuranosyltransferase. *Mol Microbiol* **69**: 1191-206.
- Blanchard, J.S. (1996) Molecular mechanisms of drug resistance in *Mycobacterium tuberculosis*. *Annu Rev Biochem* **65**: 215-39.
- Bligh, E.G., and Dyer, W.J. (1959) A rapid method of total lipid extraction and purification. *Can J Biochem Physiol* **37**: 911-7.
- Bloch, H. (1950) Studies on the virulence of tubercle bacilli; isolation and biological properties of a constituent of virulent organisms. *J Exp Med* **91**: 197-218, pl.
- Boonyarattanakalin, S., Liu, X., Michieletti, M., Lepenies, B., and Seeberger, P.H. (2008) Chemical synthesis of all phosphatidylinositol mannoside (PIM) glycans from *Mycobacterium tuberculosis*. *J Am Chem Soc* **130**: 16791-9.
- Brennan, P.J. (2003) Structure, function, and biogenesis of the cell wall of *Mycobacterium tuberculosis*. *Tuberculosis (Edinburgh, Scotland)* **83**: 91-7.
- Brennan, P.J., and Nikaido, H. (1995) The envelope of mycobacteria. *Annu Rev Biochem* **64**: 29-63.
- Brightbill, H.D., Libraty, D.H., Krutzik, S.R., Yang, R.B., Belisle, J T, Bleharski, J.R., et al. (1999) Host defense mechanisms triggered by microbial lipoproteins through toll-like receptors. *Science* **285**: 732-6.

- Briken, V., Porcelli, Steven A, Besra, Gurdyal S, and Kremer, L. (2004) Mycobacterial lipoarabinomannan and related lipoglycans: from biogenesis to modulation of the immune response. *Mol Microbiol* **53**: 391-403.
- Brosch, R, Gordon, S.V., Marmiesse, M, Brodin, P., Buchrieser, C., Eiglmeier, K., *et al.* (2002) A new evolutionary scenario for the *Mycobacterium tuberculosis* complex. *Proc Natl Acad Sci U S A* **99**: 3684-9.
- Camacho, L.R., Constant, P, Raynaud, C., Lanéelle, M.A., Triccas, J.A., Gicquel, B., *et al.* (2001) Analysis of the phthiocerol dimycocerosate locus of *Mycobacterium tuberculosis*. Evidence that this lipid is involved in the cell wall permeability barrier. *J Biol Chem* **276**: 19845-54.
- Camacho, L.R., Ensergueix, D., Perez, E., Gicquel, B., and Guilhot, C. (1999) Identification of a virulence gene cluster of *Mycobacterium tuberculosis* by signature-tagged transposon mutagenesis. *Mol Microbiol* **34**: 257-67.
- Chao, J., Wong, D., Zheng, X., Poirier, V., Bach, Horacio, Hmama, Z., and Av-Gay, Y. (2010) Protein kinase and phosphatase signaling in *Mycobacterium tuberculosis* physiology and pathogenesis. *Biochim Biophys Acta* **1804**: 620-7.
- Chao, J.D., Papavinasasundaram, Kadamba G, Zheng, X., Chávez-Steenbock, A., Wang, X., Lee, G.Q., and Av-Gay, Y.(2010) Convergence of Ser/Thr and two-component signaling to coordinate expression of the dormancy regulon in *Mycobacterium tuberculosis*. *J Biol Chem* **285**: 29239-46.
- Chatterjee, D., Hunter, S.W., McNeil, M., and Brennan, P.J. (1992) Lipoarabinomannan. Multiglycosylated form of the mycobacterial mannosylphosphatidylinositols. *J Biol Chem* **267**: 6228-33.
- Chatterjee, D., Khoo, K.H., McNeil, M.R., Dell, A., Morris, H.R., and Brennan, P.J. (1993) Structural definition of the non-reducing termini of mannose-capped LAM from *Mycobacterium tuberculosis* through selective enzymatic degradation and fast atom bombardment-mass spectrometry. *Glycobiology* **3**: 497-506.
- Christophe, T., Jackson, M., Jeon, H.K., Fenistein, D., Contreras-Dominguez, M., Kim, J., *et al.* (2009) High content screening identifies decaprenyl-phosphoribose 2' epimerase as a target for intracellular antimycobacterial inhibitors. *PLoS Pathog* **5**: e1000645.
- Chua, J., and Deretic, V. (2004) *Mycobacterium tuberculosis* reprograms waves of phosphatidylinositol 3-phosphate on phagosomal organelles. *J Biol Chem* **279**: 36982-92.
- Coar, T. (1982) *The aphorisms of Hippocrates with a Translation into Latin, and English*. Gryphon Editions, Birmingham, AB.

- Cole, S.T., Brosch, R., Parkhill, J., Garnier, T., Churcher, C., Harris, D., *et al.* (1998) Deciphering the biology of *Mycobacterium tuberculosis* from the complete genome sequence. *Nature* **393**: 537-44.
- Cole, S.T., Eiglmeier, K., Parkhill, J., James, K.D., Thomson, N.R., Wheeler, P.R., *et al.* (2001) Massive gene decay in the leprosy bacillus. *Nature* **409**: 1007-11.
- Converse, S.E., Mougous, J.D., Leavell, M.D., Leary, J.A., Bertozzi, C.R., and Cox, J.S. (2003) MmpL8 is required for sulfolipid-1 biosynthesis and *Mycobacterium tuberculosis* virulence. *Proc Natl Acad Sci U S A* **100**: 6121-6.
- Cox, G.L. (1923) Sanatorium treatment contrasted with home treatment. After-histories of 4,067 cases. *Br J Tuberc* **17**: 27-30.
- Cox, J S, Chen, B, McNeil, M., and Jacobs, W.R. (1999) Complex lipid determines tissue-specific replication of *Mycobacterium tuberculosis* in mice. *Nature* **402**: 79-83.
- Crellin, P.K., Brammananth, R., and Coppel, R.L. (2011) Decaprenylphosphoryl- $\beta$ -D-ribose 2'-epimerase, the target of benzothiazinones and dinitrobenzamides, is an essential enzyme in *Mycobacterium smegmatis*. *PLoS One* **6**: e16869.
- Crellin, P.K., Kovacevic, S., Martin, K.L., Brammananth, R., Morita, Y.S., Billman-Jacobe, H., *et al.* (2008) Mutations in *pimE* restore lipoarabinomannan synthesis and growth in a *Mycobacterium smegmatis* *lpqW* mutant. *J Bacteriol* **190**: 3690-9.
- Daffe, M., Brennan, P J, and McNeil, M. (1990) Predominant structural features of the cell wall arabinogalactan of *Mycobacterium tuberculosis* as revealed through characterization of oligoglycosyl alditol fragments by gas chromatography/mass spectrometry and by  $^1\text{H}$  and  $^{13}\text{C}$  NMR analyses. *J Biol Chem* **265**: 6734-43.
- Daffé, M., Lacave, C., Lanéelle, M.A., and Lanéelle, G. (1987) Structure of the major triglycosyl phenol-phthiocerol of *Mycobacterium tuberculosis* (strain Canetti). *Eur J Biochem* **167**: 155-60.
- Daffé, M., and Lanéelle, M.A. (1988) Distribution of phthiocerol diester, phenolic mycosides and related compounds in mycobacteria. *J Gen Microbiol* **134**: 2049-55.
- Daniel, T.M. (2005) Leon Charles Albert Calmette and BCG vaccine. *Int J Tuberc Lung Dis* **9**: 944-5.
- Daniel, T.M. (2004) René Théophile Hyacinthe Laënnec and the founding of pulmonary medicine. *Int J Tuberc Lung Dis* **8**: 517-8.
- Daniel, T.M. (2006) The history of tuberculosis. *Respir Med* **100**: 1862-70.
- De Libero, G., and Mori, L. (2010) How the immune system detects lipid antigens. *Prog Lipid Res* **49**: 120-7.

- Deretic, V., Singh, S., Master, S., Harris, J., Roberts, E., Kyei, G., *et al.* (2006) *Mycobacterium tuberculosis* inhibition of phagolysosome biogenesis and autophagy as a host defence mechanism. *Cellular microbiology* **8**: 719-27.
- Dinadayala, P., Kaur, D., Berg, S., Amin, A.G., Vissa, V.D., Chatterjee, D., *et al.* (2006) Genetic basis for the synthesis of the immunomodulatory mannose caps of lipoarabinomannan in *Mycobacterium tuberculosis*. *J Biol Chem* **281**: 20027-35.
- Dobson, G., Minnikin, D.E., Minnikin, S.M., Parlett, J.H., Goodfellow, M., Ridell, M., and Magnusson, M. (1985) Systematic analysis of complex mycobacterial lipids. In *Chemical Methods in Bacterial Systematics*. Goodfellow, M., and Minnikin, D.E. (eds). London: Academic Press. pp. 237-265.
- Domenech, P., and Reed, M.B. (2009) Rapid and spontaneous loss of phthiocerol dimycocerosate (PDIM) from *Mycobacterium tuberculosis* grown *in vitro*: implications for virulence studies. *Microbiology* **155**: 3532-43.
- Dover, L.G., Cerdeño-Tárraga, A.M., Pallen, M.J., Parkhill, J., and Besra, G.S. (2004) Comparative cell wall core biosynthesis in the mycolated pathogens, *Mycobacterium tuberculosis* and *Corynebacterium diphtheriae*. *FEMS Microbiol Rev* **28**: 225-50.
- Doz, E., Rose, S., Nigou, J., Gilleron, M., Puzo, G., Erard, F., *et al.* (2007) Acylation determines the toll-like receptor (TLR)-dependent positive versus TLR2-, mannose receptor-, and SIGNR1-independent negative regulation of pro-inflammatory cytokines by mycobacterial lipomannan. *J Biol Chem* **282**: 26014-25.
- Driessen, Nicole N, Ummels, Roy, Maaskant, J.J., Gurcha, S.S., Besra, G.S., Ainge, G.D., *et al.* (2009) Role of phosphatidylinositol mannosides in the interaction between mycobacteria and DC-SIGN. *Infect Immun* **77**: 4538-47.
- Durocher, D., and Jackson, S.P. (2002) The FHA domain. *FEBS Lett* **513**: 58-66.
- Dye, C. (2006) Global epidemiology of tuberculosis. *Lancet* **367**: 938-40.
- Ehlers, S. (2010) DC-SIGN and mannosylated surface structures of *Mycobacterium tuberculosis*: a deceptive liaison. *Eur J Cell Biol* **89**: 95-101.
- Ehrt, S., Guo, X.V., Hickey, C.M., Ryou, M., Monteleone, M., Riley, L.W., and Schnappinger, D. (2005) Controlling gene expression in mycobacteria with anhydrotetracycline and Tet repressor. *Nucleic Acids Res* **33**: e21.
- Ernst, W.A., Maher, J., Cho, S., Niazi, K.R., Chatterjee, D, Moody, D B, *et al.* (1998) Molecular interaction of CD1b with lipoglycan antigens. *Immunity* **8**: 331-40.
- Fine, P.E. (1995) Variation in protection by BCG: implications of and for heterologous immunity. *Lancet* **346**: 1339-45.

- Fischer, K., Scotet, E., Niemeyer, M., Koebernick, H., Zerrahn, J., Maillet, S., *et al.* (2004) Mycobacterial phosphatidylinositol mannoside is a natural antigen for CD1d-restricted T cells. *Proc Natl Acad Sci U S A* **101**: 10685-90.
- Fratti, R.A., Chua, J., and Deretic, V. (2003) Induction of p38 mitogen-activated protein kinase reduces early endosome autoantigen 1 (EEA1) recruitment to phagosomal membranes. *J Biol Chem* **278**: 46961-7.
- Fratti, R.A., Chua, J., Vergne, I., and Deretic, V. (2003) *Mycobacterium tuberculosis* glycosylated phosphatidylinositol causes phagosome maturation arrest. *Proc Natl Acad Sci U S A* **100**: 5437-42.
- Frieden, T.R., Sterling, T.R., Munsiff, S.S., Watt, C.J., and Dye, C. (2003) Tuberculosis. *Lancet* **362**: 887-99.
- Gagliardi, M.C., Lemassu, A., Teloni, R., Mariotti, S., Sargentini, V., Pardini, M., *et al.* (2007) Cell wall-associated  $\alpha$ -glucan is instrumental for *Mycobacterium tuberculosis* to block CD1 molecule expression and disable the function of dendritic cell derived from infected monocyte. *Cell Microbiol* **9**: 2081-92.
- Gagliardi, M.C., Teloni, R., Giannoni, F., Mariotti, S., Remoli, M.E., Sargentini, V., *et al.* (2009) Mycobacteria exploit p38 signaling to affect CD1 expression and lipid antigen presentation by human dendritic cells. *Infect Immun* **77**: 4947-52.
- Gande, R., Gibson, K.J.C., Brown, A.K., Krumbach, K., Dover, L.G., Sahm, H., *et al.* (2004) Acyl-CoA carboxylases (*accD2* and *accD3*), together with a unique polyketide synthase (*Cg-pks*), are key to mycolic acid biosynthesis in *Corynebacteriaceae* such as *Corynebacterium glutamicum* and *Mycobacterium tuberculosis*. *J Biol Chem* **279**: 44847-57.
- Geijtenbeek, T.B.H., Vliet, S.J. Van, Koppel, E.A., Sanchez-Hernandez, M., Vandenbroucke-Grauls, C.M.J.E., Appelmelk, B., and Kooyk, Y. Van (2003) Mycobacteria target DC-SIGN to suppress dendritic cell function. *J Exp Med* **197**: 7-17.
- George, K.M., Yuan, Y., Sherman, D.R., and Barry, C.E. (1995) The biosynthesis of cyclopropanated mycolic acids in *Mycobacterium tuberculosis*. Identification and functional analysis of CMAS-2. *J Biol Chem* **270**: 27292-8.
- Gibson, K.J.C., Eggeling, L., Maughan, W.N., Krumbach, K., Gurcha, S.S., Nigou, Jérôme, *et al.* (2003) Disruption of *Cg-Ppm1*, a polyprenyl monophosphomannose synthase, and the generation of lipoglycan-less mutants in *Corynebacterium glutamicum*. *J Biol Chem* **278**: 40842-50.
- Gilleron, M., Nigou, J., Nicolle, D., Quesniaux, V., and Puzo, G. (2006) The acylation state of mycobacterial lipomannans modulates innate immunity response through toll-like receptor 2. *Chem Biol* **13**: 39-47.

- Glickman, M.S., Cahill, S.M., and Jacobs, W.R. (2001) The *Mycobacterium tuberculosis* *cmaA2* gene encodes a mycolic acid trans-cyclopropane synthetase. *J Biol Chem* **276**: 2228-33.
- Goldman, R.C., and Laughon, B.E. (2009) Discovery and validation of new antitubercular compounds as potential drug leads and probes. *Tuberculosis (Edinburgh, Scotland)* **89**: 331-3.
- Gómez-Velasco, A., Bach, H., Rana, A.K., Cox, L.R., Bhatt, A., Besra G.S. *et al.* (2013) Disruption of the serine/threonine protein kinase H affects phthiocerol dimycocerosates synthesis in *Mycobacterium tuberculosis*. *Microbiology* **159**: 726-36.
- Goodfellow, M., and Minnikin, D.E. (1981) Identification of *Mycobacterium chelonae* by thin-layer chromatographic analysis of whole-organism methanolysates. *Tubercle* **62**: 285-7.
- Goren, M.B., Brokl, O., and Das, B.C. (1976) Sulfatides of *Mycobacterium tuberculosis*: the structure of the principal sulfatide (SL-I). *Biochemistry* **15**: 2728-35.
- Gringhuis, S.I., den Dunnen, J., Litjens, M., van der Vlist, M., and Geijtenbeek, T.B.H. (2009) Carbohydrate-specific signaling through the DC-SIGN signalosome tailors immunity to *Mycobacterium tuberculosis*, HIV-1 and *Helicobacter pylori*. *Nat Immunol* **10**: 1081-8.
- Grzegorzewicz, A.E., Pham, H., Gundi, V.A.K.B., Scherman, M.S., North, E.J., Hess, T., *et al.* (2012) Inhibition of mycolic acid transport across the *Mycobacterium tuberculosis* plasma membrane. *Nat Chem Biol* **8**: 334-41.
- Guerardel, Y., Maes, E., Ellass, E., Leroy, Y., Timmerman, P., Besra, G.S., *et al.* (2002) Structural study of lipomannan and lipoarabinomannan from *Mycobacterium chelonae*. Presence of unusual components with  $\alpha$ -1,3-mannopyranose side chains. *J Biol Chem* **277**: 30635-48.
- Guerin, M.E., Kaur, D., Somashekar, B.S., Gibbs, S., Gest, P., Chatterjee, D., *et al.* (2009) New insights into the early steps of phosphatidylinositol mannoside biosynthesis in mycobacteria: PimB' is an essential enzyme of *Mycobacterium smegmatis*. *J Biol Chem* **284**: 25687-96.
- Guerin, M.E., Kordulakova, J., Schaeffer, F., Svetlikova, Z., Buschiazzi, A., Giganti, D., *et al.* (2007) Molecular recognition and interfacial catalysis by the essential phosphatidylinositol mannosyltransferase PimA from mycobacteria. *J Biol Chem* **282**: 20705-14.
- Guerin, M.E., Korduláková, J., Alzari, P.M., Brennan, P.J., and Jackson, M. (2010) Molecular basis of phosphatidyl-myoinositol mannoside biosynthesis and regulation in mycobacteria. *J Biol Chem* **285**: 33577-83.



- Gupta, M., Sajid, A., Arora, G., Tandon, V., and Singh, Y. (2009) Forkhead-associated domain-containing protein Rv0019c and polyketide-associated protein PapA5, from substrates of serine/threonine protein kinase PknB to interacting proteins of *Mycobacterium tuberculosis*. *J Biol Chem* **284**: 34723-34.
- Gurcha, S.S., Baulard, A.R., Kremer, L., Loch, C., Moody, D Branch, Muhlecker, W., et al. (2002) Ppm1, a novel polyprenol monophosphomannose synthase from *Mycobacterium tuberculosis*. *Biochem J* **365**: 441-50.
- Gutierrez, M.C., Brisse, S., Brosch, Roland, Fabre, M., Omaïs, B., Marmiesse, M., et al. (2005) Ancient origin and gene mosaicism of the progenitor of *Mycobacterium tuberculosis*. *PLoS Pathog* **1**: e5.
- Haites, R.E., Morita, Y.S., McConville, M.J., and Billman-Jacobe, H. (2005) Function of phosphatidylinositol in mycobacteria. *J Biol Chem* **280**: 10981-7.
- Hanks, S.K., Quinn, A.M., and Hunter, T. (1988) The protein kinase family: conserved features and deduced phylogeny of the catalytic domains. *Science* **241**: 42-52.
- Harada, K., Gidoh, S., and Tsutsumi, S. (1976) Staining mycobacteria with carbolfuchsin: properties of solutions prepared with different samples of basic fuchsin. *Microsc Acta* **78**: 21-7.
- Hayman, J. (1984) *Mycobacterium ulcerans*: an infection from Jurassic time? *Lancet* **2**: 1015-6.
- Heaton, T.G. (1936) Complications of Artificial Pneumothorax: A Review. *Can Med Assoc J* **35**: 399-405.
- HersHKovitz, I., Donoghue, H.D., Minnikin, D.E., Besra, G.S., Lee, O.Y.-C., Gernaey, A.M., et al. (2008) Detection and molecular characterization of 9,000-year-old *Mycobacterium tuberculosis* from a Neolithic settlement in the Eastern Mediterranean. *PLoS One* **3**: e3426.
- Houben, E.N.G., Nguyen, L., and Pieters, J. (2006) Interaction of pathogenic mycobacteria with the host immune system. *Curr Opin Microbiol* **9**: 76-85.
- Hunter, R.L., Venkataprasad, N., and Olsen, M.R. (2006) The role of trehalose dimycolate (cord factor) on morphology of virulent *Mycobacterium tuberculosis* *in vitro*. *Tuberculosis (Edinburgh, Scotland)* **86**: 349-56.
- Hunter, S.W., and Brennan, P.J. (1990) Evidence for the presence of a phosphatidylinositol anchor on the lipoarabinomannan and lipomannan of *Mycobacterium tuberculosis*. *J Biol Chem* **265**: 9272-9.
- Jain, M., and Cox, J.S. (2005) Interaction between polyketide synthase and transporter suggests coupled synthesis and export of virulence lipid in *Mycobacterium tuberculosis*. *PLoS Pathog* **1**: e2.

- Jain, M., Petzold, C.J., Schelle, M.W., Leavell, M.D., Mougous, J.D., Bertozzi, C.R., *et al.* (2007) Lipidomics reveals control of *Mycobacterium tuberculosis* virulence lipids via metabolic coupling. *Proc Natl Acad Sci U S A* **104**: 5133-8.
- Jankute, M., Grover, S., Rana, A.K., and Besra, G.S. (2012) Arabinogalactan and lipoarabinomannan biosynthesis: structure, biogenesis and their potential as drug targets. *Future Microbiol* **7**: 129-47.
- Jassal, M., and Bishai, W.R. (2009) Extensively drug-resistant tuberculosis. *Lancet Infect Dis* **9**: 19-30.
- Jo, E.-K. (2008) Mycobacterial interaction with innate receptors: TLRs, C-type lectins, and NLRs. *Curr Opin Infect Dis* **21**: 279-86.
- Kang, P.B., Azad, A.K., Torrelles, J.B., Kaufman, T.M., Beharka, A., Tibesar, E., *et al.* (2005) The human macrophage mannose receptor directs *Mycobacterium tuberculosis* lipoarabinomannan-mediated phagosome biogenesis. *J Exp Med* **202**: 987-99.
- Kapur, V., Whittam, T.S., and Musser, J.M. (1994) Is *Mycobacterium tuberculosis* 15,000 years old? *J Infect Dis* **170**: 1348-9.
- Kaur, D., McNeil, Michael R, Khoo, K.-H., Chatterjee, Delphi, Crick, D.C., Jackson, M., and Brennan, P.J. (2007) New insights into the biosynthesis of mycobacterial lipomannan arising from deletion of a conserved gene. *J Biol Chem* **282**: 27133-40.
- Kelley, V.A., and Schorey, J.S. (2003) *Mycobacterium's* arrest of phagosome maturation in macrophages requires Rab5 activity and accessibility to iron. *Mol Biol Cell* **14**: 3366-77.
- Khoo, K.H., Dell, A., Morris, H.R., Brennan, P.J., and Chatterjee, D. (1995) Inositol phosphate capping of the nonreducing termini of lipoarabinomannan from rapidly growing strains of *Mycobacterium*. *J Biol Chem* **270**: 12380-9.
- Kirksey, M.A., Tischler, A.D., Siméone, R., Hisert, K.B., Uplekar, S., Guilhot, C., and McKinney, J.D. (2011) Spontaneous phthiocerol dimycocerosate-deficient variants of *Mycobacterium tuberculosis* are susceptible to gamma interferon-mediated immunity. *Infect Immun* **79**: 2829-38.
- Koch, R. (1932) Die aetiologie der tuberculose, a translation by Berna Pinner and Max Pinner with an introduction by Allen K. Krause. *Am Rev Tuberc* **25**: 285-323.
- Koppel, E.A., Ludwig, I.S., Hernandez, M.S., Lowary, T.L., Gadikota, R.R., Tuzikov, A.B., *et al.* (2004) Identification of the mycobacterial carbohydrate structure that binds the C-type lectins DC-SIGN, L-SIGN and SIGNR1. *Immunobiology* **209**: 117-27.

Korduláková, J., Gilleron, M., Mikusova, K., Puzo, G., Brennan, P.J., Gicquel, B., and Jackson, M. (2002) Definition of the first mannosylation step in phosphatidylinositol mannoside synthesis. PimA is essential for growth of mycobacteria. *J Biol Chem* **277**: 31335-44.

Korduláková, J., Gilleron, M., Puzo, G., Brennan, P.J., Gicquel, B., Mikusová, K., and Jackson, M. (2003) Identification of the required acyltransferase step in the biosynthesis of the phosphatidylinositol mannosides of *mycobacterium* species. *J Biol Chem* **278**: 36285-95.

Koul, A., Dendouga, N., Vergauwen, K., Molenberghs, B., Vranckx, L., Willebrords, R., *et al.* (2007) Diarylquinolines target subunit c of mycobacterial ATP synthase. *Nat Chem Biol* **3**: 323-4.

Kovacevic, S., Anderson, D., Morita, Y.S., Patterson, J., Haites, R., McMillan, B.N.I., *et al.* (2006) Identification of a novel protein with a role in lipoarabinomannan biosynthesis in mycobacteria. *J Biol Chem* **281**: 9011-7.

Kremer, L., Gurcha, S.S., Bifani, P., Hitchen, P.G., Baulard, A., Morris, Howard R, *et al.* (2002) Characterization of a putative alpha-mannosyltransferase involved in phosphatidylinositol trimannoside biosynthesis in *Mycobacterium tuberculosis*. *Biochem J* **363**: 437-47.

Kurosawa, H. (1952) The isolation of an antibiotic produced by a strain of streptomyces K-300. *Yokohama Med Bull* **3**: 386-99.

La Rosa, V., Poce, G., Canseco, J.O., Buroni, S., Pasca, M.R., Biava, M., *et al.* (2012) MmpL3 is the cellular target of the antitubercular pyrrole derivative BM212. *Antimicrob Agents Chemother* **56**: 324-31.

Lederer, E., Adam, A., Ciorbaru, R., Petit, J.-F., and Wietzerbin, J. (1975) Cell walls of mycobacteria and related organisms; Chemistry and immunostimulant properties. *Mol Cell Biochem* **7**: 87-104.

Lee, A., Wu, S.-W., Scherman, M.S., Torrelles, J.B., Chatterjee, D., McNeil, M.R., and Khoo, K.-H. (2006) Sequencing of oligoarabinosyl units released from mycobacterial arabinogalactan by endogenous arabinanase: identification of distinctive and novel structural motifs. *Biochemistry* **45**: 15817-28.

Lee, R.E., Protopopova, M., Crooks, E., Slayden, R.A., Terrot, M., and Barry, C.E. (2003) Combinatorial lead optimization of [1,2]-diamines based on ethambutol as potential antituberculosis preclinical candidates. *J Comb Chem* **5**: 172-87.

Lee, Y.C., and Ballou, C.E. (1964) Structural studies on the *myo*-inositol mannosides from the glycolipids of *Mycobacterium tuberculosis* and *Mycobacterium phlei*. *J Biol Chem* **239**: 1316-27.

- Lehmann, J. (1946) Para-aminosalicylic acid in the treatment of tuberculosis. *Lancet* **1**: 15.
- Liebermann, D., Moyeux, M., Rist, N., and Grumbach, F. (1956) Sur la preparation de nouveaux thioamides pyridiniques acitifs dans la tuberculose experimentale. *C R Acad Sci* **242**: 2409-12.
- Lienhardt, C., Glaziou, P., Uplekar, M., Lönnroth, K., Getahun, H., and Raviglione, M. (2012) Global tuberculosis control: lessons learnt and future prospects. *Nat Rev Microbiol* **10**: 407-16.
- Lima, V.M., Bonato, V.L., Lima, K.M., Dos Santos, S.A., Dos Santos, R.R., Gonçalves, E.D., *et al.* (2001) Role of trehalose dimycolate in recruitment of cells and modulation of production of cytokines and NO in tuberculosis. *Infect Immun* **69**: 5305-12.
- Liu, J., and Mushegian, A. (2003) Three monophyletic superfamilies account for the majority of the known glycosyltransferases. *Protein Sci* **12**: 1418-31.
- Ludwiczak, P., Brando, T., Monsarrat, B., and Puzo, G. (2001) Structural characterization of *Mycobacterium tuberculosis* lipoarabinomannans by the combination of capillary electrophoresis and matrix-assisted laser desorption/ionization time-of-flight mass spectrometry. *Anal Chem* **73**: 2323-30.
- Maartens, G., and Wilkinson, R.J. (2007) Tuberculosis. *Lancet* **370**: 2030-43.
- Maddy, J.A., Ananthan, S., Goldman, R.C., Hobrath, J.V., Kwong, C.D., Maddox, C., *et al.* (2009) Antituberculosis activity of the molecular libraries screening center network library. *Tuberculosis (Edinburgh, Scotland)* **89**: 354-63.
- Maeda, N., Nigou, J., Herrmann, J.-L., Jackson, M., Amara, A., Lagrange, P.H., *et al.* (2003) The cell surface receptor DC-SIGN discriminates between *Mycobacterium* species through selective recognition of the mannose caps on lipoarabinomannan. *J Biol Chem* **278**: 5513-6.
- Maggi, N., Pasqualucci, C.R., Ballotta, R., and Sensi, P. (1966) Rifampicin: a new orally active rifamycin. *Chemotherapy* **11**: 285-92.
- Mahapatra, S., Scherman, H., Brennan, P.J., and Crick, D.C. (2005) N Glycolylation of the nucleotide precursors of peptidoglycan biosynthesis of *Mycobacterium* spp. is altered by drug treatment. *J Bacteriol* **187**: 2341-7.
- Makarov, V., Manina, G., Mikusova, K., Möllmann, U., Ryabova, O., Saint-Joanis, B., *et al.* (2009) Benzothiazinones kill *Mycobacterium tuberculosis* by blocking arabinan synthesis. *Science* **324**: 801-4.

- Makarov, V., Riabova, O.B., Yuschenko, A., Urlyapova, N., Daudova, A., Zipfel, P.F., and Möllmann, U. (2006) Synthesis and antileprosy activity of some dialkyldithiocarbamates. *J Antimicrob Chemother* **57**: 1134-8.
- Malik, Z.A., Iyer, S.S., and Kusner, D.J. (2001) *Mycobacterium tuberculosis* phagosomes exhibit altered calmodulin-dependent signal transduction: contribution to inhibition of phagosome-lysosome fusion and intracellular survival in human macrophages. *J Immunol* **166**: 3392-401.
- Malone, L., Schurr, A., Lindh, H., McKenzie, D., Kiser, J.S., and Williams, J.H. (1952) The effect of pyrazinamide (aldinamide) on experimental tuberculosis in mice. *Am Rev Tuberc* **65**: 511-8.
- Matteelli, A., Carvalho, A.C., Dooley, K.E., and Kritski, A. (2010) TMC207: the first compound of a new class of potent anti-tuberculosis drugs. *Future Microbiol* **5**: 849-58.
- McNeil, M., Daffe, M., and Brennan, P J (1991) Location of the mycolyl ester substituents in the cell walls of mycobacteria. *J Biol Chem* **266**: 13217-23.
- McNeil, M., Wallner, S.J., Hunter, S.W., and Brennan, P.J. (1987) Demonstration that the galactosyl and arabinosyl residues in the cell-wall arabinogalactan of *Mycobacterium leprae* and *Mycobacterium tuberculosis* are furanoid. *Carbohydr Res* **166**: 299-308.
- Meniche, X., Sousa-d'Auria, C. de, Van-der-Rest, B., Bhamidi, S., Huc, E., Huang, H., *et al.* (2008) Partial redundancy in the synthesis of the D-arabinose incorporated in the cell wall arabinan of *Corynebacterineae*. *Microbiology* **154**: 2315-26.
- Mikusová, K., Slayden, R.A., Besra, G.S., and Brennan, P.J. (1995) Biogenesis of the mycobacterial cell wall and the site of action of ethambutol. *Antimicrob Agents Chemother* **39**: 2484-9.
- Mikusová, K., Huang, H., Yagi, T., Holsters, M., Vereecke, D., D'Haeze, W., *et al.* (2005) Decaprenylphosphoryl arabinofuranose, the donor of the D-arabinofuranosyl residues of mycobacterial arabinan, is formed via a two-step epimerization of decaprenylphosphoryl ribose. *J Bacteriol* **187**: 8020-5.
- Minnikin, D.E., and Goodfellow, M. (1980) Lipid composition in the classification and identification of acid-fast bacteria. *Soc Appl Bacteriol Symp Ser* **8**: 189-256.
- Minnikin, D.E., Kremer, L., Dover, L.G., and Besra, G.S. (2002) The methyl-branched fortifications of *Mycobacterium tuberculosis*. *Chem Biol* **9**: 545-53.
- Minnikin, D.E., Minnikin, S.M., Goodfellow, M., Stanford, J.L. (1982) The mycolic acids of *Mycobacterium chelonae*. *J Gen Microbiol* **128**: 817-22.

- Mishra, A.K., Alderwick, L.J., Rittmann, D., Tatituri, R.V.V., Nigou, J., Gilleron, M., *et al.* (2007) Identification of an  $\alpha(1\rightarrow6)$  mannopyranosyltransferase (MptA), involved in *Corynebacterium glutamicum* lipomannan biosynthesis, and identification of its orthologue in *Mycobacterium tuberculosis*. *Mol Microbiol* **65**: 1503-17.
- Mishra, A.K., Alderwick, L.J., Rittmann, D., Wang, C., Bhatt, A., Jacobs, W.R., *et al.* (2008) Identification of a novel  $\alpha(1\rightarrow6)$  mannopyranosyltransferase MptB from *Corynebacterium glutamicum* by deletion of a conserved gene, *NCgl1505*, affords a lipomannan- and lipoarabinomannan-deficient mutant. *Mol Microbiol* **68**: 1595-613.
- Mishra, A.K., Driessen, N.N., Appelmelk, B.J., and Besra, G.S. (2011) Lipoarabinomannan and related glycoconjugates: structure, biogenesis and role in *Mycobacterium tuberculosis* physiology and host-pathogen interaction. *FEMS Microbiol Rev* **35**: 1126-57.
- Mishra, A.K., Klein, C., Gurcha, S.S., Alderwick, L.J., Babu, P., Hitchen, P.G., *et al.* (2008) Structural characterization and functional properties of a novel lipomannan variant isolated from a *Corynebacterium glutamicum* *pimB'* mutant. *Antonie Van Leeuwenhoek* **94**: 277-87.
- Mishra, A.K., Krumbach, K., Rittmann, D., Appelmelk, B., Pathak, V., Pathak, A.K., *et al.* (2011) Lipoarabinomannan biosynthesis in Corynebacterineae: the interplay of two  $\alpha(1\rightarrow2)$ -mannopyranosyltransferases MptC and MptD in mannan branching. *Mol Microbiol* **80**: 1241-59.
- Molle, V., Kremer, L., Girard-Blanc, C., Besra, G.S., Cozzone, A.J., and Prost, J.-F. (2003) An FHA phosphoprotein recognition domain mediates protein EmbR phosphorylation by PknH, a Ser/Thr protein kinase from *Mycobacterium tuberculosis*. *Biochemistry* **42**: 15300-9.
- Morita, Y.S., Sena, C.B.C., Waller, R.F., Kurokawa, K., Sernee, M.F., Nakatani, F., *et al.* (2006) PimE is a polyprenol-phosphate-mannose-dependent mannosyltransferase that transfers the fifth mannose of phosphatidylinositol mannoside in mycobacteria. *J Biol Chem* **281**: 25143-55.
- Mukherjee, J.S., Rich, M.L., Socci, A.R., Joseph, J.K., Virú, F.A., Shin, S.S., *et al.* (2004) Programmes and principles in treatment of multidrug-resistant tuberculosis. *Lancet* **363**: 474-81.
- Nguyen, L., and Pieters, J. (2005) The Trojan horse: survival tactics of pathogenic mycobacteria in macrophages. *Trends Cell Biol* **15**: 269-76.
- Nigou, J., Zelle-Rieser, C., Gilleron, M., Thurnher, M., and Puzo, G. (2001) Mannosylated lipoarabinomannans inhibit IL-12 production by human dendritic cells: evidence for a negative signal delivered through the mannose receptor. *J Immunol* **166**: 7477-85.

- Nigou, J., Vasselon, T., Ray, A., Constant, P., Gilleron, M., Besra, G.S., *et al.* (2008) Mannan chain length controls lipoglycans signaling via and binding to TLR2. *J Immunol* **180**: 6696-702.
- Nikaido, H., Kim, S.H., and Rosenberg, E.Y. (1993) Physical organization of lipids in the cell wall of *Mycobacterium chelonae*. *Mol Microbiol* **8**: 1025-30.
- Noll, H., Bloch, H., Asselineau, J., and Lederer, E (1956) The chemical structure of the cord factor of *Mycobacterium tuberculosis*. *Biochim Biophys Acta* **20**: 299-309.
- Nunn, P., Williams, B., Floyd, K., Dye, C., Elzinga, G., and Raviglione, M. (2005) Tuberculosis control in the era of HIV. *Nat Rev Immunol* **5**: 819-26.
- Okamoto, Y., Fujita, Y., Naka, T., Hirai, M., Tomiyasu, I., and Yano, I. (2006) Mycobacterial sulfolipid shows a virulence by inhibiting cord factor induced granuloma formation and TNF- $\alpha$  release. *Microb Pathog* **40**: 245-53.
- Onwueme, K.C., Ferreras, J.A., Buglino, J., Lima, C.D., and Quadri, L.E.N. (2004) Mycobacterial polyketide-associated proteins are acyltransferases: proof of principle with *Mycobacterium tuberculosis* PapA5. *Proc Natl Acad Sci U S A* **101**: 4608-13.
- Papavinasundaram, K G, Chan, B., Chung, J.-H., Colston, M.J., Davis, E.O., and Av-Gay, Y. (2005) Deletion of the *Mycobacterium tuberculosis* *pknH* gene confers a higher bacillary load during the chronic phase of infection in BALB/c mice. *J Bacteriol* **187**: 5751-60.
- Pasca, M.R., Degiacomi, G., de Ribeiro, A.L., Zara, F., De Mori, P., Heym, B., *et al.* (2010) Clinical isolates of *Mycobacterium tuberculosis* in four European hospitals are uniformly susceptible to benzothiazinones. *Antimicrob Agents Chemother* **54**: 1616-8.
- Pease, A.S. (1940) Some Remarks on the Diagnosis and Treatment of Tuberculosis in Antiquity. *Isis* **31**: 380-393.
- Pethe, K., Sequeira, P.C., Agarwalla, S., Rhee, K., Kuhen, K., Phong, W.Y., *et al.* (2010) A chemical genetic screen in *Mycobacterium tuberculosis* identifies carbon-source-dependent growth inhibitors devoid of *in vivo* efficacy. *Nat Commun* **1**: 57.
- Philips, J.A., and Ernst, J.D. (2012) Tuberculosis pathogenesis and immunity. *Annu Rev Pathol* **7**: 353-84.
- Porcelli, S A, Segelke, B.W., Sugita, M., Wilson, I A, and Brenner, M B (1998) The CD1 family of lipid antigen-presenting molecules. *Immunol Today* **19**: 362-8.
- Porcelli, S. A., and Besra, G. S. (2002) Immune recognition of the mycobacterial cell wall. In *Intracellular Pathogens in Membrane Interactions and Vacuole Biogenesis*. J.P., G. (ed.). ASM Press, Washington, D.C. pp. 230-249.

- Portevin, D., De Sousa-D'Auria, C., Houssin, C., Grimaldi, C., Chami, M., Daffé, Mamadou, and Guilhot, C. (2004) A polyketide synthase catalyzes the last condensation step of mycolic acid biosynthesis in mycobacteria and related organisms. *Proc Natl Acad Sci U S A* **101**: 314-9.
- Prigozy, T.I., Sieling, P.A., Clemens, D., Stewart, P.L., Behar, S.M., Porcelli, S.A., *et al.* (1997) The mannose receptor delivers lipoglycan antigens to endosomes for presentation to T cells by CD1b molecules. *Immunity* **6**: 187-97.
- Protopopova, M., Hanrahan, C., Nikonenko, B., Samala, R., Chen, P., Gearhart, J., *et al.* (2005) Identification of a new antitubercular drug candidate, SQ109, from a combinatorial library of 1,2-ethylenediamines. *J Antimicrob Chemother* **56**: 968-74.
- Pérez, J., Garcia, R., Bach, Horacio, de Waard, J.H., Jacobs, W.R., Av-Gay, Y., *et al.* (2006) *Mycobacterium tuberculosis* transporter MmpL7 is a potential substrate for kinase PknD. *Biochem Biophys Res Commun* **348**: 6-12.
- Quesniaux, V., Fremond, C., Jacobs, M., Parida, S., Nicolle, D., Yermeev, V., *et al.* (2004) Toll-like receptor pathways in the immune responses to mycobacteria. *Microbes Infect* **6**: 946-59.
- Quesniaux, V.J., Nicolle, D.M., Torres, D., Kremer, L., Guérardel, Y., Nigou, J., *et al.* (2004) Toll-like receptor 2 (TLR2)-dependent-positive and TLR2-independent-negative regulation of proinflammatory cytokines by mycobacterial lipomannans. *J Immunol* **172**: 4425-34.
- Rao, A., and Ranganathan, A. (2004) Interaction studies on proteins encoded by the phthiocerol dimycocerosate locus of *Mycobacterium tuberculosis*. *Mol Genet Genomics* **272**: 571-9.
- Rao, V., Fujiwara, N., Porcelli, S.A., and Glickman, M.S. (2005) *Mycobacterium tuberculosis* controls host innate immune activation through cyclopropane modification of a glycolipid effector molecule. *J Exp Med* **201**: 535-43.
- Rao, V., Gao, F., Chen, B., Jacobs, W.R., and Glickman, M.S. (2006) *Trans*-cyclopropanation of mycolic acids on trehalose dimycolate suppresses *Mycobacterium tuberculosis*-induced inflammation and virulence. *J Clin Invest* **116**: 1660-7.
- Raviglione, M.C., and Uplekar, M.W. (2006) WHO's new Stop TB Strategy. *Lancet* **367**: 952-5.
- Reed, M.B., Domenech, P., Manca, C., Su, H., Barczak, A.K., Kreiswirth, B.N., *et al.* (2004) A glycolipid of hypervirulent tuberculosis strains that inhibits the innate immune response. *Nature* **431**: 84-7.
- Remuiñán, M.J., Pérez-Herrán, E., Rullás, J., Alemparte, C., Martínez-Hoyos, M., Dow, D.J., *et al.* (2013) Tetrahydropyrazolo[1,5-*a*]pyrimidine-3-carboxamide and *N*-



- benzyl-6',7'-dihydrospiro[piperidine-4,4'-thieno[3,2-c]pyran] analogues with bactericidal efficacy against *Mycobacterium tuberculosis* targeting MmpL3. *PLoS One* **8**: e60933.
- Riedel, S. (2005) Edward Jenner and the history of smallpox and vaccination. *Proc (Bayl Univ Med Cent)* **18**: 21-5.
- Rousseau, C., Turner, O.C., Rush, E., Bordat, Y., Sirakova, T.D., Kolattukudy, P.E., et al. (2003) Sulfolipid deficiency does not affect the virulence of *Mycobacterium tuberculosis* H37Rv in mice and guinea pigs. *Infect Immun* **71**: 4684-90.
- Rousseau, C., Winter, N., Pivert, E., Bordat, Y., Neyrolles, O., Avé, P., et al. (2004) Production of phthiocerol dimycocerosates protects *Mycobacterium tuberculosis* from the cidal activity of reactive nitrogen intermediates produced by macrophages and modulates the early immune response to infection. *Cell Microbiol* **6**: 277-87.
- Rozwarski, D.A., Grant, G.A., Barton, D.H., Jacobs, W.R., and Sacchettini, J.C. (1998) Modification of the NADH of the isoniazid target (InhA) from *Mycobacterium tuberculosis*. *Science* **279**: 98-102.
- Russell, D.G. (2001) *Mycobacterium tuberculosis*: here today, and here tomorrow. *Nat Rev Mol Cell Biol* **2**: 569-77.
- Russell, D.G. (2007) Who puts the tubercle in tuberculosis? *Nat Rev Microbiol* **5**: 39-47.
- Sacksteder, K.A., Protopopova, M., Barry, C.E., Andries, K., and Nacy, C.A. (2012) Discovery and development of SQ109: a new antitubercular drug with a novel mechanism of action. *Future Microbiol* **7**: 823-37.
- Sakula, A. (1983) BCG: who were Calmette and Guerin? *Thorax* **38**: 806-812.
- Schaeffer, M.L., Khoo, K.H., Besra, G.S., Chatterjee, D., Brennan, P.J., Belisle, J.T., and Inamine, J.M. (1999) The *pimB* gene of *Mycobacterium tuberculosis* encodes a mannosyltransferase involved in lipoarabinomannan biosynthesis. *J Biol Chem* **274**: 31625-31.
- Schatz, A., Bugie, E., and Waksman, S.A. (2005) Streptomycin, a substance exhibiting antibiotic activity against gram-positive and gram-negative bacteria. 1944. *Clin Orthop Relat Res* 3-6.
- Scherman, H., Kaur, D., Pham, H., Skovierová, H., Jackson, M., and Brennan, P.J. (2009) Identification of a polyprenylphosphomannosyl synthase involved in the synthesis of mycobacterial mannosides. *J Bacteriol* **191**: 6769-72.
- Schleifer, K.H., and Kandler, O. (1972) Peptidoglycan types of bacterial cell walls and their taxonomic implications. *Bacteriol Rev* **36**: 407-77.

Schlesinger, L.S. (1993) Macrophage phagocytosis of virulent but not attenuated strains of *Mycobacterium tuberculosis* is mediated by mannose receptors in addition to complement receptors. *J Immunol* **150**: 2920-30.

Schlesinger, L.S., Hull, S.R., and Kaufman, T.M. (1994) Binding of the terminal mannosyl units of lipoarabinomannan from a virulent strain of *Mycobacterium tuberculosis* to human macrophages. *J Immunol* **152**: 4070-9.

Schluger, N.W., and Rom, W.N. (1998) The host immune response to tuberculosis. *Am J Respir Crit Care Med* **157**: 679-91.

Seidel, M., Alderwick, L.J., Birch, H.L., Sahm, H., Eggeling, L., and Besra, G.S. (2007) Identification of a novel arabinofuranosyltransferase AftB involved in a terminal step of cell wall arabinan biosynthesis in *Corynebacteriaceae*, such as *Corynebacterium glutamicum* and *Mycobacterium tuberculosis*. *J Biol Chem* **282**: 14729-40.

Sendide, K., Deghmane, A.-E., Reyrat, J.-M., Talal, A., and Hmama, Z. (2004) *Mycobacterium bovis* BCG urease attenuates major histocompatibility complex class II trafficking to the macrophage cell surface. *Infect Immun* **72**: 4200-9.

Sharma, K., Gupta, M., Pathak, M., Gupta, N., Koul, A., Sarangi, S., *et al.* (2006) Transcriptional control of the mycobacterial *embCAB* operon by PknH through a regulatory protein, EmbR, in vivo. *J Bacteriol* **188**: 2936-44.

Sieling, P.A., Chatterjee, D, Porcelli, S A, Prigozy, T.I., Mazzaccaro, R.J., Soriano, T., *et al.* (1995) CD1-restricted T cell recognition of microbial lipoglycan antigens. *Science* **269**: 227-30.

Silva, C.L., Ekizlerian, S.M., and Fazioli, R.A. (1985) Role of cord factor in the modulation of infection caused by mycobacteria. *Am J Pathol* **118**: 238-47.

Silva, P.E.A. Da, Groll, A. Von, Martin, A., and Palomino, J.C. (2011) Efflux as a mechanism for drug resistance in *Mycobacterium tuberculosis*. *FEMS Immunol Med Microbiol* **63**: 1-9.

Simonsen, A., Gaullier, J.M., D'Arrigo, A., and Stenmark, H. (1999) The Rab5 effector EEA1 interacts directly with syntaxin-6. *J Biol Chem* **274**: 28857-60.

Singer, J.J. (1936) Collapse Therapy in Pulmonary Tuberculosis. *Cal West Med* **45**: 120-5.

Skovierová, H., Larrouy-Maumus, G., Pham, H., Belanová, M., Barilone, N., Dasgupta, A., *et al.* (2010) Biosynthetic origin of the galactosamine substituent of Arabinogalactan in *Mycobacterium tuberculosis*. *J Biol Chem* **285**: 41348-55.

- Skovierová, H., Larrouy-Maumus, G., Zhang, J., Kaur, D., Barilone, N., Korduláková, J., *et al.* (2009) AftD, a novel essential arabinofuranosyltransferase from mycobacteria. *Glycobiology* **19**: 1235-47.
- Snapper, S.B., Melton, R.E., Mustafa, S., Kieser, T., and Jacobs, W.R. (1990) Isolation and characterization of efficient plasmid transformation mutants of *Mycobacterium smegmatis*. *Mol Microbiol* **4**: 1911-9.
- Stanley, S.A., Grant, S.S., Kawate, T., Iwase, N., Shimizu, M., Wivagg, C., *et al.* (2012) Identification of novel inhibitors of *Mycobacterium tuberculosis* growth using whole cell based high-throughput screening. *ACS Chem Biol* **7**: 1377-84.
- Stock, J.B., Ninfa, A.J., and Stock, A.M. (1989) Protein phosphorylation and regulation of adaptive responses in bacteria. *Microbiol Rev* **53**: 450-90.
- Stover, C.K., Cruz, V.F. de la, Fuerst, T.R., Burlein, J.E., Benson, L.A., Bennett, L.T., *et al.* (1991) New use of BCG for recombinant vaccines. *Nature* **351**: 456-60.
- Supply, P., Marceau, M., Mangenot, S., Roche, D., Rouanet, C., Khanna, V., *et al.* (2013) Genome analysis of smooth tubercle bacilli provides insights into ancestry and pathoadaptation of *Mycobacterium tuberculosis*. *Nat Genet* **45**: 172-9.
- Tahlan, K., Wilson, R., Kastrinsky, D.B., Arora, K., Nair, V., Fischer, E., *et al.* (2012) SQ109 targets MmpL3, a membrane transporter of trehalose monomycolate involved in mycolic acid donation to the cell wall core of *Mycobacterium tuberculosis*. *Antimicrob Agents Chemother* **56**: 1797-809.
- Tailleux, L., Schwartz, O., Herrmann, J.-L., Pivert, E., Jackson, M., Amara, A., *et al.* (2003) DC-SIGN is the major *Mycobacterium tuberculosis* receptor on human dendritic cells. *J Exp Med* **197**: 121-7.
- Takayama, K., and Goldman, D.S. (1970) Enzymatic synthesis of mannosyl-1-phosphoryl-decaprenol by a cell-free system of *Mycobacterium tuberculosis*. *J Biol Chem* **245**: 6251-7.
- Tatituri, R.V.V., Illarionov, P.A., Dover, L.G., Nigou, J., Gilleron, M., Hitchen, P., *et al.* (2007) Inactivation of *Corynebacterium glutamicum* NCgl0452 and the role of MgtA in the biosynthesis of a novel mannosylated glycolipid involved in lipomannan biosynthesis. *J Biol Chem* **282**: 4561-72.
- Telenti, A., Philipp, W.J., Sreevatsan, S., Bernasconi, C., Stockbauer, K.E., Wieles, B., *et al.* (1997) The emb operon, a gene cluster of *Mycobacterium tuberculosis* involved in resistance to ethambutol. *Nat Med* **3**: 567-70.
- Thomas, J.P., Baughn, C.O., Wilkinson, R.G., and Shepherd, R.G. (1961) A new synthetic compound with antituberculous activity in mice: ethambutol (dextro-2,2'-(ethylenediimino)-di-*l*-butanol). *Am Rev Respir Dis* **83**: 891-3.

- Titgemeyer, F., Amon, J., Parche, S., Mahfoud, M., Bail, J., Schlicht, M., *et al.* (2007) A genomic view of sugar transport in *Mycobacterium smegmatis* and *Mycobacterium tuberculosis*. *J Bacteriol* **189**: 5903-15.
- Torrelles, J.B., Azad, A.K., and Schlesinger, L.S. (2006) Fine discrimination in the recognition of individual species of phosphatidyl-myo-inositol mannosides from *Mycobacterium tuberculosis* by C-type lectin pattern recognition receptors. *J Immunol* **177**: 1805-16.
- Torrelles, J.B., DesJardin, L.E., MacNeil, J., Kaufman, T.M., Kutzbach, B., Knaup, R., *et al.* (2009) Inactivation of *Mycobacterium tuberculosis* mannosyltransferase pimB reduces the cell wall lipoarabinomannan and lipomannan content and increases the rate of bacterial-induced human macrophage cell death. *Glycobiology* **19**: 743-55.
- Torrelles, J.B., and Schlesinger, L.S. (2010) Diversity in *Mycobacterium tuberculosis* mannosylated cell wall determinants impacts adaptation to the host. *Tuberculosis (Edinburgh, Scotland)* **90**: 84-93.
- Trivedi, O.A., Arora, P., Sridharan, V., Tickoo, R., Mohanty, D., and Gokhale, R.S. (2004) Enzymic activation and transfer of fatty acids as acyl-adenylates in mycobacteria. *Nature* **428**: 441-5.
- Trivedi, O.A., Arora, P., Vats, A., Ansari, M.Z., Tickoo, R., Sridharan, V., *et al.* (2005) Dissecting the mechanism and assembly of a complex virulence mycobacterial lipid. *Mol Cell* **17**: 631-43.
- van Heijenoort, J. (2001) Formation of the glycan chains in the synthesis of bacterial peptidoglycan. *Glycobiology* **11**: 25R-36R.
- Varela, C., Rittmann, D., Singh, A., Krumbach, K., Bhatt, K., Eggeling, L., *et al.* (2012) *MmpL* genes are associated with mycolic acid metabolism in mycobacteria and corynebacteria. *Chem* **19**: 498-506.
- Vergne, I., Chua, J., and Deretic, V. (2003) Tuberculosis toxin blocking phagosome maturation inhibits a novel  $Ca^{2+}$ /calmodulin-PI3K hVPS34 cascade. *J Exp Med* **198**: 653-9.
- Vergne, I., Chua, J., Singh, S.B., and Deretic, V. (2004) Cell biology of *Mycobacterium tuberculosis* phagosome. *Annu Rev Cell Dev Biol* **20**: 367-94.
- Vergne, I., Fratti, R.A., Hill, P.J., Chua, J., Belisle, J., and Deretic, V. (2004) *Mycobacterium tuberculosis* phagosome maturation arrest: mycobacterial phosphatidylinositol analog phosphatidylinositol mannoside stimulates early endosomal fusion. *Mol Biol Cell* **15**: 751-60.
- Vignal, C., Guérardel, Y., Kremer, L., Masson, M., Legrand, D., Mazurier, J., and Elass, E. (2003) Lipomannans, but not lipoarabinomannans, purified from *Mycobacterium chelonae* and *Mycobacterium kansasii* induce TNF- $\alpha$  and IL-8

secretion by a CD14-toll-like receptor 2-dependent mechanism. *J Immunol* **171**: 2014-23.

Villeneuve, C., Gilleron, M., Maridonneau-Parini, I., Daffé, M., Astarie-Dequeker, C., and Etienne, G. (2005) Mycobacteria use their surface-exposed glycolipids to infect human macrophages through a receptor-dependent process. *J Lipid Res* **46**: 475-83.

Vollmer, W., and Höltje, J.-V. (2004) The architecture of the murein (peptidoglycan) in gram-negative bacteria: vertical scaffold or horizontal layer(s)? *J Bacteriol* **186**: 5978-87.

Watanabe, M., Aoyagi, Y., Mitome, H., Fujita, T., Naoki, H., Ridell, M., and Minnikin, D.E. (2002) Location of functional groups in mycobacterial meromycolate chains; the recognition of new structural principles in mycolic acids. *Microbiology* **148**: 1881-902.

WHO (2012) WHO report 2012: Global tuberculosis report. *World Health Organization*, Geneva  
[http://www.who.int/tb/publications/global\\_report/gtbr12\\_main.pdf](http://www.who.int/tb/publications/global_report/gtbr12_main.pdf).

Welin, A., Winberg, M.E., Abdalla, H., Särndahl, E., Rasmusson, B., Stendahl, O., and Lerm, M. (2008) Incorporation of *Mycobacterium tuberculosis* lipoarabinomannan into macrophage membrane rafts is a prerequisite for the phagosomal maturation block. *Infect Immun* **76**: 2882-7.

Wietzerbin, J, Das, B.C., Petit, J.F., Lederer, E, Leyh-Bouille, M., and Ghuysen, J.M. (1974) Occurrence of D-alanyl-(D)-meso-diaminopimelic acid and meso-diaminopimelyl-meso-diaminopimelic acid interpeptide linkages in the peptidoglycan of Mycobacteria. *Biochemistry* **13**: 3471-6.

Wilson, L.G. (1990) The historical decline of tuberculosis in Europe and America: its causes and significance. *J Hist Med Allied Sci* **45**: 366-96.

Wilson, R., Kumar, P., Parashar, V., Vilchèze, C., Veyron-Churlet, R., Freundlich, J.S., *et al.* (2013) Antituberculosis thiophenes define a requirement for Pks13 in mycolic acid biosynthesis. *Nat Chem Biol* .

Winder, F.G., and Collins, P.B. (1970) Inhibition by isoniazid of synthesis of mycolic acids in *Mycobacterium tuberculosis*. *J Gen Microbiol* **63**: 41-8.

Wolinsky, E., Reginster, A., and Steenken, W. (1948) Drug-resistant tubercle bacilli in patients under treatment with streptomycin. *Am Rev Tuberc* **58**: 335-43.

Wolucka, B.A., and de Hoffmann, E. (1998) Isolation and characterization of the major form of polyprenyl-phospho-mannose from *Mycobacterium smegmatis*. *Glycobiology* **8**: 955-62.

Wolucka, B.A. (2008) Biosynthesis of D-arabinose in mycobacteria - a novel bacterial pathway with implications for antimycobacterial therapy. *FEBS J* **275**: 2691-711.

- Young, D.C., and Moody, D.B. (2006) T-cell recognition of glycolipids presented by CD1 proteins. *Glycobiology* **16**: 103R-112R.
- Zajonc, D.M., Ainge, G.D., Painter, G.F., Severn, W.B., and Wilson, I.A. (2006) Structural characterization of mycobacterial phosphatidylinositol mannoside binding to mouse CD1d. *J Immunol* **177**: 4577-83.
- Zhang, N., Torrelles, J.B., McNeil, M.R., Escuyer, V.E., Khoo, K.-H., Brennan, P.J., and Chatterjee, D. (2003) The Emb proteins of mycobacteria direct arabinosylation of lipoarabinomannan and arabinogalactan via an N-terminal recognition region and a C-terminal synthetic region. *Mol Microbiol* **50**: 69-76.
- Zhang, Y. (2003) Isoniazid. In *Tuberculosis*. W Rom, S.G. (ed.). Lippincott, New York. pp. 739-58.
- Zhang, Y., Heym, B, Allen, B., Young, D., and Cole, S. (1992) The catalase-peroxidase gene and isoniazid resistance of *Mycobacterium tuberculosis*. *Nature* **358**: 591-3.
- Zhang, Y. (2005) The magic bullets and tuberculosis drug targets. *Annu Rev Pharmacol Toxicol* **45**: 529-64.
- Zhang, Y., Wade, M.M., Scorpio, A., Zhang, H., and Sun, Z. (2003) Mode of action of pyrazinamide: disruption of *Mycobacterium tuberculosis* membrane transport and energetics by pyrazinoic acid. *J Antimicrob Chemother* **52**: 790-5.
- Zheng, X., Papavinasasundaram, K.G., and Av-Gay, Y. (2007) Novel substrates of *Mycobacterium tuberculosis* PknH Ser/Thr kinase. *Biochem Biophys Res Commun* **355**: 162-8.
- Zink, A., Haas, C.J., Reischl, U., Szeimies, U., and Nerlich, A.G. (2001) Molecular analysis of skeletal tuberculosis in an ancient Egyptian population. *J Med Microbiol* **50**: 355-66.